

Polymeric Photosensitizer Nanocomplex Encapsulated T-lymphocyte Delivery System for Photodynamic Therapy of Cancer

Dissertation

zur

Erlangung des Doktorgrades
Der Naturwissenschaften
(Dr. rer. nat.)

dem
Fachbereich Pharmazie
der
Philipps Universität Marburg

Vorgelegt von
Mohammad Yahya Momin
M.S. (Pharm.)
aus **Indien**

Marburg/Lahn, 2016

Erstgutachter: **Prof. Dr. Marc Schneider**
Zweitgutachter: **Prof. Dr. Udo Bakowsky**

Tag der mündlichen Prüfung am: **21.12.2016**
Eingereicht am: **08.11.2016**

Hochschulkennziffer: **1180**

Contents

Acknowledgement	1
List of Abbreviations	3
List of Figures	4
List of Tables	6
A ZUSAMMENFASSUNG	7
B SUMMARY	9
C GENERAL INTRODUCTION	11
1. Photodynamic therapy	11
1.1. History of photodynamic therapy	11
1.2. Mechanism of photodynamic therapy	13
1.3. Application of photodynamic therapy in patients	16
1.4. Advantages of photodynamic therapy	16
1.5. Nanoparticles in photodynamic therapy	17
2. Cancer immunotherapy	20
2.1. Animal studies in cancer immunotherapy	23
2.2. Modalities of anticancer immunotherapy	24
3. Photoimmunotherapy	29
4. Photosensitizer	31
5. Drug profile	34
5.1. Description	34
5.2. Spectral properties	35
5.3. Solubility	35
5.4. Chemical structure	35
5.5. Mechanism of action	35
5.6. Side effects	36
6 Polystyrene sulphonate	36

7	Kollidone [®] 25 (Polyvinylpyrrolidone/PVP)	36
	7.1. Kollidone [®] 25	37
	7.2. Polyvinylpyrrolidone as a complexing agent	38
8	Chitosan-hydrochloride (Protasan [®])	38
D	INTRODUCTION	40
E	MATERIALS AND EQUIPMENT	43
1	List of Materials used in experiment	43
2	List of equipment used in experiment	44
F	EXPERIMENTAL	46
1	Analytical method development by UV and fluorescence spectroscopies	47
	1.1. UV spectroscopy of mTHPP in ethanol and isopropanol	47
	1.2. Fluorescence spectroscopy of mTHPP in ethanol and isopropanol	48
2	Development of mTHPP-Polymer loaded Jurkat Cell based delivery system	49
	2.1. Synthesis of mTHPP-Polymer nanocomplexes	49
	2.2. Preparation of nanocomplex loaded Jurkat Cell based delivery system	50
3	Quantification of mTHPP	51
	3.1. Amount of mTHPP complexed with polymer	51
	3.2. Amount of intra-Jurkat cellular-mTHPP complexed with polymer	51
	3.3. Determination of complexation efficiency	52
4	Characterization of mTHPP-Polymer nanocomplex	52
	4.1. Spectral characterization	52
	4.2. Molecular modeling	53
	4.3. Atomic force microscopy (AFM)	53
	4.4. Confocal laser scanning microscopy (CLSM)	53
5	Cell culture studies	54
	5.1. MTT assay of mTHPP-Polymer nanocomplexes	54
	5.2. Haemotoxicity studies of mTHPP-Polymer nanocomplexes	54

5.3. Blood clotting study with mTHPP-Polymer nanocomplexes	54
5.4. Anticancer activity of mTHPP-Polymer nanocomplexes.....	55
G RESULTS AND DISCUSSION	56
1. Analytical method development	56
2. Synthesis of Polymer-mTHPP nanocomplexes	57
3. Complexation efficiency study	65
4. Spectral characterization	67
5. Particle size, morphology and surface charge	72
6. Confocal laser scanning microscopy	76
7. Cell culture studies	77
7.1. Cellular toxicity studies.....	77
7.2. Intra-Jurkat-cellular quantification of mTHPP.....	80
7.3. Haemocompatibility studies.....	82
7.4. Invitro anticancer activity.....	85
H CONCLUSION	88
I REFERENCES	89
J ERKLÄRUNG	100
K CURRICULUM VITAE	101

Acknowledgement

In the name of “Allah” Who is merciful and always showered blessing on me in challenging situations.

The doctoral work and then writing of this dissertation have been one of the most significant challenges in my academic career. The PhD work had taught many life-principles, instilled and improved qualities like self-control, dedication, patience and hard work. While completing doctoral thesis, support and guidance of the following people is highly acknowledged. I owe to them my deepest gratitude.

My sincere thanks to Prof. Dr. U. Bakowsky, who has been caring me like a father, guiding and teaching as a great philosopher. I am also grateful of Prof. Dr. M. Schneider for accepting my PhD candidature whose care, guidance and a friendly approach made me feel very much comfortable and encouraged to open up and share innovative ideas. In fact their keenness, foresightedness and feedbacks during group and personal meetings, and in other occasions had given me ample opportunity to explore my scientific arena and grow both personally and on professional front. The liberty provided by both, has inculcated within me a sense of responsibility and made me strong with clear vision. They have taught me science along with basic principles and facts of life. It gives me immense pleasure to acknowledge them, as with their kind supervision and support only, this thesis has taken shape as of today.

I am extremely thankful to Prof. Dr. F. Hucho (Free University of Berlin) for recommendation to do PhD at Institute of Pharmacy, Philipp’s University of Marburg.

Management and scientific assistantship of Philipps University of Marburg are highly appreciated for providing the resources, facilities and financial support to successfully complete this project in a beautiful city like Marburg.

I feel privileged to have worked with all members of both research groups (AK Bakowsky and AK Schneider) and special thanks to Eva, Shashank and Gihan for scientific help, discussion and feedbacks. Konrad is acknowledged for fun moments in lab ☺ and AFM imaging. Thanks to Agnes for AFM imaging too.

A brief period spent with Prof. Dr. Keck and members of AG Keck is memorable.

I am grateful of Prof. Dr. Kahmann at Max Planck Institute of Terrestrial Microbiology-Marburg for granting permission to carry out CLSM. Steffi and Malengo are acknowledged for extending friendly assistance towards confocal imaging of photosensitizer loaded Jurkat cells.

Thanks to Dr. P. Nair (Flinders University, Australia) for molecular modelling of each nanocomplex.

Finally I feel pleasure to thank the most important people in my life; first my parents (Khatoon & late Mohammad Saeed) and sisters (Saba and Huda) who were always there within my soul to positively influence my performance in each area of life.

- M.Y. Momin

List of Abbreviations

Abbreviation	Full form
µg	Microgram
mg	Milligram
µL	Microlitre
mL	Millilitre
NC	Nanocomplex
mTHPP	5,10,15,20-Tetrakis(3-hydroxyphenyl) prophyrine
mTHPC	5,10,15,20-Tetrakis (3-hydroxyphenyl) chlorin
Hb	Haemoglobin
UV	Ultraviolet
HPLC	High performance liquid chromatography
PNC	Photosensitizer-polymer nanocomplex
PVP	Polyvinylpyrrolidone
PSS	Polystyrene sulphonate sodium
Chitosan	Chitosan hydrochloride (Protasan [®])
EtOH	Ethanol
IPA	Isopropanol/Isopropyl alcohol

List of Figures

Figure No.	List of Figures	Page No.
01	Graphical abstract of the project	10
02	Energy level diagram illustrating mechanism of photodynamic therapy	14
03	type I (a) and type II (b) mechanisms involved in PDT	15
04	T cells recognize and bind with cancer cells through T cell receptor leading to their destruction	22
05	UV spectrum of mTHPP in EtOH (3µg/mL)	34
06	UV spectrum of mTHPP in isopropanol (2µg/mL)	34
07	Chemical structure of mTHPP; Mw: 680	35
08	Chemical structure of polystyrene sulphonate sodium	36
09	Chemical structure of polyvinylpyrrolidone	37
10	Chemical structure of Chitosan hydrochloride	39
11	Experimental design of PhD work	46
12	UV-calibration curves of mTHPP in EtOH and IPA (500 to 0.05 µg/mL)	47
13	UV-calibration curves of mTHPP in EtOH and mTHPP in IPA	48
14	Fluorescence spectrums of mTHPP in EtOH and IPA	48
15	Fluorescence calibration curves of mTHPP in EtOH and IPA	49
16	Behaviour of mTHPP in water, alone and as complexed with polymer	60
17	Polymer-mTHPP nanocomplex and mTHPC	61
18	Molecular model showing interaction of mTHPP and PSS in nanocomplex	62
19	Molecular model showing interaction of mTHPP and PVP in nanocomplex	62

20	Molecular model showing interaction of mTHPP and Chitosan in their nanocomplex	63
21	Solubility enhancement model; water soluble polymer and water insoluble drug forms water soluble drug-polymer	64
22	Comparison of amount of mTHPP complexed with different polymers by direct and indirect methods.	66
23	UV spectrums of a) mTHPP, PSS and mTHPP-PSS NC	68
24	UV spectrums of a) mTHPP, Chitosan and mTHPP-Chitosan NC	69
25	UV spectrums of a) mTHPP, PVP and mTHPP-PVP NC	70
26	AFM of mTHPP-PSS nanocomplex (height and 3D view)	73
27	AFM image of mTHPP-Chitosan nanocomplex (height and 3D view)	74
28	AFM image of mTHPP-PVP nanocomplex (height and 3D view)	75
29	CLSM image of mTHPP-PSS NC loaded Jurkat cell	76
30	CLSM image of mTHPP-Chitosan NC loaded Jurkat cell	76
31	CLSM image of mTHPP-PVP NC loaded Jurkat cell	77
32	In vitro toxicity of Jurkat cells (1×10^4) following incubation with serial dilutions of 1000 $\mu\text{g/mL}$ PSS NC, mTHPP-PVP NC and mTHPP-Chitosan NC	78
33	Schematic molecular model of mTHPP-Polymer NCs showing molecular interaction between mTHPP and a polymer chain segment containing 28 monomers.	79
34	Viability testing of electroporated 1×10^6 Jurkat cells	82
35	In vitro hemolysis following incubation of human RBCs with 15×10^4 cells Blank JC, mTHPP-PSS NC, mTHPP-PVP NC and mTHPP-Chitosan NC loaded JCs in normal saline. Positive Control shows 100% haemolysis	83
36	In-vitro anticancer activity of NC loaded JC against A549 cells	87

List of Tables

Table No.	List of Tables	Page No.
01	Brief history of photodynamic therapy	12
02	Classification of photosensitizers	32
03	List of materials or chemicals used in the experiments	43
04	List of equipment used in the experiments	44
05	Size, zeta potential and complexation efficiency of all mTHPP-Polymer nanocomplexes	67
06	Physical and spectral properties, and CE of mTHPP-Polymer nanocomplexes	71
07	mTHPP uptake by JC by electroporation	81
08	Blood clotting studies with all Polymer-mTHPP nanocomplex	84

A. ZUSAMMENFASSUNG

Eine geeignete Modellschubstanz für mTHPC (m-tetra (Hydroxy) phenyl Chlorin) als Antikrebsmedikament stellt mTHPP oder 5,10,15,20-Tetrakis-(3-hydroxyphenyl) Porphyrin dar. Die Substanz mTHPP ist ein hocheffektives Medikament, jedoch weist es biopharmazeutische und physiologische Grenzen auf. Aufgrund der geringen Wasserlöslichkeit ist die Formulierung von mTHPP eine große Herausforderung. Desweiteren hat mTHPP die Tendenz sich in der Zellmembran anzureichern, was zu einer erhöhten Gewebetoxizität führt. Durch die Verpackung von mTHPP in Nanopartikel können diese Probleme effektiv gelöst werden, jedoch ist die gezielte Zerstörung von Krebszellen durch Nanocarrier eine große Schwierigkeit. T-Lymphozyten sind in der Lage Krebszellen zu identifizieren und zu attackieren. Durch vorhandene T-Zell-Rezeptoren auf den Krebszellen erwerben sie die Fähigkeit, Krebszellen zu erkennen, anzugreifen und eine „Tumor Autoimmune machinery“ zu bilden. Durch die Einschleusung von mTHPP (als mTHPP Nanocomplex) in T-Lymphozyten wird ein „immune cell based delivery system“ erzeugt. Ein solches System kann Krebszellen selektiv auswählen und mTHPP übertragen.

mTHPP bindet durch nicht-kovalente Bindungen an folgenden Polymere: Polystyrolsulfonat-Na, Polyvinylpyrrolidone und Chitosan HCl (Protasan®). Diese physikalischen Bindungen sind schwach und erleichtern somit die Freisetzung von mTHPP. Interessanterweise besitzen diese Nanokomplexe auch eine photodynamische Aktivität. Somit stellen sie ideale „Carrier“ für mTHPP zur photodynamischen Therapie dar. Polymer-mTHPP Nanokomplexe werden durch Elektroporation in Jurkat-Zellen (JZ) eingeschleust, da dies ist eine einfache, kosten und zeitsparende Methode ist. Da PNC geladene JZs ein auf Immunzellen basierendes Transportsystem bilden, können sie durch eine direkte Verabreichung im Blut, Krebszellen identifizieren und dran binden. Der von Krebs betroffene Bereich wird mit einer bestimmten Wellenlänge des Lichts angeregt, was zu einer Anregung von PNC führt. Dies wiederum führt zu Erzeugung von ROS (Reaktive Sauerstoffspezies), die die umgebenen Krebszellen einschließlich der Jurkat-Zellen abtötet.

PNC wurden durch UV-Spektroskopie charakterisiert um die Bildung von mTHPP-Polymer-NC zu bestätigen und um die Fluoreszenzeigenschaft zu charakterisieren, da dies die Voraussetzung für eine photodynamische Aktivität ist. Die Charakterisierung mittels AFM zeigte die Morphologie sowie die PNC Teilchengröße zwischen 10-80 nm. Solche kleinen Größen von Nanopartikeln sind geeignet, um in T-Lymphozyten aufgenommen zu werden. Außerdem wurden UV und- Fluoreszenz-Spektroskopie zur Quantifizierung von mTHPP genutzt.

So konnte ein Beweis des Konzeptes erbracht werden, die Wasserlöslichkeit von mTHPC durch die Komplexbildung mit unterschiedlichen Polymeren zu verbessern. Ebenso wurde ein „T-Lymphocyte based delivery system“ für die Phototherapie gegen Krebs entwickelt. Die Substanz mTHPP diente als Model für mTHPC und Jurkat-Zellen wurden als T-Lymphozyten eingesetzt.

B. SUMMARY

mTHPP or 5,10,15,20-Tetrakis (3-hydroxyphenyl) porphyrine is a best suited model anticancer drug for mTHPC or m-tetra (hydroxy) phenyl chlorin which is used as a second generation photosensitizer in photodynamic therapy (Chatterjee et al, 2008). Though, mTHPP is an effective anticancer drug, suffers from biopharmaceutical and physiological limitations. The problem pertaining to formulation development arises due to very low aqueous solubility (Konan et al, 2002) and tendency of mTHPP to accumulate in cell membrane from where it slowly releases and degrades (Ochsner et al, 1997). These hurdles can be effectively circumvented by designing nanoparticles but targeting cancerous cells through these nanocarriers still remains a major challenge. Due to presence of T cell receptors on cancerous cells, they acquire the ability to recognise and attack cancerous cells and make a tumor targeting autoimmune machinery. This autoimmune mechanism can be exploited to develop an immune cell (T cell) based delivery system by loading mTHPP (as nanocomplex) into T cells. Such safe homing of mTHPP into T cell is capable of selective delivery and targeting cancer cells as well as avoiding numerous side effects associated with mTHPP while present in blood.

mTHPP binds with each polymer viz, polystyrene sulphonate Na, polyvinylpyrrolidone and Chitosan hydrochloride (Protasan[®]) through non-covalent bondings. These physical bonds are weak therefore facilitates release of drug. Interestingly, these nanocomplexes also possess fluorescence, thus acting as an ideal carrier for mTHPP for photodynamic therapy. Polymeric nanocomplexes of mTHPP (PNC) are internalized into Jurkat cell (JC) by electroporation because this is simple, time saving and economic method of intracellular delivery. PNC loaded JCs form an immune cell based delivery system which is intended to be administered directly into blood following identification and binding with cancer cells. Exposure of cancer affected area with suitable wavelength of light leads to excitation of PNC and generation of ROS (Reactive oxygen species) which kill surrounding cancer cells including Jurkat cells.

PNC were characterized by UV spectroscopy to confirm formation of mTHPP-polymer NC while keeping fluorescence property intact which is prerequisite for photodynamic activity. Characterization by AFM revealed morphology and particle size of PNC

between 10-80 nm which is smaller enough for effective intracellular delivery. Analytical methods by UV and fluorescence spectroscopies were developed for quantification of mTHPP.

Thus, a proof of concept was designed pertaining to enhancement of aqueous solubility of mTHPC by complexation with different polymers and development of its T lymphocyte based delivery system for photoimmunotherapy of cancer using mTHPP as a model drug for mTHPC and JCs as model cell for T lymphocytes respectively.

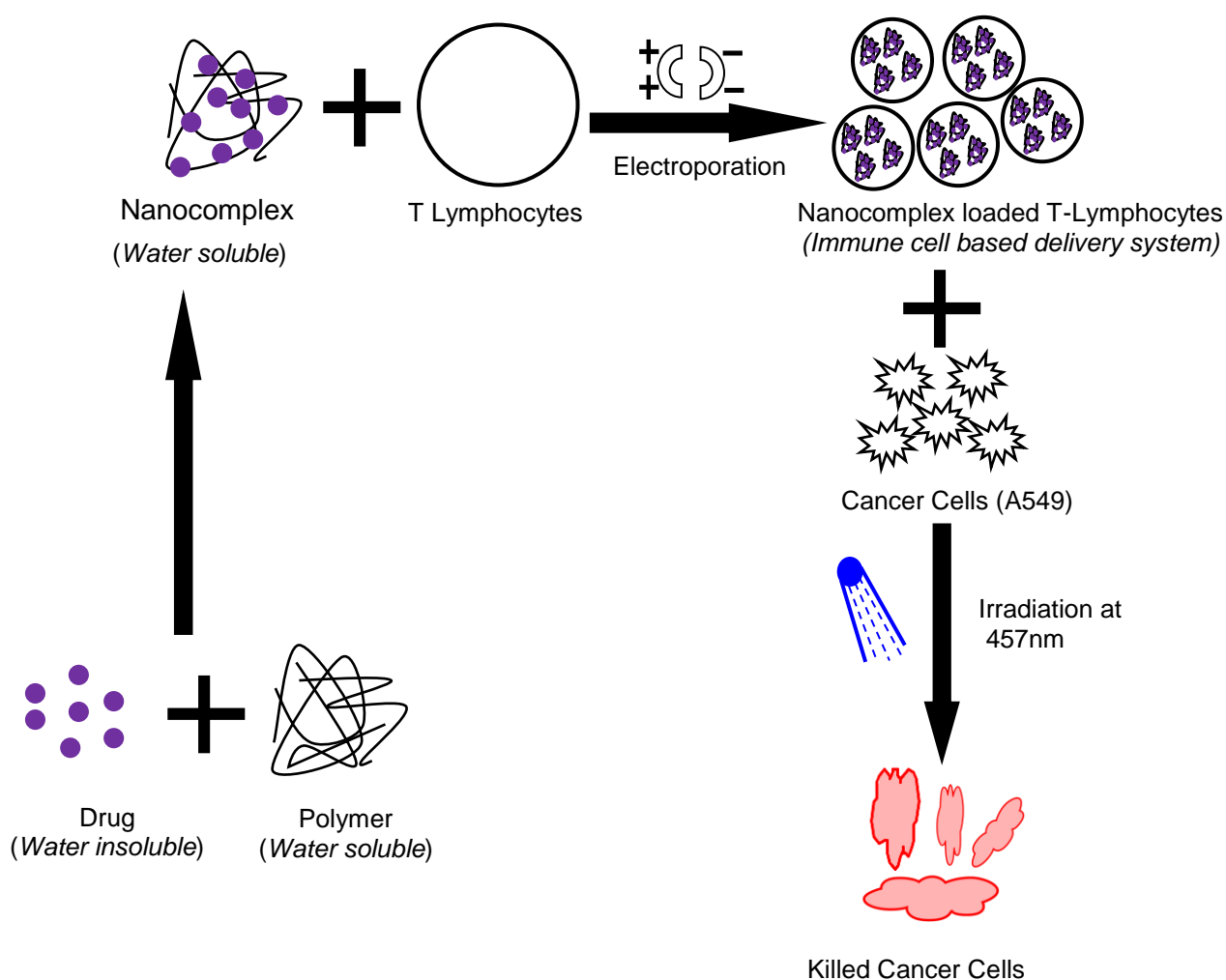


Fig.1: *Graphical abstract*; water soluble polymer and mTHPP form photosensitizer-polymer NC. These NCs are internalized into T lymphocyte by electroporation. PNC loaded T lymphocytes are incubated with A549 lung carcinoma cell line followed by irradiation at 457 nm resulting into killing cancer cells.

C. GENERAL INTRODUCTION

1. Photodynamic therapy

Photodynamic therapy (PDT) is a mode of treatment in which special drugs (photosensitizers) are used along with light in presence of oxygen to kill cancer cells. Photosensitizers are effective only after activation by certain kinds of light. PDT is also called as *photoradiation therapy*, *phototherapy*, or *photochemotherapy*.

1.1. History of PDT

Role of light for therapeutic purpose is known to human mankind since thousands of year (Ackroyd et al, 2001 & Daniell et al, 1991). Skin cancer and various other diseases like psoriasis and rickets had been treated by light in ancient Indian, Chinese, Greek and Egyptian civilization (Jain et al, 2002 & Lukšienė et al, 2003). It was more than a century ago when cell death was observed due to combination of light and some chemical compounds, and today clinical use of PDT is under testing for treatment of cancers of head and neck, brain, lung, pancreas, intraperitoneal cavity, breast, prostate and skin (Dolmans et al, 2003). A medicine student in Germany named Oscar Raab had reported that certain wavelengths of light are lethal to aquatic creature infusoria in the presence of acridine (Raab, 1900). At the same time, a French neurologist named J. Prime found that oral delivery of Eosin in patients suffering from epilepsy have developed dermatitis in areas of body which are easily exposed to sun (Prime et al, 1900). In 19th century, Niels Finsen in Denmark had found that red light has the potential to treat small pox postules and UV radiation from sun can cure cutaneous tuberculosis. He had first time used light for modern day phototherapy and achieved Noble Prize (Dolmans et al, 2003). Currently PDT is not only used in treatment of cancer but also in the treatment of many other diseases. United States Food and Drug Administration (US FDA) has approved PDT as a mode of treatment in endobronchial and endo-esophageal cancer (Dougherty, 2002; Oleinik & Evans, 1998) as well as premalignancies and early stage malignant lesion of skin (actinic keratosis), oral cavity, breast bladder and stomach (Pass, 1993). There are many fluorescent drug molecules especially porphyrine derivatives under investigation for their photodynamic effect in cancer and other diseases. Recently, the potential phototoxicity of Chlorin e6 loaded liposomes was confirmed in Neuro2a and SKOV5 cell lines along with improvement in the loading efficiency of Chlorin e6 by assembling

with cationic lipid 1,2-Dioleoyl-3-trimethylammonium-propane (Mahmoud et al, 2015). PEGylated G4.5 PAMAM-Ce6 dendrimers were developed for improved photodynamic therapy in a preclinical study of cancer (Bastien et al, 2015).

Several other studies pertaining to photosensitizers in PDT are underway. A brief history of evolution of photodynamic therapy since 1900 is presented in Table1.

Table 1: Brief history of photodynamic therapy (Dolmans et al, 2003)

1900	Oscar Raab	showed cytotoxic effect of acridine in presence of light against infusoria (<i>Paramecium caudatum</i>)
1901	Niels Finsen	used light for treatment of smallpox and cutaneous tuberculosis
1903	Niels Finsen	achieved Noble Prize for discovery in phototherapy
1903	H von Tappeiner & A Jesionek	Used eosin topically in presence of white light to treat skin cancer
1907	von Tappeiner & A Jodlbauer	first time used the term "photodynamic"
1911	W Hausmann	defined photosensitive and phototoxicity haematoporphyrine
1913	Friedrich Meyer-Betz	first used porphyrines for photodynamic therapy in humans. He used haematoporphyrines on his hands
1955	Samuel Schwartz	synthesized haematoporphyrine derivatives (HPD) by acetylation and reduction which were twice phototoxic than haematoporphyrine
1960	Richard Lipson & Baldes	described HPD about its accumulation and photodetection of tumor
1972	Diamond	proved HPD induced phototoxicity in brain tumor
1975	Thomas Dougherty	carried out successful treatment of skin cancer
1975	JF Kelly	HPD for bladder cancer and twice enhanced toxicity of HPD than haematoporphyrine

1978	Dougherty	first controlled clinical trials of PDT in human
1999	QLT PhotoTherapeutics	first approval of PDT in Canada

1.2. Mechanism of PDT

In 1903, Herman Von Tappeiner and A Jesionek have first described the overall phenomenon of PDT as “photodynamic action” during treatment of skin tumors with topically applied eosin (Fisher, 2001). Today PDT is established in clinical practice for treatment of several diseases such as actinic keratosis (Kübler, 2005 & Monfrecola et al 2009) and other forms of cancer (Berman et al, 2009; Choudhary et al, 2009; Smits et al, 2009), blindness associated with macular degeneration due to aging (Brown et al, 2004). The procedure of PDT involves a series of events for which three elements are essential viz, photosensitizer (PS), light of suitable wavelength preferably in red region ($\lambda \leq 600$ nm) because at this wavelength oxygen is highly permeable to deeply seated human tissues. Third requirement is molecular oxygen in singlet state. After administration of the photosensitizer, excitation at a wavelength corresponding to the absorbance band of the PS in presence of oxygen leads to a multistep photochemical events. It results in direct destruction of tumor cell, microvasculature damage in parallel to induction of a local inflammatory reaction (Songca et al, 2013).

There are numerous mechanisms possible for the destruction of cells by photosensitizer. However, major pathway is type II mechanism (Fig 2 & 3b). The first step in type II mechanism starts by absorption of a light by the photosensitizer in the singlet ground state to promote it to the short-lived singlet excited state (P_1) (Fig 1). The singlet state decays back to the lowest energy level of excited state via intersystem crossing to form a stable triplet excited state (P_3) where the promoted electron in a higher orbit undergoes a spin conversion. The triplet state is sufficiently long-lived to take part in chemical reactions and therefore, the photodynamic action takes place mostly in the triplet state of PS. Then the reaction between triplet excited PS molecule (P_3) and triplet state oxygen (3O) is the key step which leads to formation of singlet state oxygen (1O) or reactive oxygen species (ROS). ROS has potential to kill tumor cells directly by apoptosis and/or necrosis.

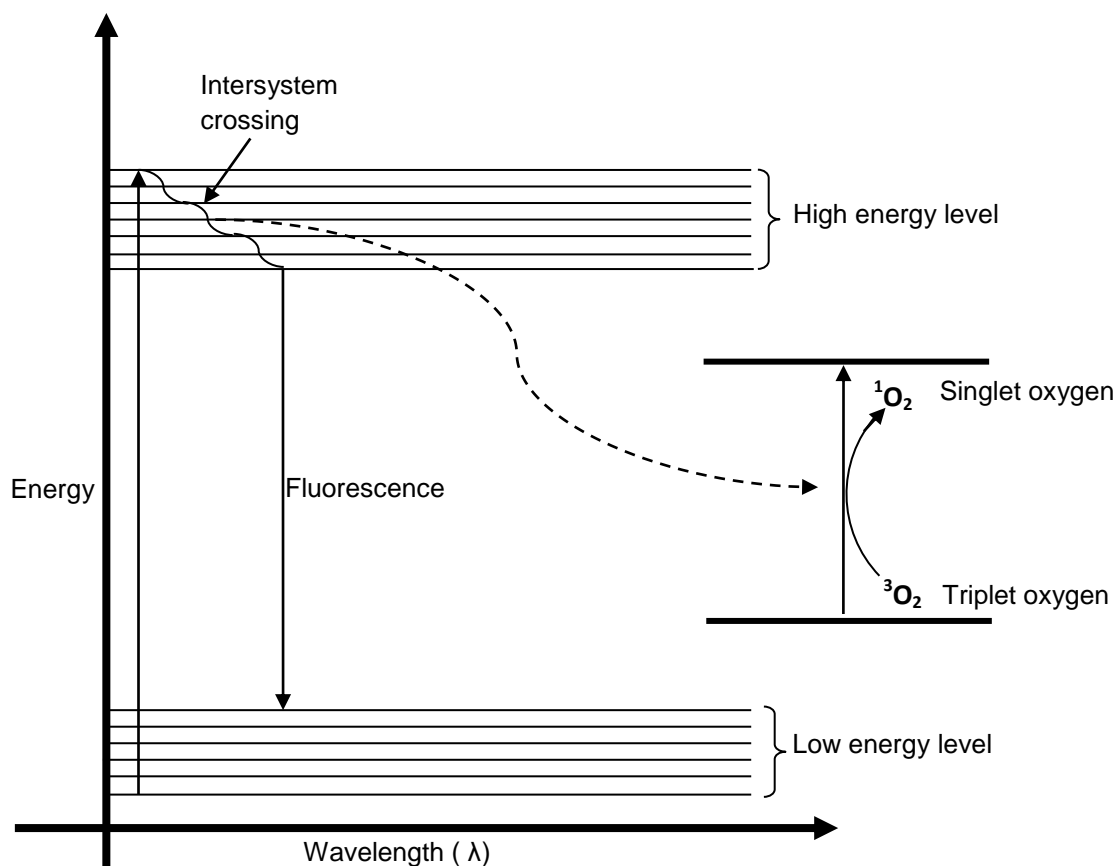


Fig.2: Energy level diagram illustrating mechanism of PDT

The destructive effect exerted by ROS could hamper ion channels e.g. Ca^{++} channels, ion pumps e.g. sarcoplasmic reticulum and sarcolemmal Ca^{++} pumps, ion exchangers e.g. $\text{Na}^+/\text{Ca}^{++}$ exchanger and Na^+/H^+ exchanger, and ion co-transporters such as K^+-Cl^- , $\text{Na}^+-\text{K}^+-\text{Cl}^-$ co-transporters. These ionic pathways are blocked by oxidation, peroxidation of cellular components and inhibition of membrane bound enzymes (Kourie et al, 1998).

The major mechanisms of cell death during anti-tumour photodynamic activity involve cell damage alongwith vasculature shut-down followed by triggering immune system against tumours. Direct cell damage involves destruction of mitochondria and cytoplasm through apoptosis, endoplasmic reticulum undergoes autophagy and cell membrane is disintegrated by necrosis (Mroz et al, 2011). Vasculatures get depleted of oxygen and nutrients through all three processes viz, apoptosis, necrosis and

autophagy leading to tumour infraction (Castano et al, 2005). Consequently an immune response through stimulation of cytotoxic T cells against tumor cells is activated (Plaetzer et al, 2003).

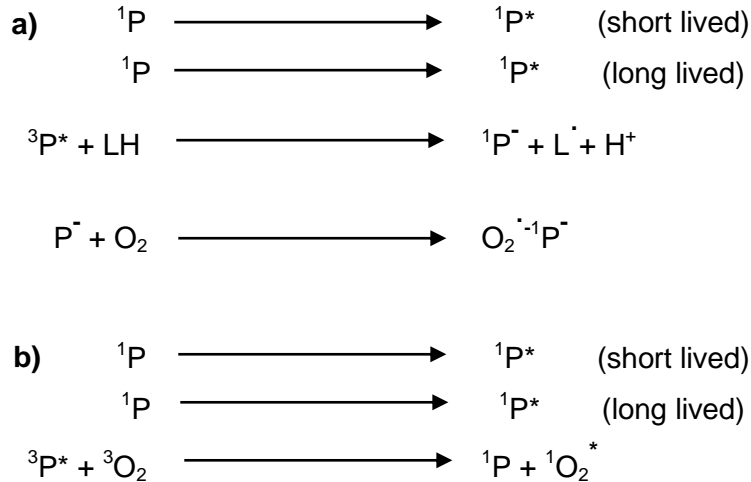


Fig.3: type I (a) and type II (b) mechanisms involved in PDT

Photodynamic therapy majorly involves Type II mechanism. In this mechanism, photosensitizer interacts in excited state with triplet state of molecular oxygen (${}^3\text{O}_2$) to generate reactive oxygen species (ROS) and radicals. They can interact with cellular components such as nucleic acids, amino acids and unsaturated lipids (Josefsen et al, 2008).

Other pathway referred as type I mechanism is described in Fig. 3a. PS is excited to triplet state like type II mechanism where it directly reacts with biomolecules to bring permanent chemical changes within them. This triplet state PS interacts with lipid molecules embedded in cell membrane and extract an electron to from cationic lipid and PS itself becomes anionic radical (Agostinis et al, 2011). This anionic PS radical react with molecular oxygen to produce superoxide radical and singlet state photosensitizer. The cationic lipid may also be converted to neutral lipid by accepting an electron. This radical lipid molecule interacts with proteins embedded in cell membrane.

1.3. Application of PDT in patient

Since inception of PDT in early 1900s, Diamond et al have found potential of hematoporphyrine derivative in destruction of tumor cells through sensitization by visible light (Diamond et al 1972). Then first time PDT was demonstrated by Dougherty et al in 1975 and it has undergone thorough investigation to enable application in patients (Dougherty et al, 1975). Thereafter, promising results were obtained during clinical studies of PDT of various malignant tumours (Dougherty et al, 1978). Studies pertaining to PDT in patients are briefly described here.

A combined approach of PDT using hematoporphyrine derivative (HPD) for intravenous injection and 5-aminolevulinic acid (ALA) for topical application were tested in 26 patients with 41 skin cancer lesions in head and face. The results of this combined PDT were compared against alone PDT using HPD on 28 patients and the ALA following CO₂ laser ablation on 41 skin cancer patients. The combined PDT has shown reduction in dose of HPD as well as period of photosensitive period (Wang et al, 2016). In case of long term PDT, 78% cure rate was achieved upon 12 months follow up when 20% ALA solution was applied over 14-18 hours and irradiated with blue light dose 10J/cm², 10mW/cm² (Tschen et al, 2006). A similar treatment protocol resulted in 89% cure rate upon 3 months follow up (Piacquadio et al, 2004). In case of single treatment pertaining to light-dose ranging investigation, 3 hours application of 20% ALA cream using red light dose 100 J/cm², 30mW/cm² had shown 89% cure rate over two months follow up in the low fluence rate group (Ericson et al, 2004). Using similar protocol for PDT using red light dose 70mW/cm², 70J/cm², two treatments resulted in 85% complete response (Sandberg et al, 2006).

1.4. Advantages of PDT

Among all methods of anticancer therapy which are practiced today, PDT is the most economic and simple mode of treatment. Since last three decades, clinical application of PDT has unraveled some advantages over conventional modalities of anticancer therapy (Chatterjee et al, 2008). Chemotherapy requires nurses to get special training as well as post treatment course in intensive care. Radiotherapy needs an engineer, computerized dosimetry calculation and additional cost due to retreatment using isotope. Surgical operations in cancer therapy requires blood transfusion and sophisticated operation theatres. Overall, chemotherapy, radiotherapy and surgery are

complex and expensive against PDT which is simple and cost effective (Songca et al, 2013). Further, cure rate associated with PDT is higher such as palliative treatment of head and neck cancer (Hopper et al, 2004) and Barrett's oesophagus (Hur et al, 2003).

1.5. Nanoparticles in PDT

Though photodynamic therapy makes use of inert components (light, photosensitizer and oxygen), is non- or minimal invasive, offers possibility of repeating treatment without cumulative toxicity, excellent cosmetic results, reduced long-term morbidity and promise for improved quality of life of patient. Its clinical application as first line oncological intervention is yet to be accepted because of some limitations. It is challenging to develop a suitable photosensitizer formulation, optimization of dose for complete and effective cancer treatment, and hurdles in planning, execution and monitoring of responses following treatment (Lucky et al, 2015).

Nanooncology has emerged as an effective therapeutic strategy by exploiting anticancer drug-nanoparticles in diagnosis and treatment of cancer. Designing nanoparticles of a photosensitizer can circumvent the physiological and physicochemical limitations (Konan et al 2002, Bechet et al, 2008).

Nanoparticles in PDT are functionally classified as passive or active (Konan et al, 2002). An active nanoparticulate delivery system of photosensitizer makes use of target tissue receptors or antigens while the passive one are intended for parenteral administration for passive targeting such as polymeric nanoparticles, hydrophilic polymer-PS conjugates, liposomes, oil-dispersions (Chatterjee et al, 2008).

Passive nanoparticles for PDT are produced either from biodegradable polymers or non-polymeric materials such as ceramic and metallic nanoparticles. PLGA (poly-dl-lactide-co-glycolide) and PLA (Poly-lactide) based nanoparticles have been emerged as better alternative than liposomes because of their high entrapment capacity of photosensitizers (Thakor et al, 2013). Photosensitizers have poor inherent aqueous solubility which produces hurdles in formulation development as well as shows physiological limitations due to accumulation in tissues upon parenteral administration (Ochsner et al, 1997). Optimization of polymer matrix composition leads to controlled degradation and release of photosensitizers at the site of action. In addition,

photosensitizer-nanoparticles have shown more phototoxicity than free photosensitizers. Size of nanoparticles also plays important role in photosensitizer effect; smaller the size of nanoparticles, more the accessibility and internalization into cancer cells via endocytosis. Further, smaller size has more surface area to volume ratio leading to more exposure of nanoparticles to surrounding environment which facilitates faster release of photosensitizers (Konan-Kouakou et al, 2005).

These nanoparticles also allow for active targeting by the incorporation of site-specific moieties. Modifying the surface of nanoparticles with polymers like poly (ethylene glycol) and poly (ethylene oxide) increases circulation times (McCarthy et al, 2005). Polymeric nanoparticles based on PLA and PLGA and second generation photosensitizers have been widely explored; p-THPP was entrapped into biodegradable nanoparticles based on three polyesters viz, poly (d,l) lactide-co-glycolide (50:50 PLGA, 75:25 PLGA) and poly (d,l) lactide (PLA) by emulsification-diffusion evaporation technique which produced < 150 nm particles with drug loading of up to 7% (w/w) (Konan et al, 2003a & Konan et al, 2003b). Photodynamic activity of these p-THPP loaded polymeric nanoparticles was evaluated on EMT-6 mouse mammary tumor cells against free p-THPP (Konan et al, 2003a). Moreover, verteporfin loaded PLGA nanoparticles against skin and prostate cancer (Konan-Kouakou et al, 2005), meso-tetraphenylporpholactol-encapsulated PLGA nanoparticles in mouse cancer model (Dougherty et al, 1978) have also been tested. Hypericin loaded PLA nanoparticles were investigated in NuTu ovarian cancer cell line (Zeisser-Labouebe et al, 2006).

Non-biodegradable nanoparticles play differently in PDT than the biodegradable polymeric nanoparticles. As they can't control release of drug therefore not applied for drug delivery purposes but they act as catalyst to produce toxic substances from dissolved oxygen. Further, control over size preferably <50 nm is desirable (Chatterjee et al, 2008). Photosensitizer loaded non-biodegradable nanoparticles have advantages over organic polymeric nanoparticles in terms of stability, control over size, shape, porosity and resistance to microbial attack and pH variation as well as functionalizing nanoparticles for selective targeting of cancer cells which avoids accumulation in normal cells and decreases required photosensitizer concentration for

phototherapeutic effect and thereby increases phototherapeutic index of photosensitizers (Thakor et al, 2013).

The first ceramic-based nanoparticles for PDT was developed using silica-based spherical particles loading antineoplastic drug 2-devinyl-2-(1-hexyloxyethyl) pyropheophorbide (HPPH) with 30 nm size. Irradiation with suitable wavelength light resulted in efficient generation of singlet oxygen, where the inherent porosity of the nanoparticles played important role (Roy et al, 2003). The HPPH-loaded nanoparticles caused < 10% viability of HeLa cell upon irradiation at 650 nm. Development of gold nanoparticles, whereby the photosensitizer is bound to the surface of the nanoparticle (Wieder et al, 2006).

Apart from biodegradable and non-biodegradable nanoparticles, self-lighting nanoparticles have also been used in PDT. Self-lighting PDT consists of a combination of radiation therapy and PDT. Scintillation or persistent luminescence nanoparticles are attached with photosensitizers such as porphyrine compounds. Exposure to radiation such as X-rays, scintillation luminescence emits from the nanoparticles and activates the photosensitizers to produce singlet oxygen which kill cancer cells. However, use of conventional radiation therapy can damage healthy tissues therefore lowering the dose of radiation is recommended (Chen et al, 2006).

An approach combining the effect of X-ray and fluorescence emission of photosensitizer can reduce the external radiation dose and minimize associated phototoxic side effects (Morgana et al, 2009). The emission spectra of many doped nanoparticles such as $\text{LaF}_3\text{:Ce}^{3+}$, $\text{CaF}_2\text{:Mn}^{2+}$ and semiconductor nanoparticles like ZnO, TiO_2 perfectly match with the absorption spectra of some porphyrine derived photosensitizers. As an example, excitation of $\text{BaFBr:Eu}^{2+}\text{:Mn}^{2+}$ nanoparticles by X-rays exhibits three peaks in emission bands at 400, 500 and 640nm. This emission spectrum matches well with the absorption spectrum of hematoporphyrine. The direct application of this approach in biological systems has not yet been reported (Chen et al, 2006). Similarly, core-excited nanoparticles therapy (CENT) uses energy like X-ray absorbed by core nanoparticles and transfer energy to and heat the shell. The heated nanoparticles heat and destroy surrounding cell (Tersigni et al, 2012).

Upconverting nanoparticles (UCN) are modified nanometer-sized composites which generate higher energy light from lower energy radiation, usually near-infrared (NIR) or infrared (IR), through the use of transition metal, lanthanide, or actinide ions doped into a solid state host (Boyer et al, 2006). Upconversion nanoparticles can be synthesized using several different ionic materials – usually rare earth ions like lanthanides and actinides doped in a suitable crystalline matrix (Zijlmans et al, 1999). Heer et al, have identified micrometer-sized $\text{Er}^{3+}/\text{Yb}^{3+}$ or $\text{Tm}^{3+}/\text{Yb}^{3+}$ co-doped hexagonal NaYF_4 as the materials with the highest upconversion efficiencies (Heer et al, 2004).

Nanocomplexes of therapeutic substances have also been explored in anti-cancer therapy. Nazaran et al, have investigated anticancer potential of MnCl_2 (Nazaran et al, 2014) and BCl_3 NCs (Nazaran et al, 2015) designed by nanochelating technology in animal models. A combination of p53 gene carrying targeted liposomal nanocomplex and Docetaxel attached with anti-transferin receptor antibody were studied in a clinical trial Phase 1b for safety and efficacy in advanced solid tumour (Pirollo et al, 2016). Photosensitizer entrapped mesoporous silica nanoparticles spread on with folate modified lipid bilayer-coated gold nanorods were used to design organic-inorganic nanocomplex and tested for synergistic photo-therapy. A combined approach consists of photodynamic therapy and magnetic hyperthermia was adopted to effectively kill cancer cells using photoresponsive magnetic liposomes. This smart nanoplatform consists of hybrid liposomes for an enhanced anticancer effect in which the aqueous core was loaded with iron oxide nanoparticles and the lipid bilayer was embedded with a photosensitizer (Di Corato et al, 2015).

2. Cancer immunotherapy

According to International Agency for Research on Cancer (IARC), 14.1 million new cancer cases had been diagnosed and 8.2 million resulted in death in 2012 (22000 deaths per day). Further, deaths due to cancer are expected to rise to 13.1 million by 2030 (Abastado J-P et al, 2014 & Anderson et al, 2014). Among several modes of cancer treatment, cancer immunotherapy (CIT) makes use of certain parts of human immune system to fight disease such as cancer. Immune cells such as T lymphocytes, B cells, dendritic cells etc. are commonly used for cancer immunotherapy. Harnessing the immune system aiming for eliminating tumor is ongoing area of research and

promising for a mainstream approach for anticancer therapy (Liu et al, 2014). The prestigious journal *Science* has listed Cancer Immunotherapy as top 10 breakthroughs of the Year 2013 (Couzin-Frankel et al, 2013). Thus, it has a huge impact on the lives of millions of people in the coming decades. The CIT is carried out in different ways either by stimulating own immune system to attack and destroy cancer cells or providing immune system with immune components such as man-made immune system proteins. Choice of the modes of treatment depends on cancer types. Sometime boosting body immune system helps eradication of cancer and other way through training immune system against cancer cells appear better strategy. We had approached towards harnessing T lymphocytes with polymeric photosensitizer nanocomplex to enable them to effectively kill cancer cells.

The immune system is collection of organs, specialized cells and substances which help protecting from infection and other disease condition. In case of entry of antigens such as bacteria, viruses, threatening pathogens into body, the immune system is stimulated and raises alarm to unrecognizable substances. The immune system identifies them as foreign bodies and attacks them. Cancer cells are also recognised as foreign body by immune system and immune cells such as T lymphocytes, B cells attempt to attack and destroy them. Immune cells identify and kill these cancer cells as a part of human defence mechanism. In this thesis, the immune system mediated by T lymphocyte is exploited for delivery of anticancer-photosensitizing agent to kill tumours.

However, the immune system faces tougher time to target cancer cells because of their uncontrolled growth. Sometimes similarity of cancer cells with normal cells to avoid recognition and a weak anticancer response from immune system is achieved. There have been various mechanisms suggested to downregulate the anticancer activities mediated by immune cell. Overall, the ability of immune system despite recognising cancer cell antigen is limited therefore need arises to identify the cancer cells by immune system and strengthen them to fight against cancer cells.

Immune cell based anticancer therapy is an emerging field in oncology. An overview of body immune system and its mechanistic understanding in killing cancer cell is prerequisite to gain insight into cancer immunotherapy. Cancer immunotherapy or

immuno-oncology is a treatment modality which makes use of body's immune system to treat cancer. Thus immune cells targeting cancer cells frame autoimmune machinery which is exploited in different ways to serve the purpose of anticancer therapy.

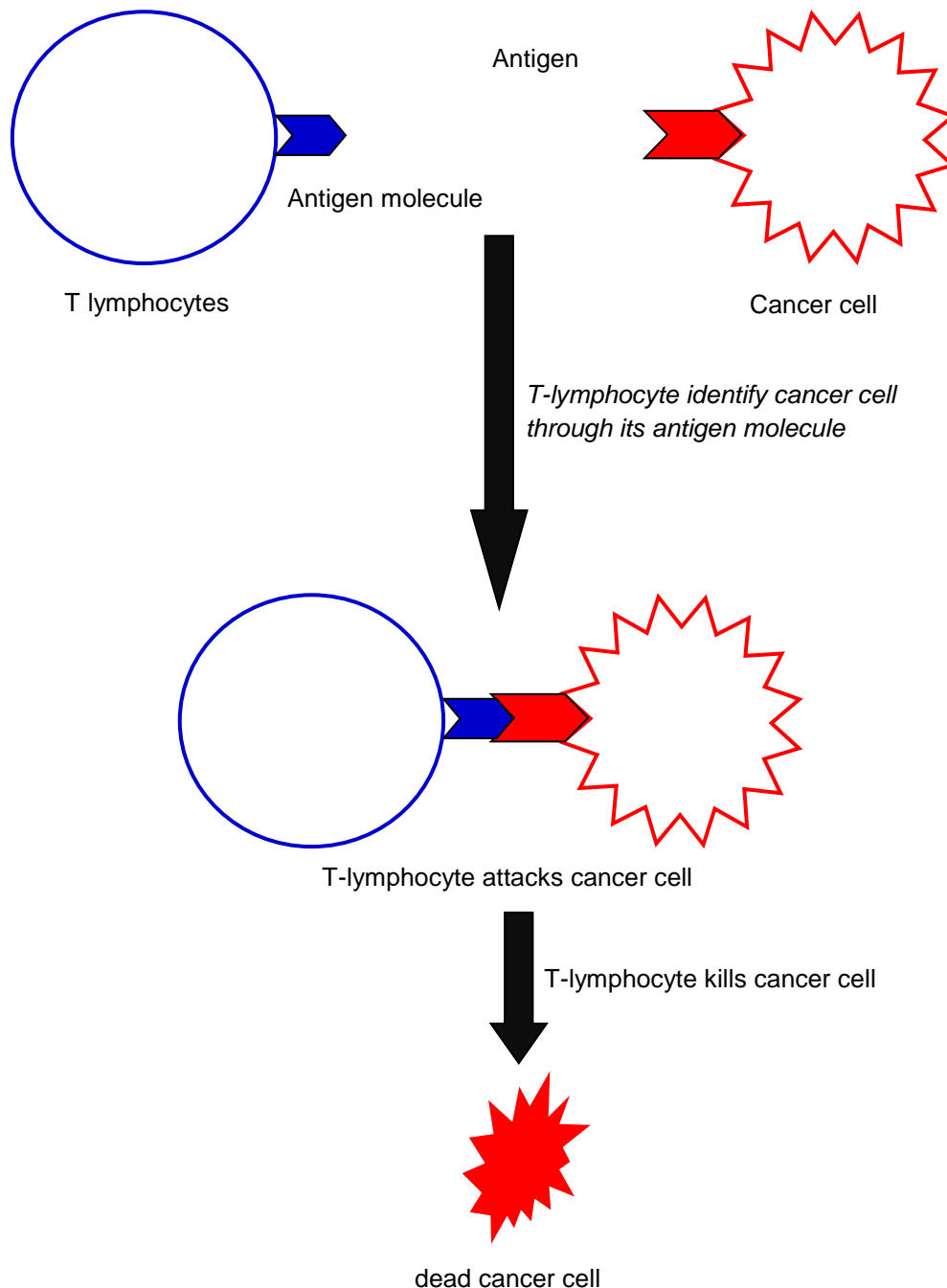


Fig.4: T cells recognize and bind with cancer cells through T cell receptor leading to their destruction

In view of the fact that all cancer cells and viruses often produce a protein molecule on its surface which is identified by immune cells and it is termed as antigen. This molecule is capable of stimulating an immune response upon entry inside the body.

Antigens associated with cancerous cells are bound to class I MHC molecules which are proteins, and brought to the surface of the cell by the class I MHC molecule, where they can be recognized by the T lymphocytes. If the T cell receptor is specific for that antigen, it binds to the complex of the class I MHC molecule and the antigen and the T cell destroys the cell (Milstein et al, 2011).

2.1. Animal studies in cancer immunotherapy

The breakthrough in cancer immunotherapy came in light from animal studies. Beside, different check-point receptors help cancer cells recognizing immune cells signal and avoid immune system attack as well as creating an immunosuppressive microenvironment. Thus, development of check point receptor inhibitors is exciting research in cancer immunotherapy. A combination therapy involving check point receptor inhibitors requires consideration over regulatory and budgetary control for clinical trial approval. Therefore, pre-clinical study with mouse model is needed for accurate determination of optimal therapy with combination immunotherapies (Liu et al, 2014). Three important anticancer therapies in clinical trial are showing great promises viz, chimeric antigen receptors, anti-CTLA therapy and anti PD1 therapy. Research carried out on animals makes critical contribution in these therapeutic approaches.

Adoptive T cell therapy using T lymphocytes modified with chimeric antigen receptors (CARs) have demonstrated activity in hematologic malignancies in early phase clinical trials. Barrett et al have tested the hypothesis in robust leukemia xenograft model mice that multiple infusions of RNA CAR into cytotoxic T cells followed by lymphodepleting chemotherapy can show antitumor responses (Barrett et al, 2013). Highly reactive TCRs with anticancer potential govern the gene therapy against cancer. TCRs responsive to melanoma/melanocyte antigens were generated by both immunization of transgenic mice and a high throughput screening of human T-lymphocytes. This adoptive T cell therapy had shown cancer regression in 36 patients (Johnson et al, 2009). In a study pertaining to relationship between autoimmunity and improved

antitumor immunity, destruction of melanocytes in mice model had shown enhanced number of CD8+ T cells. This finding suggested that adaptive immune responses to cancer can be triggered from immune-mediated destruction of normal cells (Byrne et al, 2011). Monoclonal antibodies specific for CTLA4 (cytotoxic T lymphocyte 4) antigen had shown anticancer potential in mouse tumor model and human, however in advanced stages of cancer therapeutic effect is not appreciable. These problems were addressed in two preclinical studies using mice models viz, TC-1 tumor model and mouse memory carcinoma (MMC) model. Anti CTLA4 therapy had shown effect in TC-1 model but not in MMC model which could be due to lower blockage of CTLA4 receptors in MMC model (Persson et al, 2011). PD-1 and its ligand (B7-H1 and B7-DC) play crucial role in tumor suppression. Blocking both ligands by antibodies was investigated in murine pancreatic cancer model. Administration of blocking antibodies significantly decreased tumor growth in vivo (Okudaira et al, 2009).

2.2. Modalities of anticancer immunotherapy

There are three main types of immunotherapy viz, cellular, antibody and cytokine. All immunotherapies provoke the immune system to attack tumor cells by targeting antigens on cancer cells. Cellular cancer immunotherapies are designed to provoke lymphocyte activation to increase immune response against tumor cells or to enhance recognition of tumor cells (Fry et al, 2001). In clinical practice, vaccines are used for cell based cancer immunotherapy. A vaccine is a biological preparation which is used to acquire active immunity in treatment of a particular disease. Typically it contains an antigen or a microorganism which can cause disease but are either half-killed by destroying its potential to cause disease or completely killed. They trigger the immune system's recognition ability of any disease causing agent and record it through which entry of any such agent is noticed even in later stages. The goal of cancer vaccine is to help treating cancer by provoking immune system.

Vaccine can act in anticancer therapy in different ways; either through blocking the suppression of immunity induced by tumors or by blocking or removing the cellular function through suppression activity, or inducing sensitivity towards apoptosis. Cancer cells express suppressive factors which induces immune escape (Baxevanis et al, 2009). Vaccines designed against cancer either prevent the occurrence of cancer or treat the cancer. Some cancers are caused by viruses; therefore vaccines

which help protection against viral infections might also help preventing cancer associated with those viruses. Some strains of human papilloma virus (HPV) are linked to cervical, anal, throat and other cancers. Anti-HPV vaccine may help preventing such types of cancers. In same way, chronic hepatitis B virus (HBV) infection has higher risk for liver cancer therefore anti-HBV vaccine may lower the risk of liver cancer. These vaccines do not target directly cancer cells but they help reducing the cancer. Moreover, these vaccines are useful only for specific types of cancer which are caused by viral infection.

Vaccines designed to treat cancer work in different way than cancer-preventing vaccines. These vaccines provoke immune system to mount an attack against cancer cells, hence they are meant to destroy tumor indirectly. Some cancer treating vaccines consist of tumor cells, antigens or parts of cells capable to provoke immune system working against cancer cells. Patient's own cells are also removed to prepare vaccines in the lab which are re-injected into the body to enhance immunity against cancer cells. Vaccines could also be combined with adjuvants (other cells) which play role in further boosting immune response. PROVENGE[®] (sipuleucel-T) is indicated in autologous cellular immunotherapy for the treatment of advanced prostate cancer which has acquired resistance to hormone therapy. In order to prepare this vaccine, immune cells of patient are removed from blood and exposed to certain chemicals which turn them into dendritic cells. They are also exposed to prostatic acid phosphatase (PAP) which is a protein, to produce anti prostate cancer immune response. Intravenous administration of dendritic cell back into the body helps other immune cells to attack prostate cancer.

Regulation of immune system involves an intricate balance of stimulatory and inhibitory signals from respective receptors. Some monoclonal antibodies have ability to stimulate the immune response by interaction with immune receptor molecule. They act either as an antagonist on crucial receptors which suppress immune response or as an agonist to activate those receptor which stimulate immune response. An antibody is a protein which circulates throughout the body to identify and attach specific proteins called antigen. Then, they recruit other parts of immune system to destroy antigen-containing cells.

Researchers have designed antibodies that specifically target an antigen expressed on cancer cells. While the copies of such antibodies engineered in lab are called monoclonal antibodies (MCAs). MCAs were first produced by Kohler and Milstein through hybridoma technology which has been now modified for therapeutic application in cancer. Monoclonal antibodies are hybridoma of myeloma cells and spleen derived antibodies which are monospecific for cancer cells. It is an emerging strategy in cancer immunotherapy and initial clinical trials of these MCAs have shown promising results (Melero et al, 2007). Different types of MCAs in anticancer therapies are naked MCAs, conjugated MCAs, bispecific MCAs and now trispecific MCAs are also available on the market.

Naked MCAs are common type of antibodies in cancer therapy. They work by themselves without being labelled with drug or radioactive materials. Some MCAs act by boosting antitumor immune response by attaching to cancer cells and serve as a marker for immune system of body to destroy cancer cells. For example, alemtuzumab (Campath[®]) is indicated in chronic lymphocytic leukemia. It attaches with CD52 antigen expressed on lymphocytes including leukemia cells. After binding, this antibody recruits immune cells towards cancer cell destruction. In some cases, naked MCAs bind and block antigens expressed by cancer cells or nearby cells which help growth and proliferation of cancer cells. Trastuzumab (Herceptin[®]) is such an antibody which attaches and blocks HER2 protein that help growing breast and stomach cancer cells upon activation.

Conjugated MCAs are combination of MCAs and a chemotherapeutic agent or radioactive substance. MCA provides homing to its conjugates and direct them to target cancer cells. This conjugate circulates throughout body and reaches to targeted cancer antigen where it binds and selectively delivers toxic substances to destroy tumor. This selective delivery strategy reduces collateral damage to normal cells. Ibritumomab tiuxetan (Zevalin[®]) is a radiolabeled MCA acts against CD20 antigen expressed on cancerous B cells. The antibody delivers radioactive substances selectively to cancerous B cells and also applied in non-Hodgkin lymphoma. Such type of cancer treatment is also called as radioimmunotherapy. Brentuximab vedotin (Adcetris[®]) is the conjugate of antibody and MMAE which is chemotherapeutic agent. It acts against CD30 antigen expressed on lymphocytes. Adcetris[®] is intended for

Hodgkin lymphoma anaplastic large cell lymphoma. Ado-trastuzumab emtansine (Kadcyla[®]) is an antibody attached with DMI chemotherapeutic agent. It targets HER2 protein highly expressed on breast cancer cells.

Apart from the above mentioned antibodies, monospecific, bispecific and even trispecific antibodies are also used in anticancer therapy. Bevacizumab (Avastin[®]) is a monospecific recombinant MCAs for human use which slows down formation of blood vasculature by inhibiting angiogenesis. In addition, VEGF induced inhibition of dendritic and T cell functions may also be decreased (Melero et al, 2007). It happens through blocking the signals of VEGF-A (vascular endothelial factor-A) (Los et al, 2007). In addition it is used in variety of disease including cancer immunotherapy and was first angiogenesis inhibitor available for clinical use in USA (Shih et al, 2006). Bispecific antibodies are made up of two parts each from different antibodies means two different proteins are attached at the same time. Blinatumomab (Blinicyto[®]) is a bispecific CD19-directed CD3 T-cell engager which is intended in treatment of Philadelphia chromosome-negative relapsed or refractory Bcell precursor acute lymphoblastic leukemia. By binding to both proteins viz, CD19 and CD13, it brings cancer and immune cells in proximity leading cancer cells attacked by immune cells. Cetuximab (Erbix[®]) is an antibody targeting EGFR (Epithelial growth factor receptor) which is usually expressed on normal and cancerous skin cells. The side effect of this drug is skin rash in some recipients. Though conjugated MCAs are more powerful than naked MCAs but conjugated component can cause more side effects. A Trispecific antibody (Affimed[®], Heidelberg) in multiple myeloma is in pipeline which target has yet not been disclosed.

The immune system has ability to distinguish between normal cells and antigens. Immune cells possess certain molecules called as check points through which they selectively attack foreign bodies. The goal is to activate or deactivate check points to bring an immune response. Cancer cells often attempt to avoid these check points to bypass their recognition therefore drugs acting on these check points are very promising in anticancer therapy. Reports pertaining to check points in animal studies have been described.

PD1 is a check point proteins present on T lymphocytes while PDL1 is expressed on cancer cells. PD1 puts T lymphocytes off from attacking other cells in body, notably when PD1 binds with PDL1. This binding provokes T lymphocytes to attack other cell and therapy cancer cells evade immune attack. Treatment using MCAs targeting PD1 or PDL1 boost immune system against tumors and such a therapy has appeared very promising. Pembrolizumab (Keytruda[®]) and Nivolumab (Opdivo[®]) act on PD1 or PDL1 targets and are indicated in treating melanoma with a long lasting effect as well as in lung, kidney and colorectal cancers. However, collateral damage to normal cells is a side effect of this therapeutic approach. CTLA-4 is another check point molecule which is expressed on active T cells and deactivates its function. Currently evaluation of antibodies against this molecule is under clinical trial (Kirkwood et al, 2008). Antibodies acting against CTLA4 inhibit activity of CTLA4 which results in increased population of T cells. Thus, depletion of immunosuppressive agents from tumor microenvironment is necessary for development of an effective immunity against tumor. The microenvironment of tumor contains some immunosuppressive agents which decreases the therapeutic effect of vaccine while immunity is induced and also during effector phase of response. In order to facilitate the immune response, the negative regulator of T cell function can be blocked (Sutmuller et al, 2001). Ipilimumab (Yervoy[®]) is a MCA which binds with CTLA4 and inhibit its functioning. It is indicated in melanoma of skin and effect against other cancer type is under investigation. As Ipilimumab targets immune cells therefore immune system related serious side effects are more in comparison to PD1 or PDL1 targeting drugs.

Non-specific immunotherapies are also practiced in clinical oncology. Here cancer cells are not targeted specifically but they trigger immune system and often show better anticancer immune response. Non-specific immunotherapeutic agents are used either themselves or as an adjuvant to main therapy. This leads to boosting immune system to improve immunotherapy using vaccines. Cytokines are mainly used in non-specific immunotherapy. They are small proteins, peptides or glycoproteins (~5–20 kDa) which are secreted or remain bound on cell surface. Cytokines include interferon, interleukin, chemokines, lymphokines and tumor necrosis factor. Cytokines are produced by immune cells such as macrophages, B lymphocytes, T lymphocytes and mast cells and other cells, including immune cells as well as endothelial cells, fibroblasts and various stromal cells. They regulate differentiation,

growth and activation of immune cells and act as cell signalling molecules to help communication between cells in case of immune responses and thereby stimulate the mobility of cells towards sites of infection and inflammation.

Examples of cytokines are interferon (IFN) and interleukin (IL) (Dranoff G, 2004 & Ananya, 2015). There are different types of cytokines produced in tumor microenvironment and play vital role in cancer pathogenesis. They can be crucial in inhibiting progress and development of cancer, therefore an improved cancer immunotherapy is attributed to cytokine-tumor cell interaction (Dranoff G, 2004). As the cytokines present in the microenvironment of cancer cells makes up immunity, therefore therapeutic intervention in this surrounding can be strategized for cancer immunotherapy. There has been plethora of cytokines investigated in cancer therapy. IFN- α and IL-2 are approved by FDA while IL-3, IL-4, IL-6 IL-7, IL-10 are in different phases of clinical trial. Denileukin diftitox is a cytotoxic protein derived from recombinant DNA and consists of diphtheria toxin fragments A and B and the full-length IL-2 molecule. Upon administration it inhibits protein synthesis and kill the cells in very short time (Mahnke et al, 2007). Cancer immunotherapies through inducing the sensitivity of cancer cells to apoptosis have been well studied. Histone deacetylase (HDACs) is involved in regulation of cellular functions such as production of oncoproteins viz, PML-RAR or AML1-ETO, tumor suppression by p53 gene. Inhibiting HDACs could result in antitumor activity and thereby HDACIs (Histone deacetylase inhibitors) can be used in cancer treatment. HDACIs have shown antitumor activity through inducing apoptosis of leukemic cells by suppressing expression of oncogenes and activating death receptor pathway (TRAIL) which is tumor necrosis factor inducing ligand receptor, expressed by tumor cells (Insinga et al, 2005). It is suggested that a synergistic anticancer therapy can be achieved by combining apoptosis induction and other vaccination and targeted therapy approaches (Baxevanis et al, 2009).

3. Photoimmunotherapy

Conventional cancer treatment strategies include chemotherapy, radiotherapy, surgery, small molecule based therapy and immunotherapy as well as a combination of them is practiced. Chemotherapy shows systemic side effect and surgery is associated with high rate of recurrence. Treatment using radiation is restricted to limited dose. Advancement in search of a safe potent and cost effective cancer

treatment led to emergence of immunotherapy and photodynamic therapy. A combination of both is promising for a safe, effective and potential mode of treatment. Photoimmunotherapy (PIT) is a cancer therapy involve light and body immune cells such as antibodies, was first developed at National Cancer Institute, Bethesda, Maryland, USA (Mitsunaga et al, 2011). It is a novel type of molecular-targeted cancer therapy in which selective destruction of cancer cells is possible without damaging to normal tissues.

Conventional PDT makes use of a photosensitizer which can be activated by a non-ionizing light to kill cancer cells but these photosensitizers are non-specific. Upon exposure of photosensitizers to light of suitable wavelength, reactive oxygen species (ROS) are produced which rapidly destroy surrounding cells (Park, 2007). However, due to non-specificity of these photosensitizers, they are also taken up by not-to-be-targeted (normal) cells and results in serious side effects.

PIT treatment is aimed at circumventing these collateral phototoxic effects by creation of a targeted-photosensitizer. PIT-delivery system consists of two integral parts: a non-targeted photosensitizer and a monoclonal antibody (MCA) which identifies and binds with antigen proteins on the surface of cancer cells. Upon administration into body, MCAs with photosensitizers recognize and selectively access to cancer cells, avoid targeting to normal tissues and then upon exposure to light, they kill the cancer cells (Mitsunaga et al, 2017).

The research group at Professor Kobayashi's lab have coupled a phthalocyanine derivative, IRDye 700DX to antibodies targeting human epidermal growth factor receptors expressed on tumor cells and photosensitizer dye which was activated by near-infrared (NIR) light. IRDye 700DX was chosen for its hydrophilicity and strong cytotoxicity induced upon association with the cellular membrane and subsequent activation (Mitsunaga et al, 2017).

A variety of cancers, such as breast and pancreatic cancers over-express epidermal growth factor receptors (McKeage et al, 2002). This new photosensitizing compound utilizing IRDye 700DX NHS Ester was referred to as "mAb-IR700 conjugates". In vitro studies showed that mAb-IR700 killed tumor cells post exposure to the near-infrared

light irradiation. A positive correlation between the intensity of excitation light and percentage of cell death was observed. Infrared light alone or mAb-IR700 conjugate alone could not damage any normal cell. When tumor-xenografted mice were treated with combination of mAb-IR700 and near-infrared light, tumor shrinkage was observed. With administration of mAb-IR700 conjugate in part followed by repeated NIR light exposure, 80% tumor was destroyed to significantly prolong survival of mice (Mitsunaga et al, 2011). Current hypothesis reveals that PIT derived cellular toxicity is caused by rapid expansion of local water upon the formation of holes in the membrane.

Emission of fluorescence light upon activation during PIT using mAb-IR700 conjugate was also a required characteristic. Therefore before PIT, a lower dose of mAb-IR700 can be administered for guidance of excitation light application to targeted tumor tissues which minimizes unnecessary light exposure to collateral tissues.

As PIT is an emerging and promising selective cancer therapeutic strategy for treatment of mAb-binding cancer with minimal off-targeting. Having clinical feasibility, future direction is focused on conjugating a variety of other MCAs to photosensitizers such as phthalocyanine. As in PIT antibodies are armed with photosensitizers to get photoimmunotherapy, we had used T lymphocytes (having cancer cell receptor) model (Jurkat cells) for selective targeting of A549 lung carcinoma cell line creating a delivery system for PIT consists of T lymphocytes and polymeric photosensitizers.

4. Photosensitizer

Photosensitizers are those chemical compounds which undergo a photochemical or photophysical alteration on molecular level due to initial absorption of radiation without involvement in any chemical reaction (<http://goldbook.iupac.org/P04652.html>). An ideal photosensitizer for photodynamic therapy of cancer is capable to localize specifically in neoplastic tissues, accumulates for optimum period in tumor and possess short half-life for rapid clearance. When it is activated at desired wavelength, shows optimal penetration into tissues, possess high quantum yield to generate singlet oxygen and deprived of dark toxicity and should be chemically pure.

One of the most important characteristics of photosensitizer in cancer immunotherapy is its ability to localise in tumor which is based on the physicochemical properties of a photosensitizer. To the best of our knowledge, only animal studies have been done so far to determine the tumor:normal tissue ratio which gives insight of extent of tumor localisation of a photosensitizer against its distribution into normal tissues. Therefore, photosensitizers are classified here based on their tumor localising property (Table.2).

Table 2: Classification of photosensitizers

Photosensitizers	Examples
<p><i>Hydrophilic compounds:</i> They bind to albumin and globulin</p>	<p>Tri and tetrasulphonated derivatives of tetraphenylporphine (TPPS3, TPPS4) and chloroaluminum phthalocyanine (CIAPCS3, CIAPCS4)</p>
<p><i>Amphiphilic compounds:</i> They penetrate into outer layer of lipoprotein</p>	<p>- Benzoporphyrine derivative monoacid (BPD) - Lutetium texaphyrine (LuTex) - Monoaspartyl chlorin (e6) (MACE) which partition between high density lipoprotein (HDL) and albumin</p>
<p><i>Hydrophobic compounds:</i> They permeate into inner lipid core of lipoprotein notably low density lipoprotein (LDL) and, also high density lipoprotein (HDL) and very low density lipoprotein (VLDL). They require vehicles like liposomes, Tween 80 or cremophor-EL which help to solubilize them</p>	<p>- Unsubstituted phthalocyanines (ZnPC, CIAIPC) - Naphthalocyanins (isoBOSINC) - tinetiopurpurin (SnET2)</p>

As after administration of photosensitizer for anticancer therapy, tumor targeting out of other normal cells is highly desirable therefore tumour localisation of photosensitizer is one of the most important characteristics of photosensitizer in cancer immunotherapy.

Only animal studies have been done so far to determine the tumor:normal tissue ratio. Tumor localisation ability of a photosensitizer is based on the physicochemical properties of a photosensitizer which governs their binding to proteins (albumin, globulin), other heavy proteins and lipids of different densities. Thus, photosensitizers, based on their tumor localising ability are classified (Castano et al, 2005).

Photosensitizers are also classified based on presence of porphyrine moiety in their chemical structure and then further subclassified into first, second and third generations.

The first generation photosensitizers are hematoporphyrine, hematoporphyrine derivative and Photofrin. Hematoporphyrine was first found to possess very powerful photosensitization property and well accumulated in tumor (Meyer-Betz, 1913). However, its derivatives had shown better tumor localisation (Figge et al, 1948). Later hematoporphyrine derivatives were further purified to isolate Photofrin which is still in clinical use (Lipson et al, 1961).

Second generation PS were evolved to overcome limitations associated with first generation PS i.e. hematoporphyrine derivatives and Photofrin. Activation at 630nm where limited penetration beyond 5mm resulting in no effective treatment of lesions and accumulation in cutaneous layer leads to prolong cutaneous toxicity up to 6 weeks and these PS contains impurities too (Wohrle et al, 1998, Nayak, 2005). Thus, second generation photosensitizers were developed which could successfully circumvent above mentioned problems, they are phthalocyanins, naphthalocyanins, benzoporphyrins, chlorins, purpurins, texaphyrins, porphycens, pheophorbides, bacteriochlorins. These compounds can produce singlet oxygen effectively, have high range of absorbance wavelength i.e. 650-850 nm, give a short length photosensitivity and are free from impurities as reviewed by Juzeniene et al (Juzeniene et al, 2007). Some second generation photosensitizers like Foscan[®] containing mTHPC (Biolitec AG), Visudyne[®] containing verteporfin (Novartis AG) are used in clinical practice. Upto

second generation of photosensitizers, clinical application is evident; however an advancement to next generation of photosensitizers can be achieved by intervention of novel carriers system or antibodies. When second generation PS are linked to nanocarriers, liposomes or antibodies then they are called as third generation photosensitizer. Currently these photosensitizers are widely exploited in research (Juzeniene et al, 2007).

5. Drug (mTHPP) Profile

5.1. Description

mTHPP occurs as dark violet fluffy powder, practically odourless. It is stored in amber coloured glass bottle.

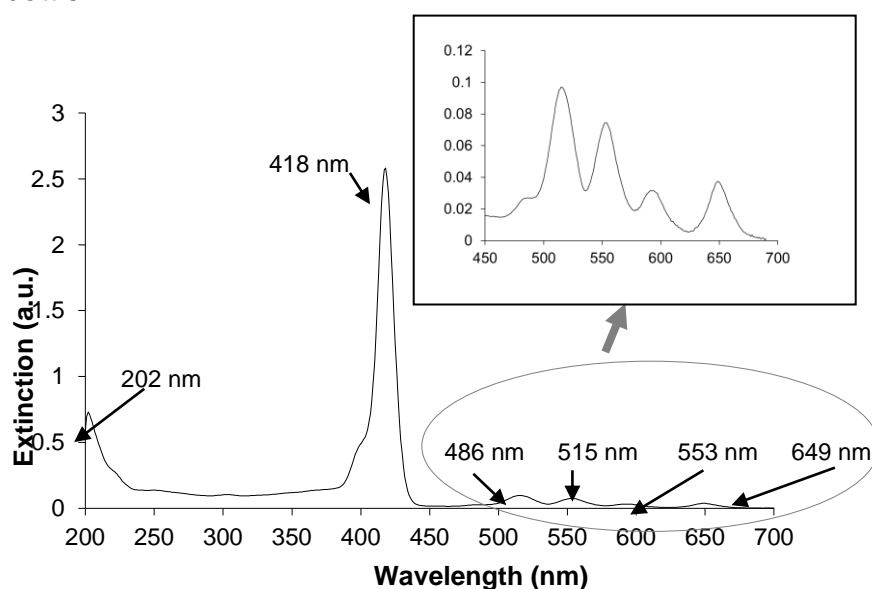


Fig. 5: UV spectrum of mTHPP in EtOH (3µg/mL)

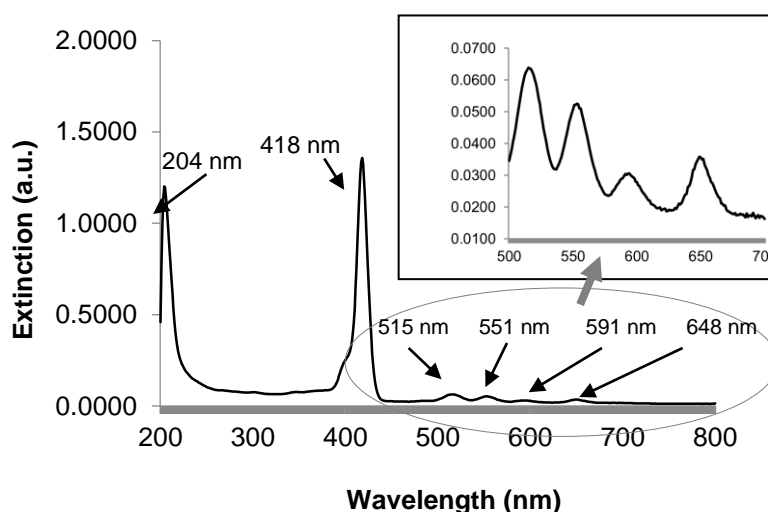


Fig. 6: UV spectrum of mTHPP in isopropanol (2µg/mL)

5.2. Spectral properties

mTHPP shows prominent UV spectrum in solvents such as ethanol and isopropanol. Alcoholic solutions viz, ethanolic solution of mTHPP (3 μ g/mL) and isopropanolic solution of mTHPP (2 μ g/mL) shows peaks at 418nm (Fig.5 & 6).

5.3. Solubility

mTHPP is practically insoluble in water and freely soluble in ethanol, isopropanol and ethyl acetate.

5.4. Chemical structure

mTHPP is a porphyrine compound. It contains a parent porphine ring which is substituted at all four carbons of exocyclic double bond each by the meta carbon of phenolic ring. Overall mTHPP contains four double bonds, four pyrrole rings in the centre and four benzene rings which enrich mTHPP with plethora of mobile electron for excitation. The presence of double bonds and lone pairs of electron make it an ideal candidate for complexation with other entities having similar chemical features.

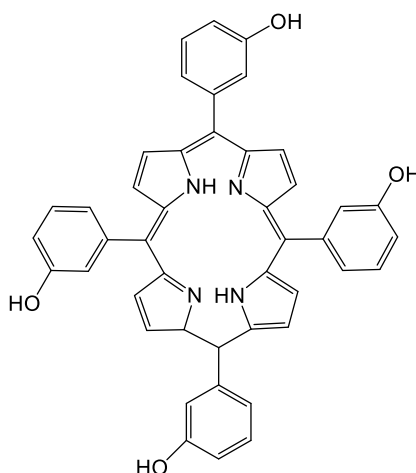


Fig. 7: Chemical structure of mTHPP; Mw: 680

5.5. Mechanism of action

The mechanism of action of mTHPP is similar to any other photosensitizer used in photodynamic therapy to kill cancerous cells. Infact mTHPP is inert in absence of light until activated by light to exhibit cytotoxic effect. Upon administration of mTHPP compound, it selectively accumulates in the target cells. Then it destroys the lesion

with laser light at 425nm or 649nm. Later wavelength is generally used in clinical practice for mTHPC. Interestingly, light and mTHPP are individually non-toxic but the combination of both elements in the presence of oxygen selectively destroys the target tissue (Lukšienė et al, 2003). Excitation of mTHPP followed by emission of fluorescent light along with production of radical oxygen species leading to antiproliferative effect is previously described under photodynamic therapy.

5.6. Side effects

Apart from killing cancer cells, mTHPP can kill the surrounding normal cells.

6. Polystyrene sulphonate (PSS)

Polystyrene sulfonates are polymers derived from polystyrene containing sulfonic acid or sulfonate functional groups. The crosslinked material (called a resin) does not dissolve in water and typically appears amber colored but the linear polymer which is Ca^{++} and Na^+ salts appear white when very pure and is water-soluble. PSS is insoluble in organic solvent like ethanol, ethyl acetate. Salts are used as Ca^{++} and Na^+ replenisher upon oral delivery (Dardel et al, 2008).

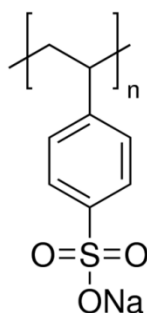


Fig. 8: Chemical structure of polystyrene sulphonate sodium

These polymers are classified as polysalts and ionomers. The fluorescein tagged PSS appears dark yellow fluppy powder, practically odourless.

7. Kollidone® (Polyvinyl pyrrolidone/PVP)

Kollidone® is chemically Polyvinylpyrrolidone. It is a widely used synthetic excipient in pharmaceutical and cosmetic industries. There are four different grades of Kollidone®; Soluble Kollidone® (povidone) grades, Insoluble Kollidone® (crospovidone) grades,

Kollidone® VA64 grades (copovidone) and Kollidone® SR. Initially W. Reppe at BASF (the chemical company), had synthesized soluble Kollidone® (povidone) grades which was later on followed by synthesis of other insoluble grades and now has become one of the most important pharmaceutical and cosmetic excipient.

As a matter of fact all grades are based on water soluble polyvinylpyrrolidone which are further chemically modified to synthesize other grades of Kollidone®. A physical cross linking process of vinylpyrrolidone results in insoluble grades of Kollidone® while water soluble co-polymerisation of vinylpyrrolidone and vinyl acetate forms Kollidone® VA 64 or copovidone. A mixture of polyvinyl acetate and povidone (8:2) is available on the market with the tradename of Kollidone®SR for sustained release purposes.

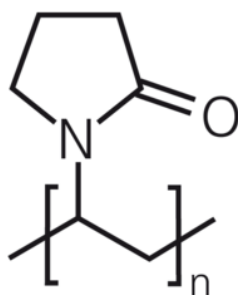


Fig. 9: Chemical structure of Polyvinylpyrrolidone

Considering the design of mTHPP nanaocomplex using PVP, we had used water soluble Kollidone® grades or povidone. The soluble PVP is obtained by radical polymerization of vinylpyrrolidone in water or 2-propanaol. There are six grades of soluble Kollidone® viz, 12PF, 17FP, 25, 30 and 90F among which first two are endotoxin free. Kollidon® 25 was used in the PhD project for synthesis of PVP-mTHPP nanocomplex.

7.1. Kollidone® 25

Kollidone® 25 or PVP or polyvidone or povidone, is a water-soluble polymer consists of monomer *N*-vinylpyrrolidone. It is amorphous and appears as white free flowing powder, tasteless and has faint ammonia like odour. PVP is more than 10% soluble in water, methanol, ethanol, diethylene glycol, propylene glycol, glycerol and less than 1% soluble in ethyl acetate, diethyl ether and liquid paraffin. It is officially included in

Pharmacopoeias of Europe, USA and Japan. All pharmacopoeias have described K value for each soluble Kollidone[®] based on the relative viscosity in water and molecular weight of PVP. The K value of Kollidone[®] 25 is 22.5 to 27.0. It is non-toxic, biodegradable and a good complexing agent and used as a soluble carrier for proteins (von Specht et al, 1973). Its good complexation ability is attributed to the presence of lone pair of electrons on N and O atoms of lactam unit and active binding sites for hydrogen donors (Rothschild et al, 1972). PVP is used as a plasma volume expander (Motiff et al, 1975) and due to its property of binding with certain drugs, dyes and toxins acts as a carrier to eliminate toxins and retard drugs.

PVP has also been explored for designing drug delivery and medical devices. Taxol is a novel antitumor alkaloid possessing anti tumor activity against several types of tumours. Using PVP, a novel polymer based Taxol nanoparticulate formulation was prepared by reverse microemulsion method. These 50-60 nm particles were evaluated in B16F10 murine melanoma transplanted in C57B1/6 mice (Sharma et al, 1996). Water-soluble macromolecules such as FITC–dextran (FITC–Dx)-encapsulating injectable hydrogel polymeric nanoparticles of polyvinylpyrrolidone cross-linked with *N,N'*-methylene bis-acrylamide were prepared as a reverse micellar droplets. This revealed PVP as a potential carrier for hydrophilic drug too (Bharali et al, 2003).

7.2. Polyvinylpyrrolidone as a complexing agent

Polyvinylpyrrolidone holds an excellent candidature of complexing agent and has been widely used because of its complexation attribute in designing biosensors and drug delivery purposes. Povidone-Iodine is a commonly known complex of antiseptic iodine and PVP. This complex reduces toxicity and obliterating the staining property of iodine while keeping up antiseptic activity of iodine intact (USP). Biosensors for detection of glucose level in diabetes make use of PVP alongwith graphene, nickel and Chitosan (Saroj et al, 2013).

8. Chitosan hydrochloride (Protasan[®])

Chitosan is a linear polysaccharide composed of randomly distributed β -(1-4)-linked D-glucosamine (deacetylated unit) and N-acetyl-D-glucosamine (acetylated unit). It is made by treating shrimp and other crustacean shells with the alkali sodium hydroxide. Chitosan is available in various grades for biomedical applications.

Protasan[®] is a brand of Chitosan hydrochloride which is available in different molecular weights. PROTASAN[®] is a Chitosan in which > 90 percent of the acetyl groups are removed. The polymer with cationic head is a highly purified and well-characterized water-soluble chloride salt. The functional properties are described by the molecular weight and the degree of deacetylation. The average molecular weight for PROTASAN[®] is 100,000 g/mol range (measured as a Chitosan hydrochloride). The ultra-low levels of endotoxins and proteins allow for a big variety of in vitro and in vivo applications.

Chitosan has a number of commercial and biomedical applications. A novel drug delivery systems based on Chitosan nanoparticles containing aminolevulinic acid derivatives such as prodrug (5-ALA and its ester derivative 8-ALA) were developed, characterized and evaluated for the in vitro cytotoxic activity. Further the synergistic effect of combined classical PDT and electrochemotherapy, were investigated in treatment of cutaneous neoplasms (Ferreira et al, 2013). Tamoxifen is a broad spectrum drug with limited clinical application. The smart pH-responsive drug delivery system based on Chitosan nanoparticles for controlled release Tamoxifen was developed. Tamoxifen loading into Chitosan nanoparticles and its release at pH 7.4 (tumor microenvironment pH) has shown improved anticancer activity in human breast cancer MCF-7 cells (Vivek et al, 2013).

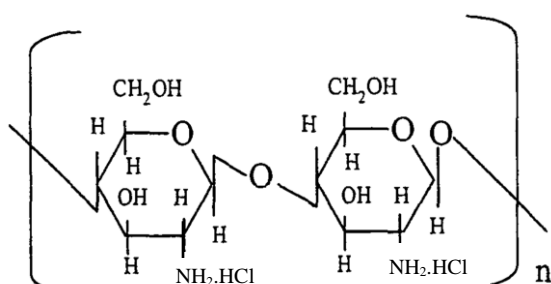


Fig. 10: Chemical structure of Protasan[®] (Chitosan hydrochloride)

D. INTRODUCTION

Last few decades have witnessed a phenomenal advancement in science and technology which led nanotechnology to emerge as a versatile field in delivering plethora of drug molecules for therapeutic purpose. Nanoparticulate delivery systems have been widely investigated in designing treatment strategies and circumventing associated toxicities and side effects of drug molecules. Different treatment strategies for major diseases like cancer, tuberculosis, diabetes etc. have been extensively improved by designing nanoparticles of drug molecules and toxicity associated with drug molecules were reduced. Wu et al, have designed PLGA/HPMCP nanoparticles for oral delivery of insulin and investigated its antidiabetic potential (Wu et al 2012). Kumar and co-workers have reduced the toxicity issues associated with amphotericin B (Italia et al, 2009) and cyclosporin A (Italia et al, 2007) in parallel to enhancement in oral bioavailability and solving biopharmaceutical hurdles arise from high molecular weight and low aqueous solubility. Schneider and co-workers have formulated nanoparticles of several drug molecules for improved therapy including cancer. Recently, tetranidine loaded poly-dl-lactide-co-glycolide (PLGA) nanoparticles (Schi et al, 2015), idarubicin encapsulated PLGA and maleate polyester-polymer nanocomplexes (Blaudszun et al, 2015) were designed and their anticancer potential was investigated against cancer cell lines. A drug multilayer based nanocarrier consists of Gold nanoparticle core multiple times layered by the polymeric nanocomplex of the model photosensitizer drug 5,10,15,20-Tetrakis (3-hydroxyphenyl) porphyrine or mTHPP for photodynamic therapy of cancer (Reum et al, 2010).

All chemotherapies of cancer practiced nowadays are associated with severe side effects; therefore amount of drug used in anticancer treatment must be minimised. However, this leads to a non effective therapy due to sub-therapeutic dose of drug reaching to tumor tissues. Moreover, selective accessibility of anticancer drug to cancer cells is also challenging. This limitation of existing cancer chemotherapy has suggested the growing need of an effective delivery system which can be fulfilled through interdisciplinary research of engineering, pharmaceutical science and molecular biology. Advent of nanoparticles in advanced drug delivery is very promising to overcome the limitations of existing cancer chemotherapy (Bechet et al, 2008). Different nanocarriers such as polymeric nanoparticles, liposomes and micelles have

been introduced to modulate the pharmacokinetics of conventional chemotherapeutics (Khan et al, 2010). These nanocarriers are associated with many advantages such as they are internalized into cells without recognition from efflux mechanism e.g. p-glycoprotein which enhances intracellular concentration of drugs (Cho et al, 2008). One of the main advantages is that it facilitates transport of hydrophobic drugs in the body without aggregation and loss of drug activity. When coated with poly (ethylene glycol), blood circulation time increases leading to enhanced tumor tissues accumulation by Enhanced permeation and retention (EPR) effect (Matsumura and Maeda, 1986; Duncan et al 2003). Further, the immunogenicity is minimized and resistant to microbial attack is acquired (Bechet et al 2008 & Chatterjee et al 2008).

Among several nanocarriers in anticancer therapy, Doxil[®] is clinically approved as well as PEGylated liposome based formulation (Gabizon et al, 2001). These PEG-lipids make hydrophilic corona in micelles which allows micellar based delivery system for longer time circulation in blood (Blanco et al, 2009). While the PEG moiety helps accumulation of drug at tumor site, a steric hindrance between cancer cells and nanocarrier appears which reduces tumor cell uptake (Gabizon, 2001 & Hatakeyama et al, 2007). Mixed micelles of monoclonal antibody (MCA) 2C5-DSPE-polyethylene glycol and polyhistidine-polyethylene glycol incorporating paclitaxal were synthesised for an improved anticancer efficacy by enhancing specific internalization into tumor cells through endocytosis mediated by antibody and drug release triggered by lower pH of endosome (Wu et al, 2013).

During angiogenesis, the defective pores are formed on vasculatures innervating cancer cells. Small size nanocarriers ($\leq 100\text{nm}$) extravagate through these pores from blood circulation to the tumor cells (Maeda et al, 2000). DaunoXome is a liposomal formulation of Daunorubicin which is a cytostatic agent in treatment of cancer- Kaposi sarcoma (Torchilin, 2007), or ovarian and recurrent breast cancer (Wang et al, 2008). Some other liposomal-based formulations are CPX-1 and LE-SN38 which contains a topoisomerase I inhibitor in colorectal cancer or colon cancer therapy. At present, they are in Phase-II clinical trials (Kraut et al, 2005; Batist et al, 2009). Polymers such as poly-DL-lactide-co-glycolide (PLGA) which is approved by US FDA, has also been widely explored due to its biocompatibility and biodegradability. Vincristin and

verapamil co-loaded PLGA nanoparticles were synthesised to get enhanced efficacy and reduced toxicity against multidrug resistant breast cancer (Chen et al, 2014).

Though nanocarrier based drug delivery system in cancer therapy appear promising, it faces several obstacles in effective delivery of drug to tumor tissues such as transfer of drug from its 'nanohoming' to cancerous cells at tumor site is very difficult. It might be possible that the lethal dose of drug does not reach to the tumor tissues resulting in a non-effective killing of cancer cells. In addition, these nanocarriers are prone to opsonisation during circulation and thereby less amount of delivery system reaches to cancer cells within tumor site (Gabizon et al, 2001; Photos et al., 2003).

These limitations of nanocarriers for anticancer therapy can be very well circumvented by designing Immune cell based delivery systems which are one of the advanced drug-delivery systems used in cancer immunotherapy. In brief they are made by first internalizing anticancer macromolecules or nanomaterials into immune cells and then to target cancer cells.

In addition, 5,10,15,20-Tetrakis (3-hydroxyphenyl) porphyrine or mTHPP which is the model drug of anticancer agent 5,10,15,20-Tetrakis (3-hydroxyphenyl) chlorin (mTHPC) is suffering from physiological and biopharmaceutical problems due to accumulation in tissue after delivery and poor solubility in water during formulation development.

Considering the problems associated with mTHPP, adeptness of autoimmune machinery in attacking cancer cells, we had proposed to design mTHPP nanocomplex loaded T lymphocyte for an effective and safe immune cell based delivery system for cancer immunotherapy. Precisely, complexation of mTHPP with water soluble polymers viz, polystyrene sulphonate, polyvinyl pyrrolidone and chitosan produces water soluble mTHPP-polymer nanocomplex which is internalised into Jurkat cells (model T cells) to develop immune cell based delivery system. Upon injecting this immune cell based delivery system into blood; they identify and target cancer cells.

E. MATERIALS AND EQUIPMENT

1. Materials

Table 3: List of materials or chemicals used in the experiments

Materials/Chemicals	Specifications/Grade	Supplier
mTHPP	-	Sigma Aldrich
PSS Na	4300 Da	Sigma Aldrich
PVP	31000 Da, Kollidone [®] 125;	BASF
Chitosan HCl	100,000 Da, Protasan [®]	Sigma Aldrich
Purified water	MilliQ	Stibel Eltron Comfort
Ethanol (<99% pure)	HPLC grade	Sigma Aldrich
Isopropanol	Spectrophotometric grade	Sigma Aldrich
Jurkat cells	Human lukaemic blood T-lymphocytes	Sigma Aldrich
A549 cells	Human lung carcinoma cells	Sigma Aldrich
RPMI medium	-	Sigma Aldrich
EBSS	-	Sigma Aldrich
DMEM	-	Sigma Aldrich
Trypsin EDTA	-	Sigma Aldrich
Water	Purified water	Inhouse facility
FluorSave [™]	-	Merck Millipore

2. Equipment

Table 4: List of equipment used in the experiments

Equipment	Supplier
Centrifuge	Thermoscientific [®]
Vortex	Lab Dancer [®]
Clean bench	Labguard class II biological safety cabinet
Filter	0.22µm Merk Millipore [®]
Incubator-cum-shaker	IKA [®] KS 4000
Electroporator	BIORAD Gene Pulsor [™]
Electroporation cuvette	0.4cm, Sigma Aldrich [®]
Micropipette	Metler Toledo [®]
AFM	JPK [®]
Light microscope	Nikon TMS [®]
Water purifier	Stibel Eltron Comfort [®]
UV spectrophotometer	Multiscan Go, Thermosceintific [®]
Fluorescence spectrophotometer	Fluo Star Optima [®] (Optima control software)
Atomic force microscope	JPK [®]
Confocal laser scanning microscope	- DMI6000 Leica [®] TCS SP5 - LSM880 Zeiss [®]
Autoclave	Stansautoclave Systec [®] VX-95
Weighing balance	Pioneer [™] OHAUS
Magnetic rotor-cum-heater	CAT [®] MCS66

Chemical structure drawing Chem Bio Draw Ultra 4.0
software

LED (Laser emitting diode) Lumundus Eisenach[®] GmbH

F. EXPERIMENTAL

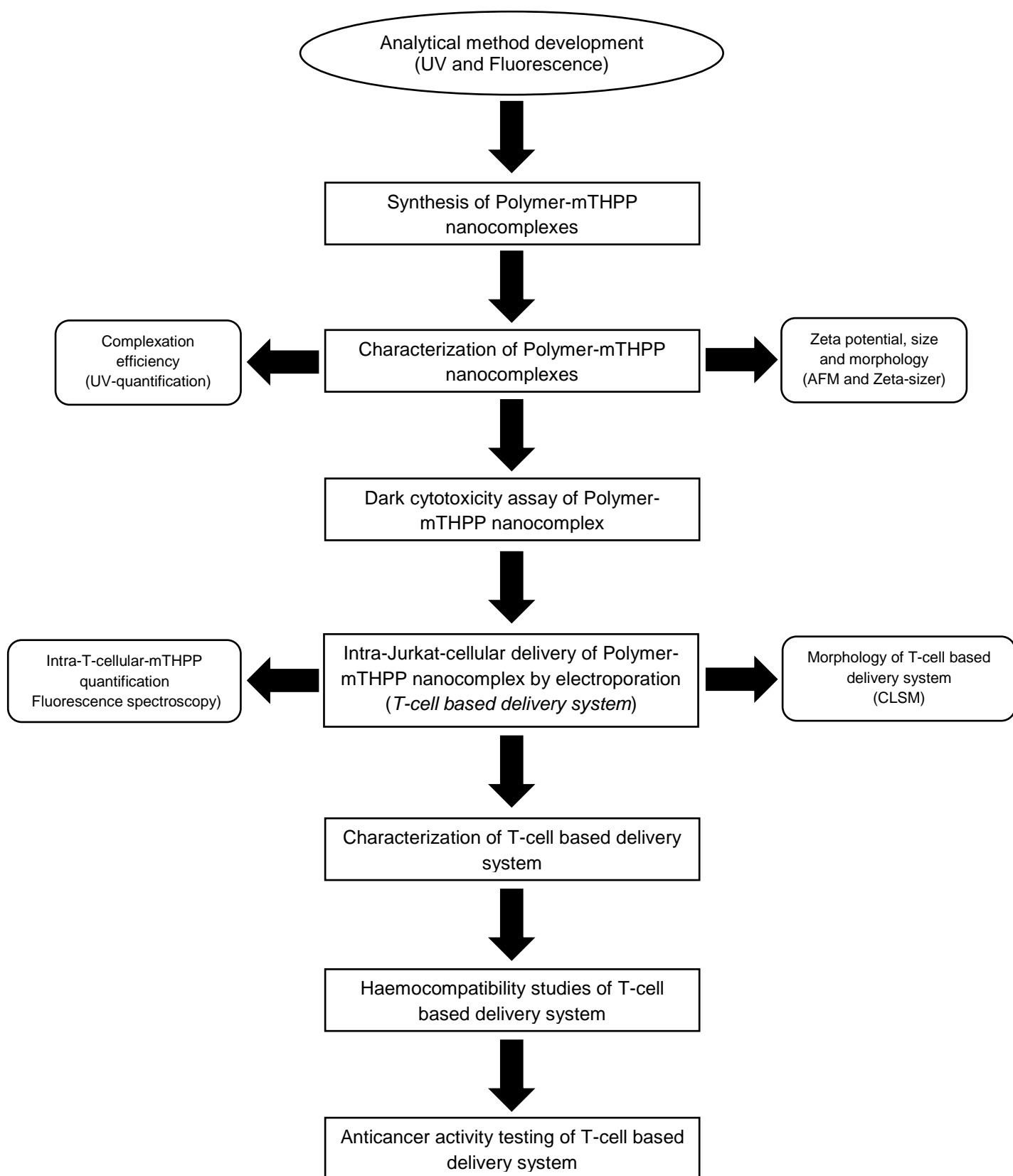


Fig. 11: Experimental design of PhD work

1. Analytical method development by UV and fluorescence spectroscopies

UV-analytical method for mTHPP was developed in ethanol and isopropanol for quantification of mTHPP and determination of complexation efficiency (CE) of each nanocomplex. An analytical method by fluorescence spectroscopy was also developed for quantification of mTHPP present intracellular as a complex with polymer.

1.1. UV spectroscopy of mTHPP in ethanol and isopropanol (IPA)

mTHPP was weighed and dissolved in ethanol and isopropanol to produce 500 µg/mL alcoholic (EtOH and IPA) solutions of mTHPP. First, the blank (ethanol and IPA) was scanned between 200-800 nm range for the baseline and then 3 µg/mL ethanolic and 2 µg/mL isopropanolic solutions of mTHPP were scanned to get the UV spectrums of mTHPP (Fig.5 & 6). Then, the absorbance of all solutions in calibration curve was measured at $\lambda_{\text{max}}=418\text{nm}$. Both alcoholic solutions of mTHPP (500 µg/mL) were serially diluted (1:10) to produce a range of concentration between 500 to 0.05 µg/mL and curves (Extinction v/s Concentration) (Fig.11) was made. In view of Beer Lambert's law, a serial dilution (1:1) was made between 50 to 0.20 µg/mL and a linear curve was extracted from absorbance values ≤ 1.4 .

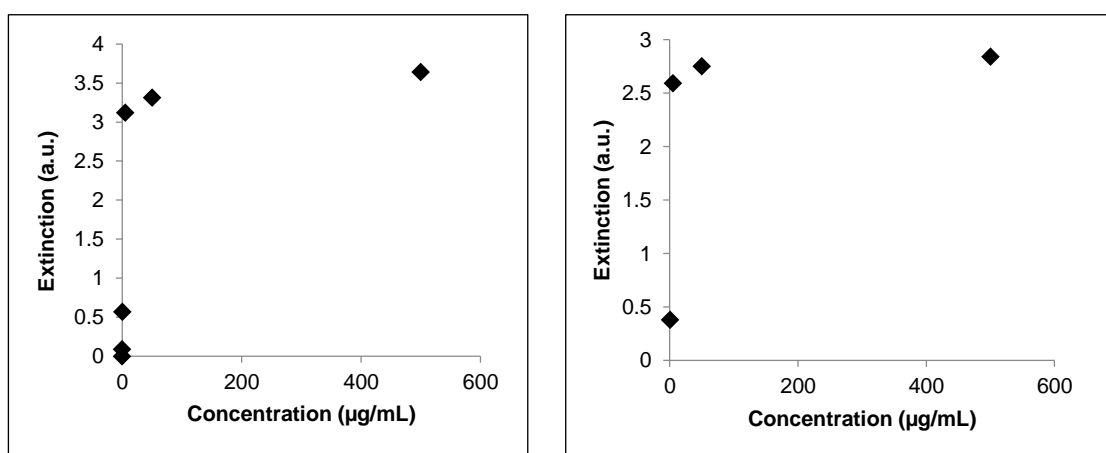


Fig.12: Calibration curve of mTHPP (500 to 0.05 µg/mL)
a) mTHPP in EtOH (L) & b) mTHPP in IPA (R)

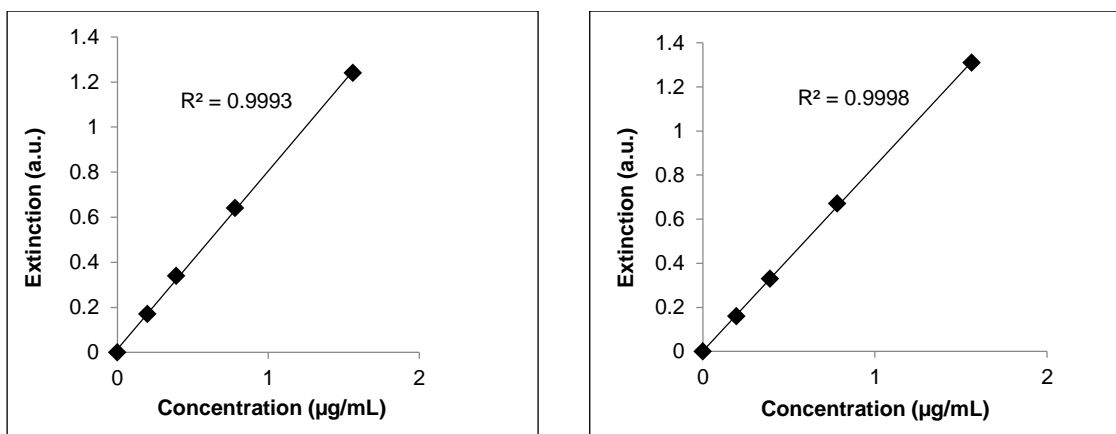


Fig.13: UV-calibration curve of mTHPP in EtOH (L) and mTHPP in IPA (R)

Finally, a standard curve (Extinction v/s Concentration) was made between concentration range 1.56 to 0.20 $\mu\text{g/mL}$ (Fig.13). This calibration curve shows a linear relationship between absorbance and concentration ($R^2 = 0.9993$ for mTHPP in EtOH and $R^2 = 0.9998$ for mTHPP in IPA).

1.2. Fluorescence spectroscopy of mTHPP in ethanol and isopropanol

As mTHPP is well extractable from its nanocomplexes in ethanol (mTHPP-PSS and mTHPP-PVP NCs) and in isopropanol (mTHPP-Chitosan), a calibration curve in ethanol and isopropanol (with 2% TritonX 100) was made by fluorescence spectroscopy.

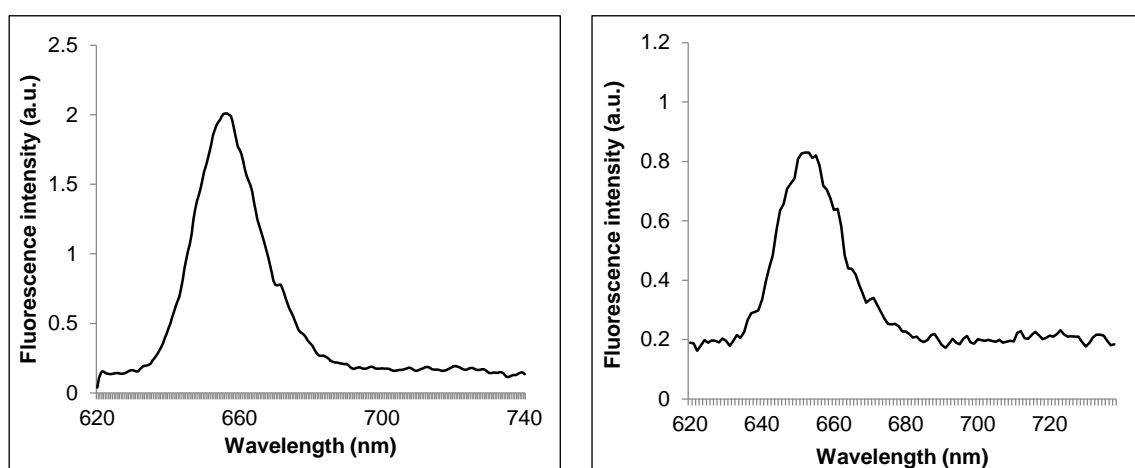


Fig.14: Fluorescence spectra of mTHPP upon excitation at $\lambda_{\text{exc}} = 405 \text{ nm}$
(L) EtOH ($\lambda_{\text{em}} = 656$) and (R) in IPA ($\lambda_{\text{em}} = 653$)

During extraction of mTHPP from intracellular NC, Triton X100 is used as cell lysing agent; therefore calibration curve was made in presence of 2% Triton X100. First the fluorescence spectrums of mTHPP in ethanol and isopropanol were obtained.

mTHPP was weighed and individually dissolved in pure ethanol and pure isopropanol to produce 250 μ g/mL solution. These solutions were serially diluted as 1:1 in light protected 96 well plates. Fluorescence emission was measured at λ_{exc} = 415 nm and at λ_{em} = 670 nm against blank ethanol and isopropanol. A standard curve was made between 7.81-250ng/mL (mTHPP in EtOH) with R^2 =0.9994 and 15.63-250ng/mL (mTHPP in IPA) with R^2 = 0.9989 (Fig.15).

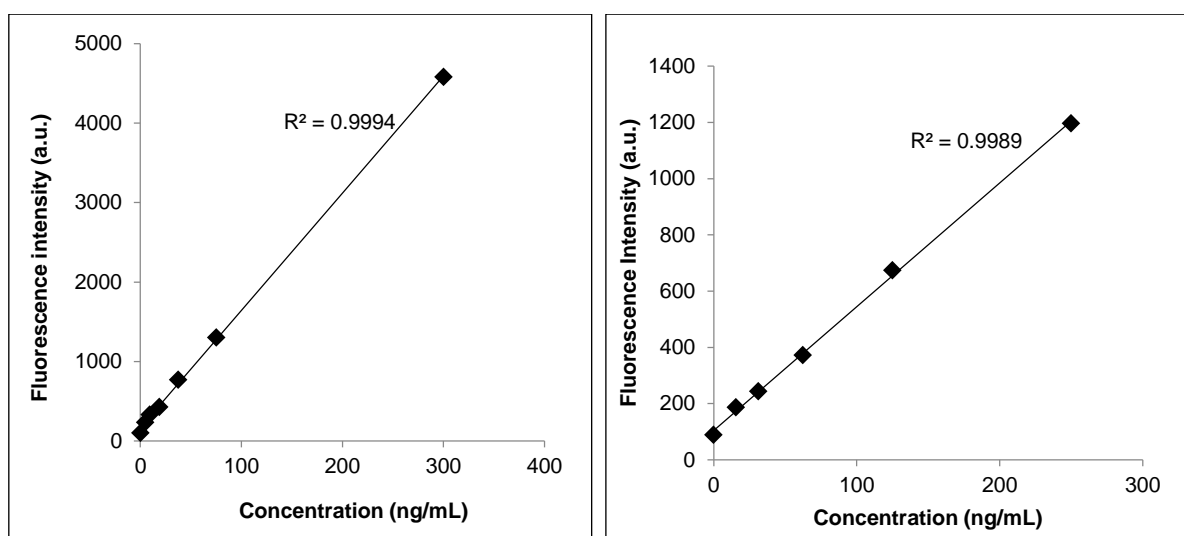


Fig.15: Fluorescence calibration curve of mTHPP in EtOH (L) and mTHPP in IPA (R)

2. Development of mTHPP- Polymer loaded Jurkat cell based delivery system

2.1. Synthesis of mTHPP-Polymer NCs

Three polymers viz, Polystyrene sulphonate-Na (4.3kDa, Sigma Aldrich), Polyvinylpyrrolidone/Kollidone[®]125 (31kDa, BASF) and Chitosan-HCl/Protasan[®] (100kDa, Sigma Aldrich) were used to synthesize the PNCs with mTHPP (680Da, Sigma Aldrich). Each polymer (15mg) was weighed and individually dissolved in 4mL purified MiliQ water (Stibel Eltron Comfort) and mTHPP (10mg) was weighed and dissolved in 4mL ethanol (>99% pure, Sigma Aldrich) for each aqueous polymeric solution. Aqueous solution of polymer was added to the ethanolic solution of mTHPP

to get a hydroalcoholic mixture. It was thoroughly mixed by vortex for 2 minutes to ensure complete interaction between polymer and mTHPP. The mixture was then kept at -80°C over 30 minutes for prefreezing. The frozen hydroalcoholic mixture was freeze dried over 24hr. The samples in 50mL tube were completely covered by aluminium foil to avoid exposure to light and small pores were made on the top to allow escape of sublimed ethanol and water during freeze drying. Sufficient quantity of water was added to freeze dried samples and stirred thoroughly on vortex (Labdancer®) followed by centrifugation (Thermoscientific®) over 3 minutes at 2500rcf. Supernatant was taken out by micropipette and filtered through polycarbonate filter (0.22µm pores, Merk Sigma Aldrich®) under vacuum. Water was again added in 50mL tube, followed by vortex, centrifugation and filtration; the procedure was repeated thrice. The filtration resulted in separation of aqueous solution of PNC as a filtrate and free mTHPP as a residue on the filter. More water was added thoroughly on filter to dissolve out any PNC adsorbed on mTHPP or filter. During the experiment care was taken to avoid exposure to sunlight by covering with aluminium foil or using light resistant apparatus. PNCs prepared by above method were taken for quantification of complexed mTHPP by UV (Multiscan GO, Thermoscientific®) analytical method.

2.2. Preparation of PNC loaded JC based delivery system

Sub-toxic concentrations of mTHPP-PSS NC, mTHPP-PVP NC and mTHPP-Chitosan NC for JC were determined by MTT assay. Jurkat Cell (Capricon Scientific®) suspensions (20×10^3 , 40×10^3 and 80×10^3 cells) in 250µL RPMI medium (Capricon Scientific®) and 250µL PNC solution were transferred to the electroporation cuvette (0.4cm, Sigma Aldrich) such that total 500µL volume contains sub-toxic concentration of PNC and above mentioned number of JCs. In parallel, two sets of 500µL JC suspension were also prepared for blank JC and electroporated blank JC, and transferred to electroporation cuvette (Merk Sigma Aldrich®). All PNCs were added to electroporation cuvette-containing JC suspension and subjected to electroporation (BIORAD Gene Pulsor™) at 250V and 250µF capacitance, and time constant (ms) was noted. After electroporation, samples were kept for minimum 5 minutes to allow resealing of cell membrane pores. JCs were centrifuged at 1000rcf for 5min and supernatant was collected. JCs were washed with RPMI, collected and immediately used for phototherapy and Confocal laser scanning microscopy (DMI6000 Leica TCS SP5; LSM880 Zeiss).

3. Quantification of mTHPP

3.1. Amount of mTHPP complexed with polymer

The amount of mTHPP which is complexed with each polymer was determined by direct and indirect methods. In case of direct method, mTHPP was extracted from mTHPP-PSS NC and mTHPP-PVP NC by ethanol and from mTHPP- Protasn[®] NC by isopropanol (spectrophotometric grade, Sigma Aldrich). For indirect method, free (uncomplexed) mTHPP on filter was dissolved in ethanol for mTHPP-PSS NC and mTHPP-PVP NC and in isopropanol (spectrophotometric grade, Sigma Aldrich) for mTHPP- Protasn[®] NC. Amount of mTHPP estimated by UV spectroscopy (Multiscan GO, ThermoScientific) in both methods were compared. For indirect method estimated amount of mTHPP was subtracted from the amount of mTHPP used for experiment.

$$\text{Amount of mTHPP complexed} = \text{Total amount of mTHPP added} - \text{Free mTHPP}$$

For direct estimation of mTHPP, 1mL each PNC was freeze dried in eppendorf tube. Extracting solvents each 1mL ethanol (mTHPP-PSS NC and mTHPP-PVP NC) and isopropanol (mTHPP-Protasn[®] NC) were added in eppendorf tube, vortexed and centrifuged at 2500rcf. Supernatant was collected and the process was repeated thrice with addition of respective organic solvent. Supernatants of each step were pooled and estimated by UV spectroscopy at 418nm.

For indirect method, after filtration step as mentioned above, the moist filter was dried in oven at 40°C, over 1hr. Then, ethanol (mTHPP-PSS NC and mTHPP-PVP NC) and isopropanol (mTHPP- Protasn[®]) were added on filter to dissolve free mTHPP and collected as filtrate under vacuum. These alcoholic solutions of mTHPP were further diluted and estimated by UV spectroscopy at 418nm.

3.2. Amount of intra-Jurkat-cellular mTHPP complexed with polymer

The amount of mTHPP internalized into JCs was determined by fluorescence spectroscopy (Fluostar Optima[®]). Three sets of JCs (80×10^4) in 500μL, each suspended in 31μg/mL (mTHPP-PSS NC), 47μg/mL (mTHPP-Chitosan NC) and 94μg/mL (mTHPP-PVP NC) solutions in RPMI medium were subjected to electroporation at 250V current and 250μF resistance between 4-6ms time constant.

The JC suspensions were allowed to rest for minimum 5 minutes to allow resealing of pores. PNC loaded JCs were centrifuged at 1000rcf for 5 minutes followed by washing with RPMI medium to remove non-encapsulated PNCs. Cell lysing agent, 2% TritonX100 (100 μ L) was added to cell pellet and vortexed to break down the cells. Ethanol for mTHPP-PSS NC and mTHPP-PVP NC, and isopropanol for mTHPP-Chitosan NC (400 μ L) were added and further vortexed to extract out mTHPP from PNCs. Extraction mixtures were centrifuged at 1000rcf for 5 minutes and supernatant was collected. The procedure with ethanol and isopropanol was repeated thrice and all extracts were pooled together. Extracts were serially diluted in a light protected 96 well plate. The amount of mTHPP internalised into JC was estimated from standard curves at λ_{exc} =415 nm and at λ_{em} = 670 nm against blank ethanol and isopropanol.

3.3. Determination of complexation efficiency

The amount of free mTHPP remaining on filter and complexed mTHPP was determined by UV-spectroscopy. CE in terms of 'number of monomers binding to one molecule of mTHPP' was calculated by converting the amount of mTHPP complexed with polymer to the molar ratio of mTHPP and number of monomers forming the complex.

4. Characterization of mTHPP-Polymer NCs

4.1. Spectral characterization

As the PNC inherits both chemical and spectral features from their parent compounds i.e. mTHPP and respective polymer, therefore overall spectrums of mTHPP, each polymer and PNC were determined. mTHPP (1mg) was dissolved in 1mL ethanol and further diluted to produce 2 μ g/mL ethanolic solution of mTHPP. Ethanol (blank) was first scanned between 200 to 800 nm to set the baseline followed by 2 μ g/mL ethanolic solution of mTHPP.

Each PNC (1mg) was weighed and individually dissolved in 1mL MilliQ water to produce 1mg/mL aqueous solution. After further dilution with MilliQ water, mTHPP-PSS and mTHPP-PVP NCs solutions (5 μ g/mL) and mTHPP-Chitosan (500 μ g/mL) were produced. First, MilliQ water (blank) was scanned between 200 to 800nm to get the baseline and then 5 μ g/mL solutions of each PNC was scanned in same way to get

spectrums. Aqueous solutions of each polymer; PSS (20µg/mL), PVP (31µg/mL), and Chitosan-HCl or Protasan[®] (500µg/mL) were also scanned for UV spectrums.

4.2. Molecular modeling characterization

The molecules viz, mTHPP, PSS, PVP and Chitosan were sketched and minimized using Powell method in Sybyl X 2.1. Gasteiger-Hückel charges were applied to the molecules during minimization. Docking studies was performed using AutoDock Vina.

4.3. Atomic force microscopy (AFM)

Aqueous solutions of all PNCs were characterized for their surface morphology and size by AFM. The system runs by JPK software. The PNC solution was placed on the mica chip stuck on glass slide surface, with the help of a pipette and allowed to air dry. The slide was kept below the cantilever (silicon tip). Images were obtained by displaying the amplitude signal of cantilever in the trace direction and the height signal in retrace direction, both signals being recorded simultaneously. The images were recorded in height and 3D view, and particle size of 50 PNC images were manually counted by JPK software.

4.4. Confocal laser scanning microscopy (CLSM)

Delivery of polymeric photosensitizer PNCs into JCs was confirmed by CLSM. Subtoxic concentration of each PNC as determined by MTT assay was individually loaded into 80×10^3 JCs by electroporation. JC suspension was taken into eppendorf tube and centrifuged at 1000rpm for 5 minutes. Supernatant was removed and cells were washed with medium to remove non-encapsulated PNC. JCs were fixed on slide with PBS/4% (w/v) paraformaldehyde. FluorSaver[™] reagent (Merk Millipore[®]) was spread on smear of cells and covered with cover slip. Imaging of cells were carried out using two confocal laser scanning microscopes; DMI6000 Leica TCS SP5 for 50µm images and LSM880 Zeiss for 5µm images. In order to get 50µm images, mTHPP-PSS NC, mTHPP-Protasan[®] NC and mTHPP-PVP NC loaded JCs were excited at 458nm, 405nm and 458nm respectively while for 5µm images, all NCs were excited at 440nm laser line. Emission wavelengths and image were recorded.

5. Cell culture studies

5.1. MTT assay of polymeric nanocomplexes

JC suspension (10,000 cells/200 μ L) was added in a V bottom 96 well plate. Next day, the plates were centrifuged at 1000rcf for 5 minutes to harvest JC in V bottom of the plate. Supernatant was carefully removed and 200 μ L serial dilutions (1:1) of 1000 μ g/mL mTHPP-PSS NC, mTHPP-PVP NC and mTHPP-Chitosan NC were added to each well. After overnight incubation, the 96 well plate was centrifuged and supernatant was carefully removed followed by addition of 200 μ L MTT dye:RPMI (1:9) to each well. Incubation overnight leads to conversion of yellow MTT dye into violet tetrazolium salt crystals by the cell metabolites at the bottom. The plate was again centrifuged and supernatant was removed followed by addition of 200 μ L DMSO (Sigma Aldrich[®]) and stirring at 200rpm to dissolve the crystal. The solutions in each well were transferred to flat bottom 96 well plate and the intensity of dye was measured by spectrophotometer at 570 nm.

5.2. Haemotoxicity studies of mTHPP-Polymer nanocomplexes

Human blood was collected with the help of technician in a tube containing 150mg EDTA/100mL blood and centrifuged at 3500rcf to separate plasma and RBC at the bottom. The plasma was taken out and RBCs were washed twice with normal saline and diluted up to 10 times in normal saline. JC suspension (80x10³ cells/500 μ L) blank and loaded with mTHPP-PSS NC, mTHPP-PVP NC and mTHPP-Chitosan NC were added to RBC suspension (150x10³ cells/500 μ L) to make up total 1mL volume in an eppendorf tube. Distilled water was added to a set of RBC (150x10³ cells) for positive control. All samples were incubated at 37°C under 40rpm stirring. Each sample was centrifuged at 0.5, 6 and 12hr interval, and supernatant was collected. Supernatant contains Hb which is released due to breakdown of RBC and forms Oxy-Hb upon exposure to air. Oxy-Hb was estimated by spectrophotometer at 540nm.

5.3. Blood clotting study

Blood clotting study was performed using human blood by slide method. The finger was pricked with needle and immediately mixed with JC (80x10³ cells/100 μ L); blank and loaded with mTHPP-PSS NC, mTHPP-PVP NC, and mTHPP-Chitosan NC. Formation of fibrin was tested every 30 seconds with needle and time was noted upon

fibrin formation. The experiment was performed at ambient temperature and controlled by clotting time estimation of only blood.

5.4. Anticancer activity of NC loaded JC against A549 lung carcinoma cells

A549 cells (10,000cells/well) were seeded in a 96 well plate one day before the experiment for both dark and laser induced toxicity studies. Next day, the sub-toxic concentrations of PNCs viz, mTHPP-PSS NC (31 μ g/mL), mTHPP-PVP NC (94 μ g/mL), and mTHPP-Chitosan NC (47 μ g/mL) were internalized into JCs by electroporation at 250V and 250 μ F capacitance. For electroporation, JC suspensions (20 $\times 10^3$, 40 $\times 10^3$ and 80 $\times 10^3$ cells) in 250 μ L RPMI and 250 μ L PNC solutions were transferred to the electroporation cuvette and 250 μ L RPMI was added such that total 500 μ L volume contains sub-toxic concentration of PNC and 20 $\times 10^3$, 40 $\times 10^3$ and 80 $\times 10^3$ JCs. Besides, 2 sets of JC suspension as blank JC (20 $\times 10^3$) and, electroporated blank JC (20 $\times 10^3$) in 500 μ L protein free RPMI medium were also prepared and transferred to electroporation cuvette. All samples were mixed gently and subjected to electroporation at 250V and 250 μ F capacitance, and time constant (ms) was noted. After electroporation, samples were kept for minimum 5 minutes to allow resealing of cell membrane pores. Then, JCs were centrifuged at 1000rcf for 5 minutes and supernatant-containing non-encapsulated PNC was removed and cell pellet was washed and suspended in 200 μ L medium. The medium of A549 cells (1 $\times 10^4$ cells/well) in 96 well plate was removed and each sample volume (200 μ L) was transferred to A549 cell and allowed to incubate over 4hr at 37°C. Then, 96-well plate was centrifuged at 1000rcf for 5min and supernatant was removed. The plates for light induced toxicity studies were irradiated (Lumundus Eisenach GmbH) at 457nm with light dose 12J/mm². The light dose was calculated into J/mm² by multiplying 40 Storm (mA) with 100W/m² times duration of light exposure in seconds. MTT dye (200 μ L; 1part dye and 9parts RPMI medium) were added to each well and MTT assay was performed as mentioned in MTT assay procedure.

G. RESULTS AND DISCUSSION

Nanocomplexes for anticancer therapy such as self-assembled micellar NC of catechin derivative with protein (Chung et al, 2014), Chitosan-micro RNA NC (Santos et al, 2015) and, siRNA and RNA-based CD30 aptamer probe co-complexed with nano-sized polyethyleneimine-citrate (Zhao et al, 2011) have been designed. However, targeting deeply localised tumours and malignancies are still challenge. A delivery system comprising polymeric mTHPP NC encapsulated in T lymphocytes is promising to successfully tackle the challenge because T cells have accessibility to even deeply seated cancer cells and photosensitizers having excitation peak between 650 to 900 nm can be irradiated from a 7-14 cm distance (Mitsunaga et al, 2011 and Weissleder et al, 2003).

Such a delivery system combining phototherapy and immunotherapy was formulated by first synthesizing polymer-mTHPP nanocomplex followed by internalization into T cells. We have used mTHPP as a model drug for mTHPC which is used in clinical practice as second generation photosensitizers and Jurkat cells (transformed T cells) to design a proof of concept focused on development of the delivery system aiming for photoimmunotherapy of cancer. Interplay of immune therapy mediated by T cells and photodynamic action exerted by the loaded photosensitizer nanocomplex can result in effective killing of cancer cells even if they are present in deep tissues.

1. Analytical method development

Quantification of the drug incorporated into the delivery system is one of the most important parts in formulation development. Different techniques are used for quantification such as UV, fluorescence spectroscopy, HPLC etc. We had chosen UV spectroscopy for quantification of mTHPP complexed with polymers because it is time saving, simple and easy technique. This quantitative information is important to not only know the amount of mTHPP complexed with polymer but also to calculate the CE of each polymer. The aim of the project is also extended to estimate the amount of mTHPP reached within JCs in form of polymer nanocomplex. As UV spectroscopy is not sensitive enough to accurately estimate the intracellular mTHPP, therefore a sensitive technique such as fluorescence spectroscopy was used for precise quantification.

2. Synthesis of Polymer-mTHPP NCs

Water soluble NCs of mTHPP with different polymers were synthesised by merely mixing the aqueous solution of polymer with ethanolic solution of mTHPP. When aqueous solution of polymer and ethanolic solution of mTHPP are mixed together, a hydroalcoholic mixture is formed which consists of hydroalcoholic solvent containing both non-complexed mTHPP suspended as free drug and complexed mTHPP as water soluble mTHPP-Polymer complex. In fact, mixing of aqueous and ethanolic solutions allows free intermolecular interaction between mTHPP and polymer to associate each other through non-covalent bondings.

Intermolecular forces arise from attraction or repulsion between molecules, atoms or ions. They are weaker than intramolecular forces which keep the whole molecule intact through co-valent bond formed by sharing of electrons. While the intermolecular interaction takes place, the level of potential energy changes; the ability of chemical entities taking part in complex formation is determined by their level of potential energy in electronic ground state (Schreck et al, 2016). Together mTHPP and all polymers (Fig.17, 18, 19, 20) are rich in mobile electrons in ground state. Presence of lone pairs of electron, H-atoms, dipoles between counterpart atoms; all of them are prerequisite for intermolecular interaction which leads to complexation.

The intermolecular forces are either permanent arising from electrostatic attraction between dipoles such as H-bonding interaction, ion-dipole, π - π interaction or temporary force like van der Waals forces (Keesom force, Debye force, and London dispersion force) which arise due to interaction of uncharged atoms and molecules.

The mobile electrons in chemical structure play key role in formation of nanocomplex and rich presence of non-covalent electrons enhance the tendency of complex formation. Interestingly, mTHPP possess plethora of mobile electrons and monomers of each polymer chain also have sufficient electrons which impart not only in complex formation through physical bonding but also able to be excited by laser to generate ROS for inducing phototoxic effect.

Looking at the chemical structures of mTHPP (Fig.17) and polymers (Fig.8, 9 & 10); the parent porphyrine ring in mTHPP is substituted at all four carbons of exocyclic double bond, each by the meta carbon of phenolic ring. mTHPP is rich in mobile electrons because of four benzene rings, four pyrrole rings, four exocyclic double bonds, and 8 lone pairs of electron together on nitrogen and oxygen. Moreover, 6 hydrogens are bonded to nitrogen and oxygen. These mobile electrons in mTHPP molecule can form hydrogen bond with hydrogen atom of counterpart as well as π - π interaction between electropositive nitrogen atoms with π -electrons is also possible to produce charge transfer complex.

Electronegativity difference between hydrogen and its electronegative oxygen creates permanent dipoles responsible for electrostatic interactions. Further, electropositive nitrogen can also induce dipole interaction with any encountered electronegative species. Thus, mTHPP is an ideal candidate for complexation with any other chemical entities possessing similar electronic and chemical attributes.

On other hand, PSS monomer contains a benzene ring, 2 exocyclic double bonds, and a sulphonate group (Fig.17a). PVP monomer has a ketonic group which produces a permanent dipole in monomer and electropositive nitrogen atom (Fig.17b) helps inducing the dipole with encountered electronegative species which trigger complex formation. In case of Chitosan hydrochloride (Protasan[®]), 6 lone pairs of electron and hydrogen bonded with oxygen and hydrogen in monomer provoke it to predominantly undergo hydrogen bonding interaction (Fig.17c). Thus electronic and chemical features of each polymer enable them to undergo complexation, therefore they were chosen for nanocomplexation with mTHPP.

An interplay of all these physical forces lead to complexation between complexing agents. Pichierri et al, have investigated dipole-dipole interactions in protein-protein complex taking Ubiquitin Dsk2 as model protein. The stability and correct alignment of protein complex was largely derived by dipole-dipole interaction (Pichierri et al, 2013). The empirical data depicting fingerprints of hydrogen bonding were studied which is responsible for complex formation between acetone and chloroform azeotrope (Schreck et al, 2016). The interactions between local anaesthetic bupivacaine and its structural analogues viz, 2,6-dimethylaniline and N-methyl-2,6-dimethylacetanilide,

cocaine and electron deficient moieties were studied by UV-visible spectroscopy and proton-NMR. Red shift in UV-visible wavelength of electron acceptor and chemical shift in NMR indicated change in electron flow and formation of charge transfer complexes through π - π interaction between bupivacaine, its analogues and aromatic acceptors (Powell et al, 2007). Solubility enhancement study and complexation through π - π interaction were investigated between phenanthrene (π -electron donor) and quinones and N-heteroaromatic cations (π -electron acceptor) by UV-visible spectroscopy and proton NMR. Charge transfer bands in UV spectroscopy and ring current shifts in NMR spectrums confirmed π - π interaction (Wijnja et al, 2004).

The mechanism of nanocomplex formation can be either explained by applying quantum mechanics, molecular mechanics or phenomenologically in view of above mentioned intermolecular forces such as dipole-dipole interactions, π - π interaction, van der Waals forces. Taking each polymer and mTHPP, the phenomena of nanocomplex formation, behaviour of polymer and mTHPP undergoing physical interaction from their chemical structure and molecular modelling are described.

In case of mTHPP and PSS, nanocomplexation is majorly driven by H-bonding, π - π interaction as well as dipole interaction. All hydrogen bonded with oxygen of phenolic ring in mTHPP take part in forming hydrogen bond with lone pairs of electron present in sulphonyl moiety of PSS monomers. Nitrogen is electron acceptor moiety in mTHPP which forms charge transfer complex with π -electrons of benzene ring in PSS. All four hydroxyl groups of mTHPP and sulphonyl group of PSS form permanent dipole and mutually create dipole-dipole interaction (Fig.17a).

In case of mTHPP-PVP nanocomplex, π -interaction from both counterparts is possible. Electropositive nitrogen of PVP forms charge transfer complex with π -electrons of benzene ring, porphyrine ring and exocyclic double bonds in mTHPP and on other hand nitrogen of mTHPP undergoes π -interaction with π -electrons of carbonyl group. Moreover, lone pairs of electron on carbonyl forms hydrogen bonding with hydrogen bonded with oxygen in mTHPP molecule. All four hydroxyl group of mTHPP and a carbonyl group of PSS form permanent dipole and mutually create dipole-dipole interaction (Fig.17b).

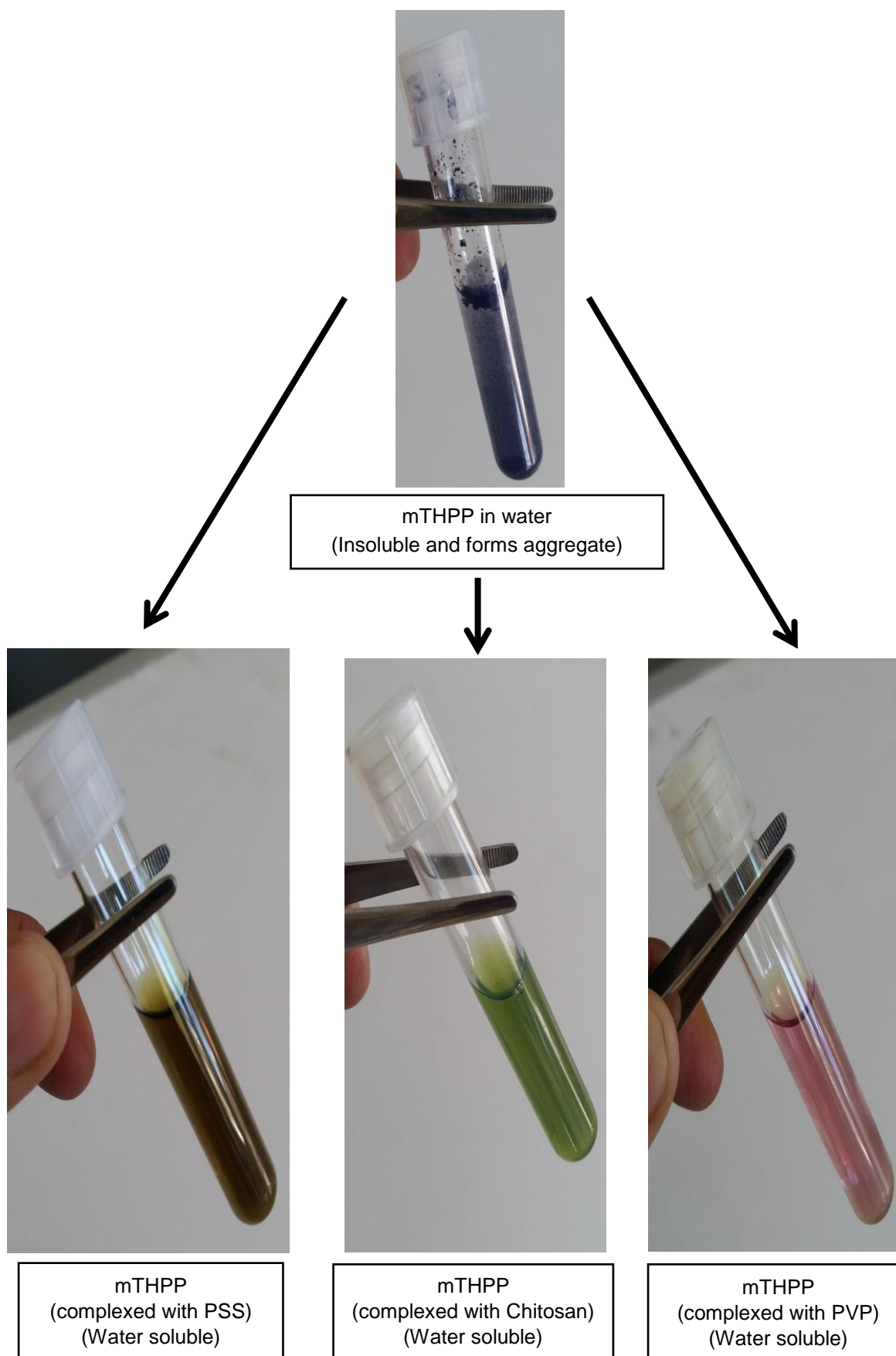


Fig.16. Behaviour of mTHPP in water, alone and as complexed with polymer

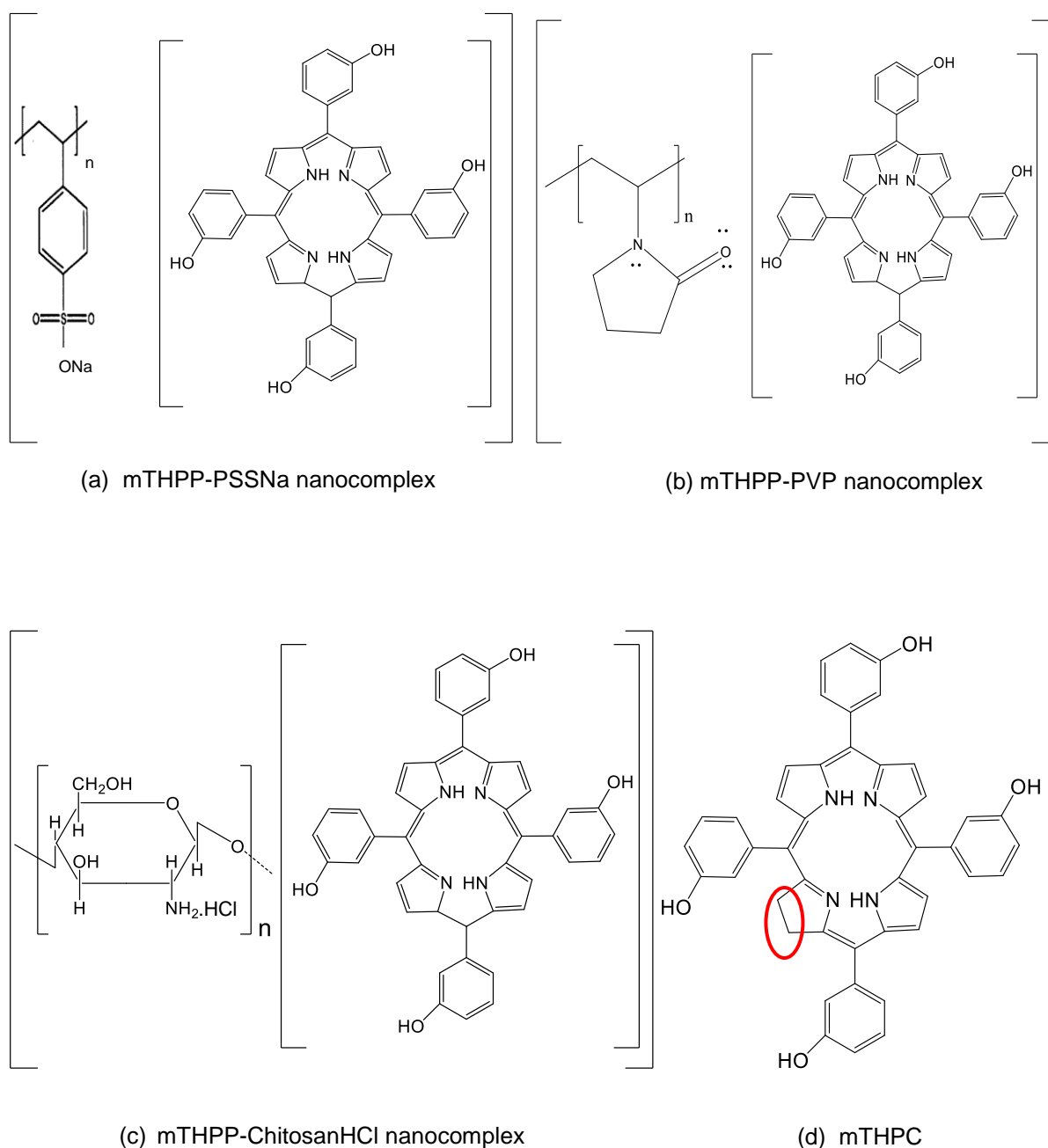


Fig. 17: Polymer-mTHPP nanocomplex and mTHPC with one less π -bond encircled

Chitosan is rich in lone pairs of electron on oxygen which forms hydrogen bond with oxygen bonded hydrogen of mTHPP. Beside, hydrogen of alcoholic group and electropositive nitrogen in Chitosan monomer can act as electron acceptor to interact with π -electrons of mTHPP to produce charge transfer complex. Further these hydrogen atoms of Chitosan form Hydrogen bondings with electronegative oxygen atoms of mTHPP (Fig.17c).

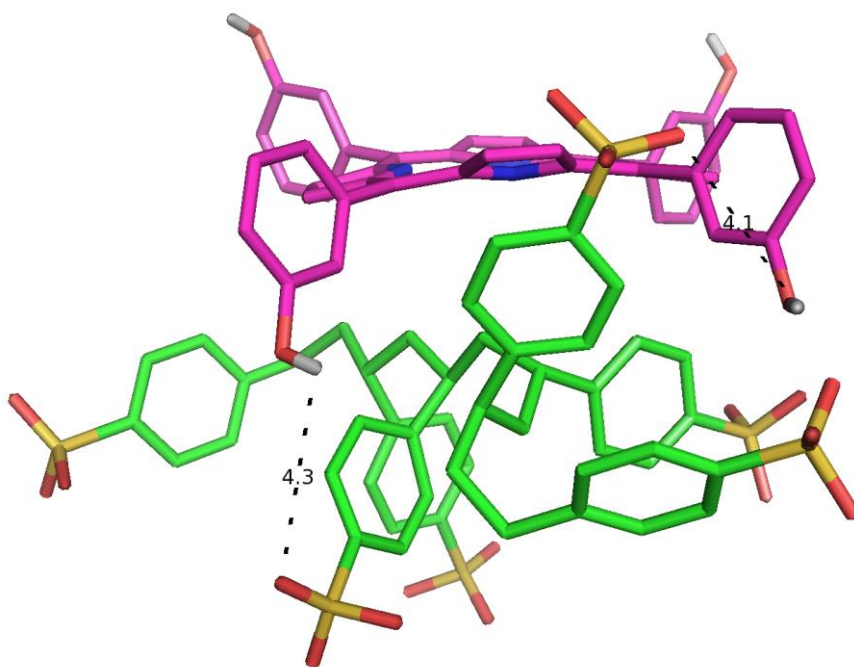


Fig.18: Molecular model showing interaction of mTHPP and polystyrene sulphonate
Dotted line indicates bond distance in Å^o

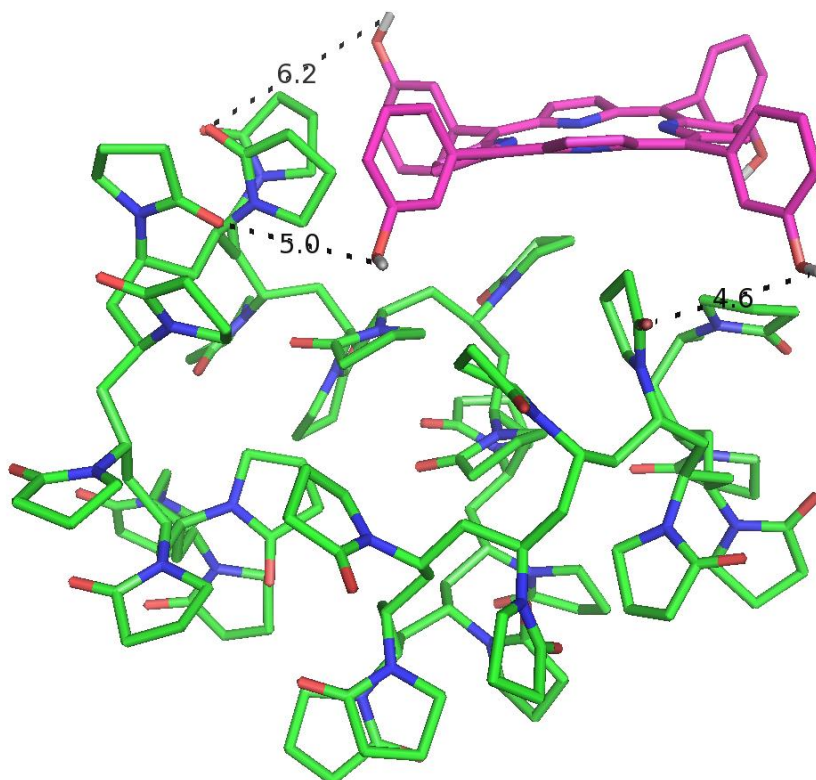


Fig.19: Molecular model showing interaction of mTHPP and polyvinylpyrrolidone
Dotted line indicates bond distance in Å^o

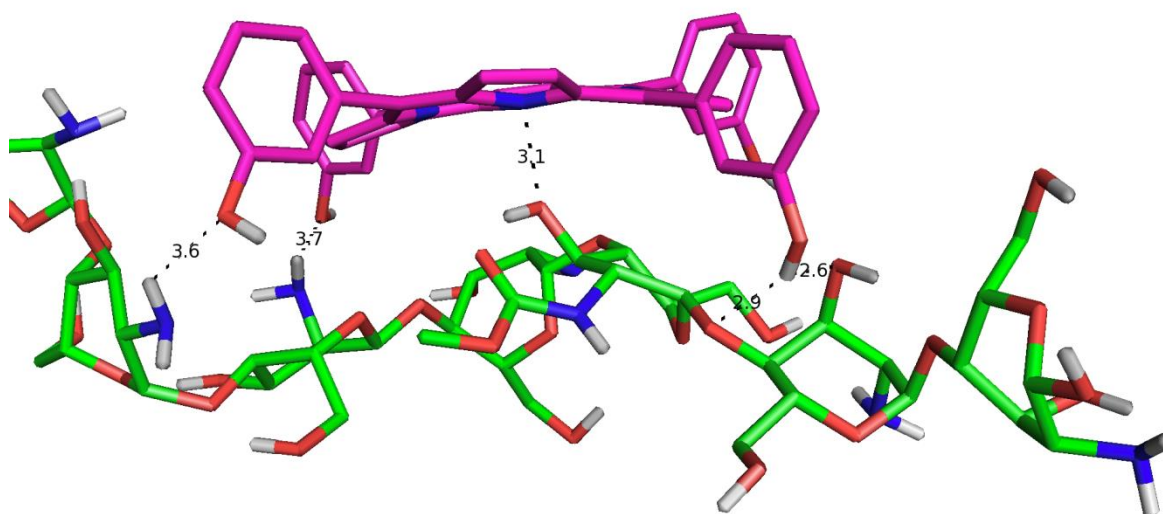


Fig.20: Molecular model showing interaction of mTHPP and Chitosan in their nanocomplex
Dotted line indicates bond distance in Å^o

Though these polymers are capable to form complex with mTHPP through various intermolecular interactions, the efficiency of a polymer in complex formation varies and largely depends upon the number of mobile electrons associated with aromatic characters. Complexation efficiency study revealed PSS as the most efficient polymer in formation of nanocomplex than Chitosan and PVP. Chitosan is more efficient than PVP for the same reason. Reasons behind varying complexation efficiencies of polymers following the order mTHPP-PSS NC > mTHPP-Chitosan NC > mTHPP-PVP NC are explained later.

We had also performed computer aided drug design studies to investigate intermolecular interaction between mTHPP and respective polymers. This study had been carried out only up to a preliminary stage to get rudimentary data. Further studies are underway until getting molecular modelling parameters which are comparable against spectrophotometric results. This can precisely unravel the behaviour of each polymer and mTHPP in aqueous solvent. Based on preliminary studies all molecular models (Fig.18, 19 & 20) show H-bonding and π - π interactions as most energetically favourable. In case of mTHPP-PSS NC, π - π and H-bonding interactions are evident while mTHPP-Chitosan NC shows only H-bonding. Interestingly, mTHPP-PVP shows poor H-bonding interaction and key interactions are

governed by hydrophobic forces e.g. van der Waals interaction between pyrrolidone and phenyl rings of the THPP.

Choice of mTHPP as a model drug for mTHPC which is second generation photosensitizer is due to cheap availability of mTHPP and very close physicochemical features to that of original drug (Fig.17d). Further, the freeze drying method was adopted to prepare nanocomplex because this method appeared to be more efficient in nanocomplex formation (Reum et al, thesis 2011).

In process of development of a drug-delivery system, journey starts from preformulation studies through solubility and permeability profiling of drug molecule. As our T lymphocyte based delivery system is intended to be administered directly into blood therefore permeability profile is ruled out but enhancing aqueous solubility of mTHPP is indispensable. Aqueous solubility of mTHPP is highly desirable in T cell based formulation development because mTHPP forms aggregate in water (Fig.16). This presents hurdle in formulation development especially when internalizing mTHPP into Jurkat cells, it must be soluble in medium so that a suitable Tcell based formulation can be developed. Moreover, poor aqueous solubility of mTHPP instigates accumulation in tissues where it slowly releases and degrades causing toxicity.

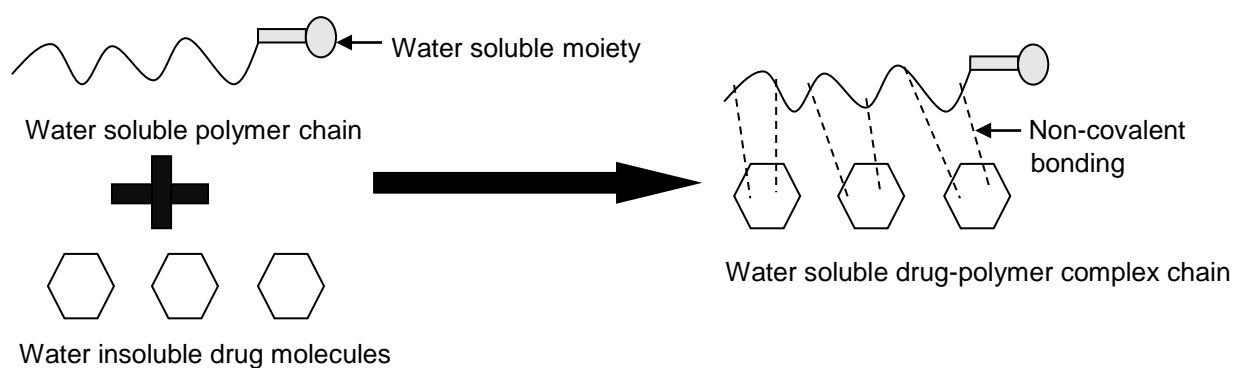


Fig.21. Solubility enhancement model; water soluble polymer and water insoluble drug forms water soluble drug-polymer

Several approaches based on nanotechnology principle have been applied to solve poor aqueous solubility problem of challenging and difficult-to-deliver drug molecules. Kumar et al have improved aqueous solubility of amphotericin B (Italia et al, 2009) and

cyclosporin (Italia et al, 2007). Solubility of Paclitaxel was improved by formulating stable PEGylated liposome (Yang et al, 2007). We had approached nanocomplexation technology to enhance aqueous solubility of mTHPP because NCs have produced as smaller size particle as 10-80 nm (Table 5; Fig.26a, 26b, 27a, 27b, 28a, 28b) and weak physical bonds alongwith high intensity of laser during photodynamic therapy facilitates faster release of mTHPP.

NCs must exhibit polarity which is prerequisite for aqueous solubility; PSS possess sulphonate group where electronegativity difference of O and S generates polarity between them, similarly PVP possess polarity due to electronegativity of O in ketonic group and amine salt group confers polarity to Chitosan hydrochloride (Protasan[®]). Intermolecular interaction of water insoluble mTHPP with these polymers produces a complex with altered solubility.

Infact, after formation of complex water soluble moiety responsible for aqueous solubility of polymers greatly imparts in making the nanocomplex water soluble and thereby increases solubility of mTHPP. According to solubility enhancement model (Fig.21), non-covalent bonding between water insoluble drug and water soluble polymer form complex and compel the drug molecule to become aqueous soluble. However, CE of polymer determines the extent of water solubility of mTHPP (Table.5). When CE of polymer is higher, all monomers together in a polymer chain bind with relatively more number of mTHPP leading to enhanced aqueous solubility.

3. Complexation efficiency study

While the complexation takes place between polymer and drug, monomers in the polymer chain exclusively take part in complex formation. As the number of monomers taking part in formation of complex with one drug molecule decreases, polymer becomes more efficient in formation of complex with given drug molecule. On contrary, number of drug molecules forming complex with a polymer chain or number of monomers in single polymer chain can also describe complexation efficiency in terms of drug molecule. Thus, Complexation efficiency (CE) in terms of monomers is defined as number of monomers in a polymer chain required to complex with one molecule of drug. Lower the CE value, more efficient is the polymer to form complex with drug. CE was determined from amounts of mTHPP and polymer taking part in

formation of complex. A molar ratio of mTHPP and polymer complexed with each other results in complexation ratio which defines CE of polymer.

Moreover, taking 10:15 (drug:polymer) ratio for nanocomplexation shows different amounts of mTHPP complexed with respective polymers (Fig.22). Both the amount of mTHPP complexed and respective CE of polymers calculated follows the order of PSS>Chitosan>PVP (Table 5).

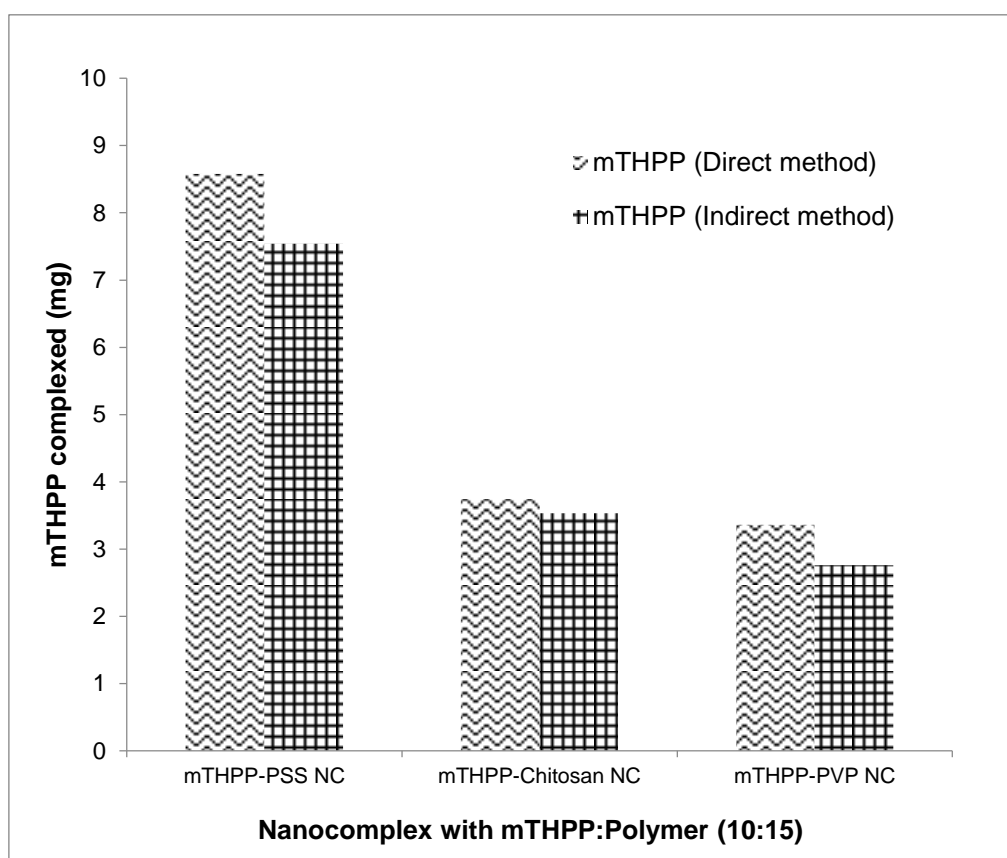


Fig.22. Comparison of amount of mTHPP complexed with different polymers by direct and indirect methods. (Values are shown as mean of 2 independent experiments)

Complexation efficiency of PSS is higher than PVP and Chitosan because in case of PSS, 6 monomers are required to form complex with one molecule of mTHPP while Chitosan and PVP need 14 and 27 monomers respectively to complex with one molecule of mTHPP. The benzene ring in PSS greatly increases aromatic character and thereby chances of π - π interaction and formation of charge transfer complex increases than other counterpart polymers. In addition, three lone pairs of electrons and two double bonds in sulphonate group also increase the probability of physical

interaction through dipole interaction and hydrogen bonding interaction. Thus, PSS appears to possess highest CE than PVP and Chitosan. Chitosan monomer with 9 lone pairs of electron and 5 hydrogen atoms exhibit stronger CE than PVP monomer which possesses only a ketonic group (Fig.17, 18, 19, 20).

Interestingly, molecular modelling of mTHPP and PVP reveal poor H-bonding and hydrophobic interaction (van der Waals forces) which can be attributed to its weakest CE than its counterpart polymers viz, PSS and Chitosan. Beside molecular model of mTHPP-PSS shows both H-bonding and π - π interactions against mTHPP-Chitosan which exhibit only H-bonding, suggest that CE of mTHPP-PSS is stronger than mTHPP-Chitosan. Thus order of CE among all polymers is mTHPP-PSS NC > mTHPP-Chitosan > mTHPP-PVP (Fig.18, 19, 20).

Table 5: Size, zeta potential and CE of all mTHPP-Polymer NCs

Nanocomplex	Particle size* (nm)	Zeta potential (mV)	CE**
mTHPP-PSS NC	65 \pm 5 nm	- 47 \pm 12.0	05.78 \pm 0.12
mTHPP-Chitosan NC	80 \pm 8 nm	+ 51 \pm 9.0	14.28 \pm 3.40
mTHPP-PVP NC	10 \pm 4 nm	+3 \pm 0.6	27.48 \pm 2.84

* Size were measured by manually counting 50 particles in AFM image

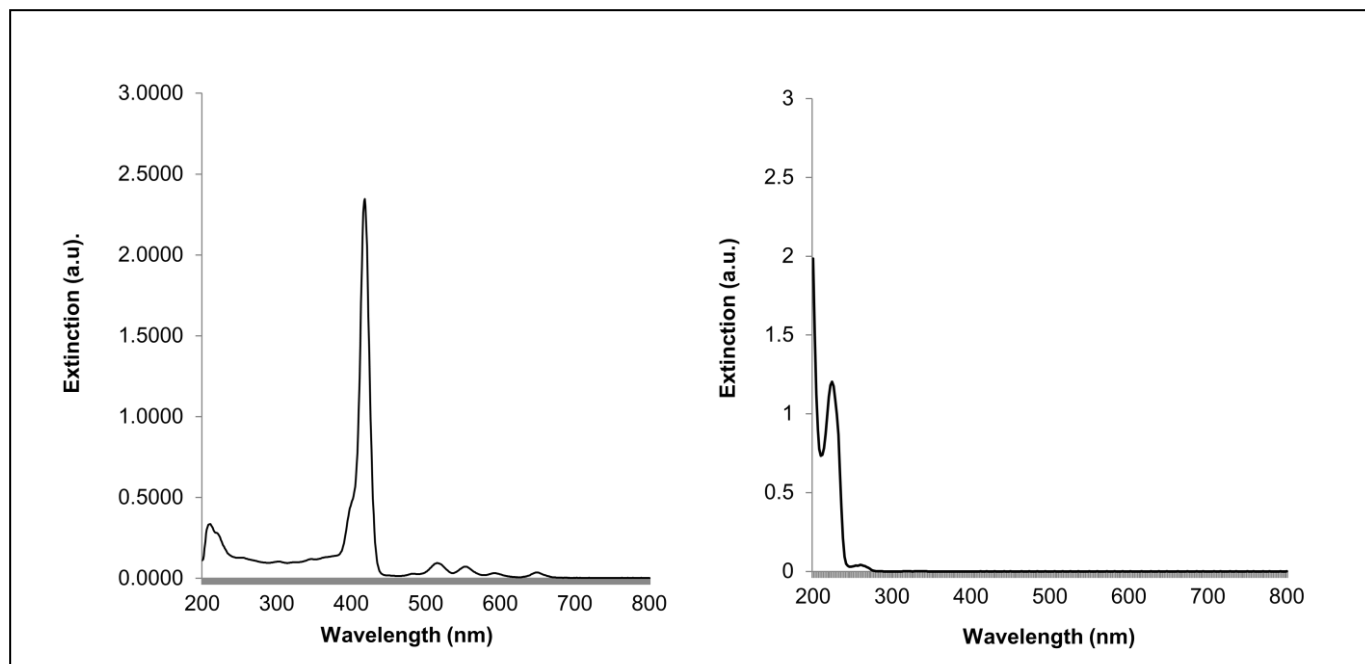
**CE is number of monomers/mTHPP molecule

4. Spectral characterization

Spectral characterization by UV spectroscopy has shown unique spectral features in respective spectrums of each nanocomplex (Fig. 23, 24, 25). Interaction between mTHPP and polymers on electronic level changes mobility of electrons resulting in absorbance shifts. The absorbance maxima of mTHPP is 418 nm in alcohol; in case of mTHPP-PSS NC peak sifts to 446 nm and of mTHPP-PVP NC towards 423 nm (red shift) while mTHPP-Chitosan NC shifts towards 412 nm (blue shift).

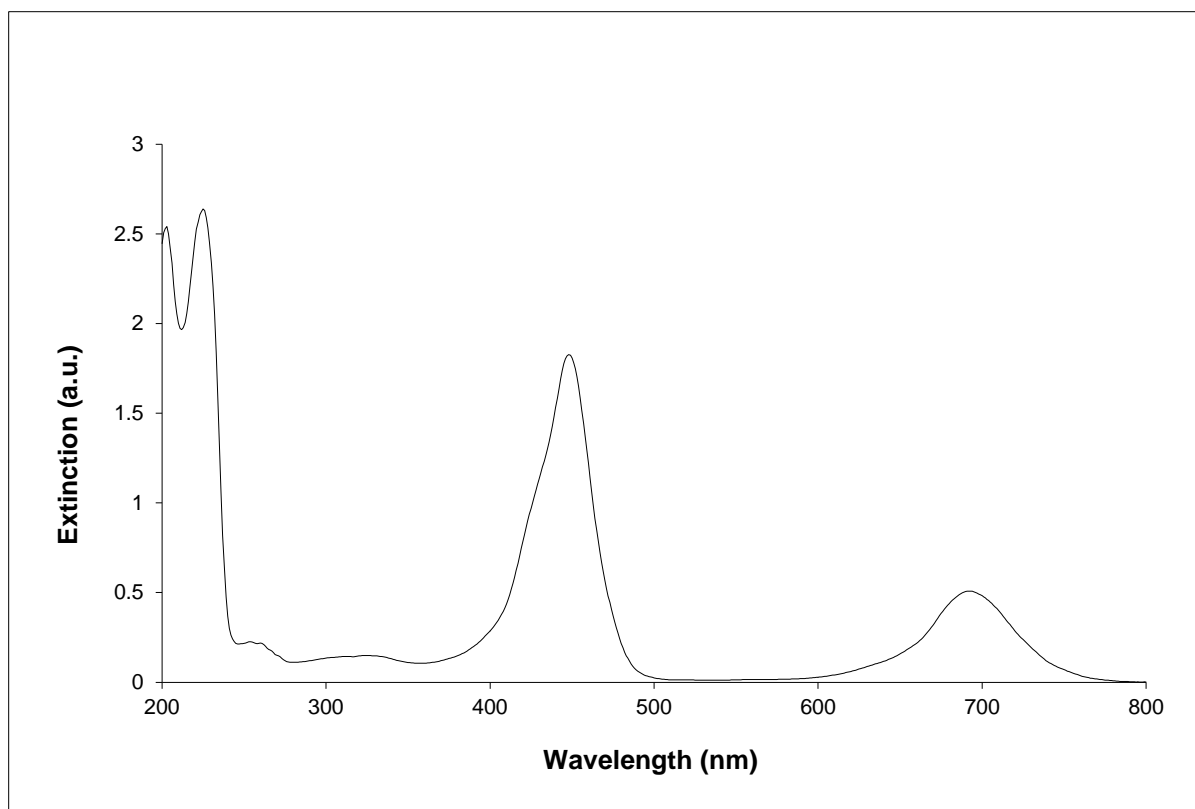
Apart from λ_{\max} of each Polymer-mTHPP NC, the absorbance peak above 600 nm is very important. The sensitivity of photosensitizers is greatly enhanced within near

infrared radiation fluorescence (NIRF) i.e. between 650 to 900 nm and penetration depth up to 7-14 cm in tissues and this range is also used in clinical practice.



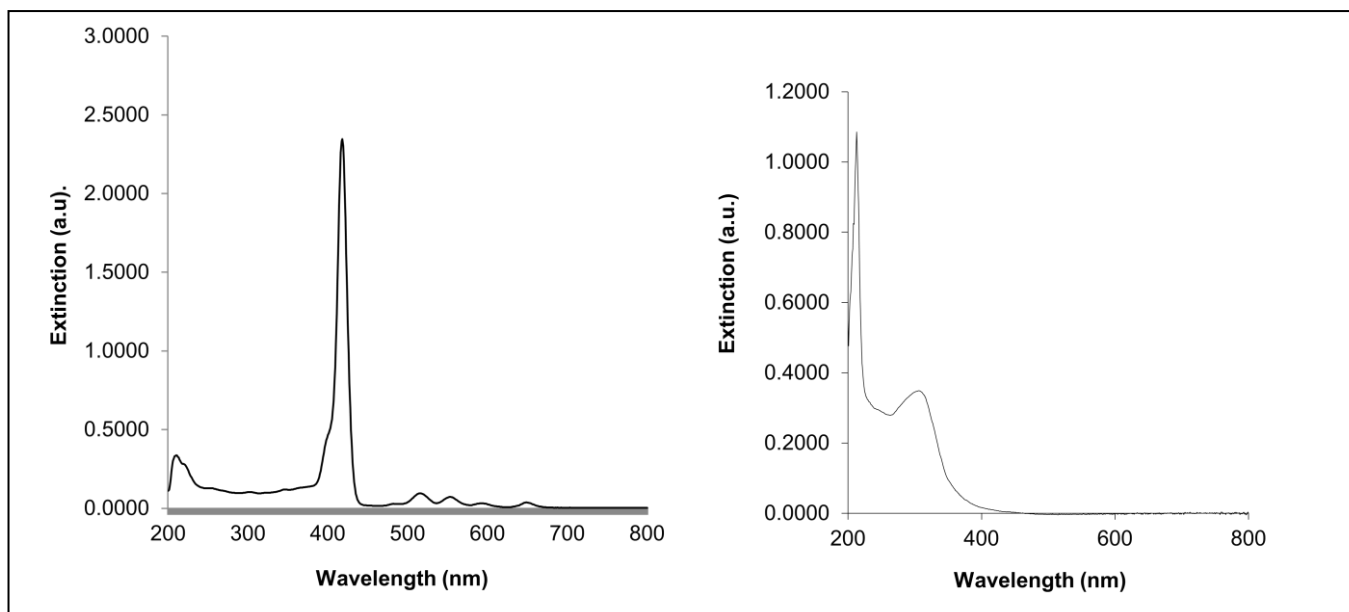
a) UV spectrum of mTHPP in EtOH (2 µg/mL)

b) UV spectrum of PSS-Na in water (20 µg/mL)



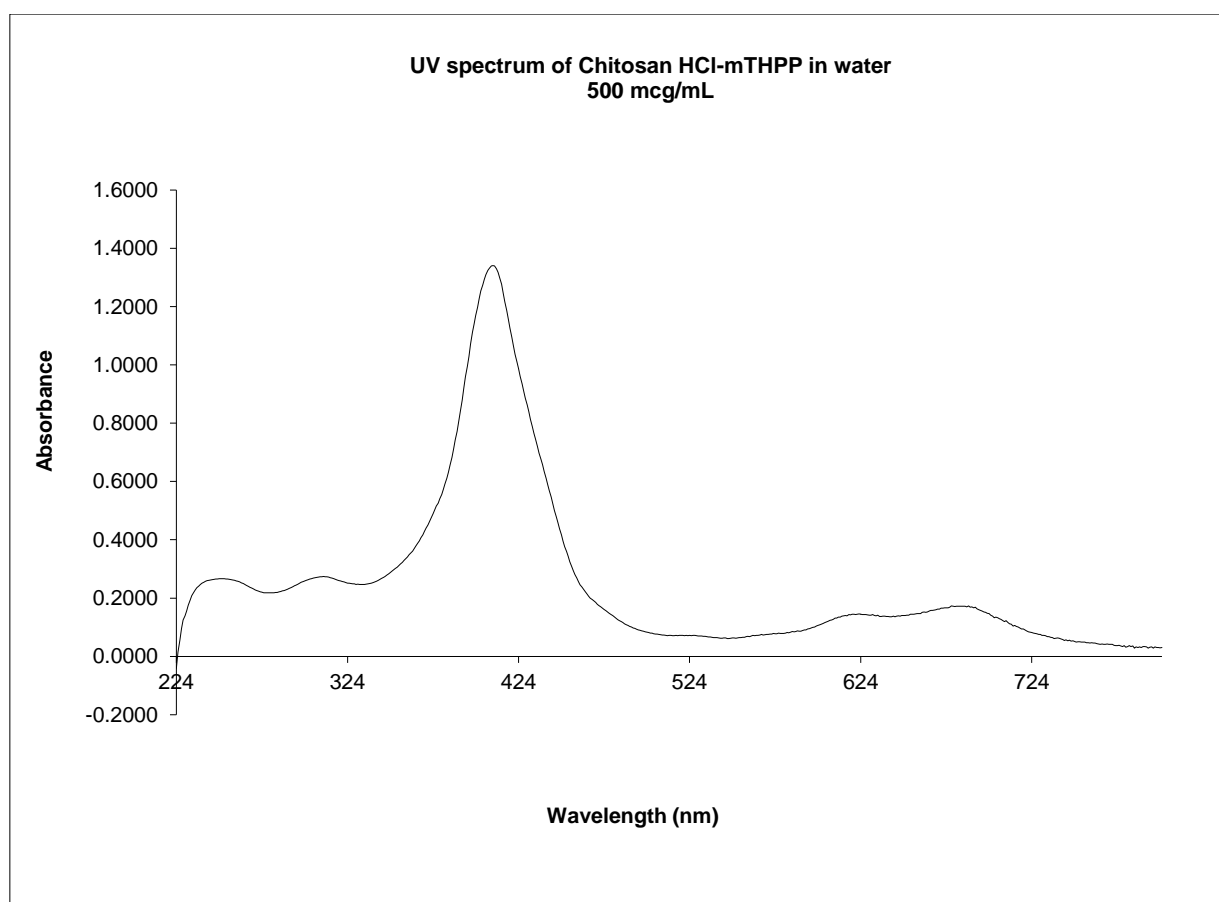
c) UV spectrum of mTHPP-PSS-Na nanocomplex in water (5 µg/mL)

Fig.23: UV spectrums of a) mTHPP, PSS-Na and mTHPP-PSS NC



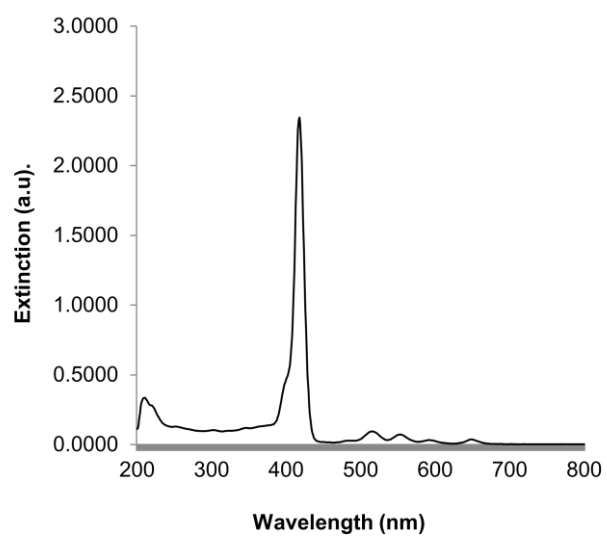
a) UV spectrum of mTHPP in EtOH (2 μg/mL)

b) UV spectrum of ChitosanHCl in water in (200 μg/mL)

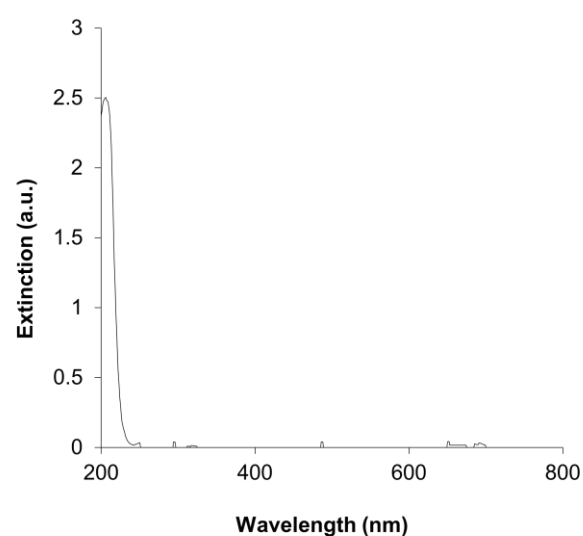


c. UV spectrum of mTHPP-ChitosanHCl NC (500 μg/mL)

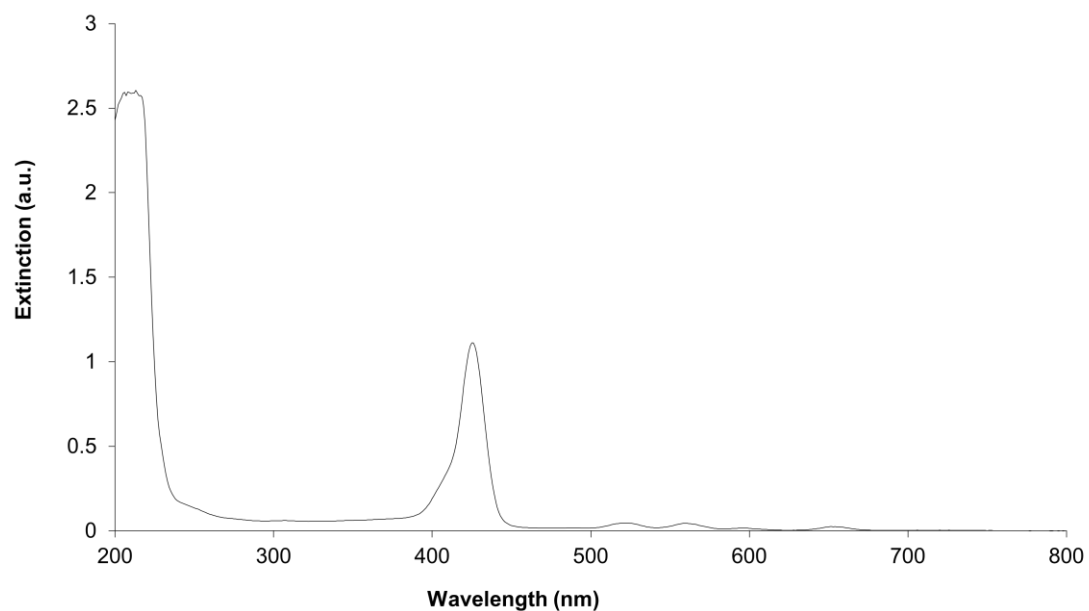
Fig.24: UV spectrums of mTHPP, ChitosanHCl and mTHPP-ChitosanHCl NC



a) UV spectrum of mTHPP in EtOH (2µg/mL)



b) UV spectrum of PVP in water in (31 µg/mL)



c) UV spectrum of mTHPP-PVP NC (5 µg/mL)

Fig.25: UV spectrums of a) mTHPP, PVP and mTHPP-PVP NC

As evident from spectrums of all nanocomplexes; they show an absorbance peak in NIR range (600-900nm). mTHPP-PSS NC shows an absorbance at 685nm, mTHPP-Chitosan shows bimodal peak at 607 and 677 nm while mTHPP-PVP NC shows at 650 nm. The absorption of light by Haemoglobin, lipids and auto fluorescence are minimal between 650-900 nm and therefore light above 600 nm can penetrate deep seated tissues from 7-14 cm (Mitsuganga et al, 2011 and Weissleder et al, 2003). Hence, absorbance peaks above 600 nm in each nanocomplex can be used in clinical application for deep seated tumours and malignancies. However, we had used λ_{\max} of each NC for our experiment in vitro pertaining to investigation their photodynamic activity because the size of JC is only about 8 μ m and targeted cancer cells lie in very close proximity.

In view of these spectral features, all NCs hold candidature for clinical application in photodynamic therapy. Further, smaller size of PSS (Mw=4.3 KDa) against Chitosan HCl (Protasan[®], Mw=100 KDa) and PVP (Mw=31 KDa) strengthen its candidature as an ideal excipient for polymeric NC because after metabolism, smaller molecular size facilitates faster renal clearance.

Table 6: Physical, spectral properties and CE of Polymer-mTHPP NCs

Drug and its nanocomplex	Spectral characteristic (UV- λ_{\max})	Physical characteristic (Colour)
mTHPP	418 nm	violet
mTHPP-PSS NC	446 nm	dark green
mTHPP-PVP NC	426 nm	Light (violet to yellow)
mTHPP-Chitosan NC	412 nm	light green

Due to weak physical forces between polymer and mTHPP, they can dissociate into the cell but such dissociation does not alter the photodynamic potential as NC and dissociated mTHPP, both possess peaks above 600 nm for excitation to exhibit fluorescence which is essential for photodynamic effect. Moreover, distinct colours of

each nanocomplex are their unique physical attributes for preliminary identification. The colour of mTHPP-PSS NC is dark green while mTHPP-PVP appears light yellow to violet and mTHPP-Chitosan light green (Table 6).

5. Particle size, morphology and surface charge

In view of internalization of each Polymer-mTHPP NC into Jurkat cells, characterization in terms of particle size measurement and determination of surface charge are crucial. Particle size greatly influences the passage of drug molecules through biological membrane inside cell. Cell membrane bears negative charge, hence surface charge on NC is also an important criterion to determine capability for intracellular delivery. Thus, size and surface charge greatly influence cellular uptake.

Ideally smaller size and positive charge must facilitate uptake of NC into JCs, however positive charge also causes damage to cellular structure (Fröhlich et al, 2012). Atomic force microscopy revealed morphology (Fig.26a&b, 27a&b, 28a&b) as well as size of each NC. As fluorescence exhibited by NC interferes with the dynamic light scattering, therefore size data rely exclusively upon counting 50 particles by Atomic force microscopy.

The size of mTHPP-PVP is much smaller (10 nm) with discrete particles than other two NCs; Chitosan-mTHPP (65 nm) and mTHPP-PSS (80 nm) (Table 5; Fig.26a&b, 27a&b, 28a&b). PSS monomer is much bigger than other counterparts; therefore its size is larger (80 nm). Overall size of NCs lie within 10-80 nm range is smaller enough to facilitate their internalization into JCs.

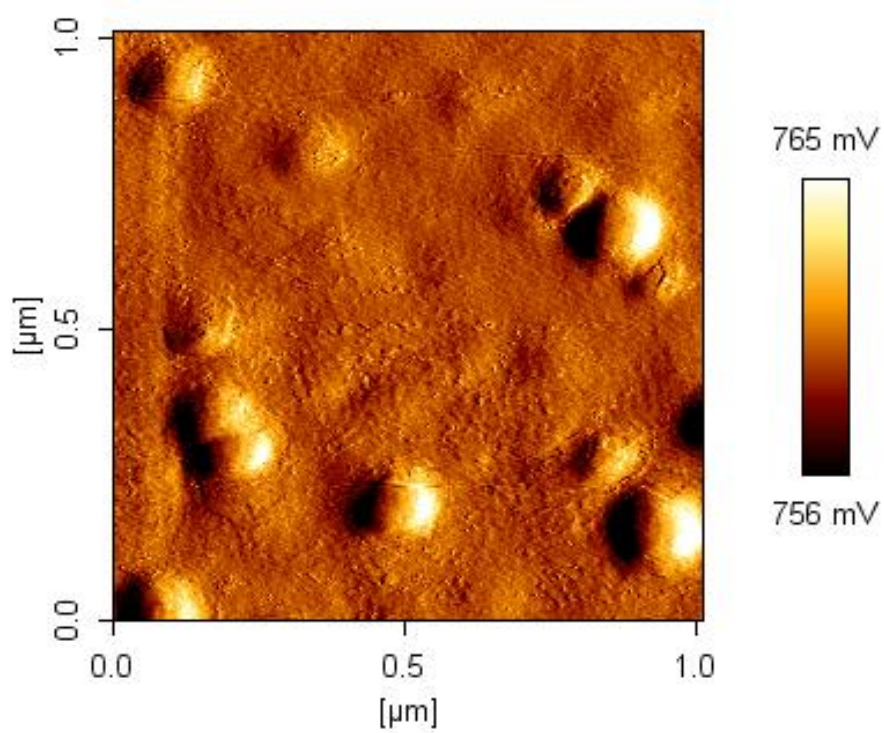


Fig.26a: AFM image of mTHPP-PSS nanocomplex (1x1 μm)

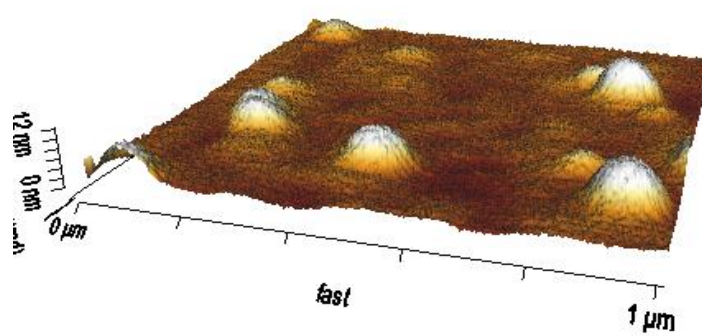


Fig.26b: 3D view; AFM image of mTHPP-PSS nanocomplex (1x1 μm)

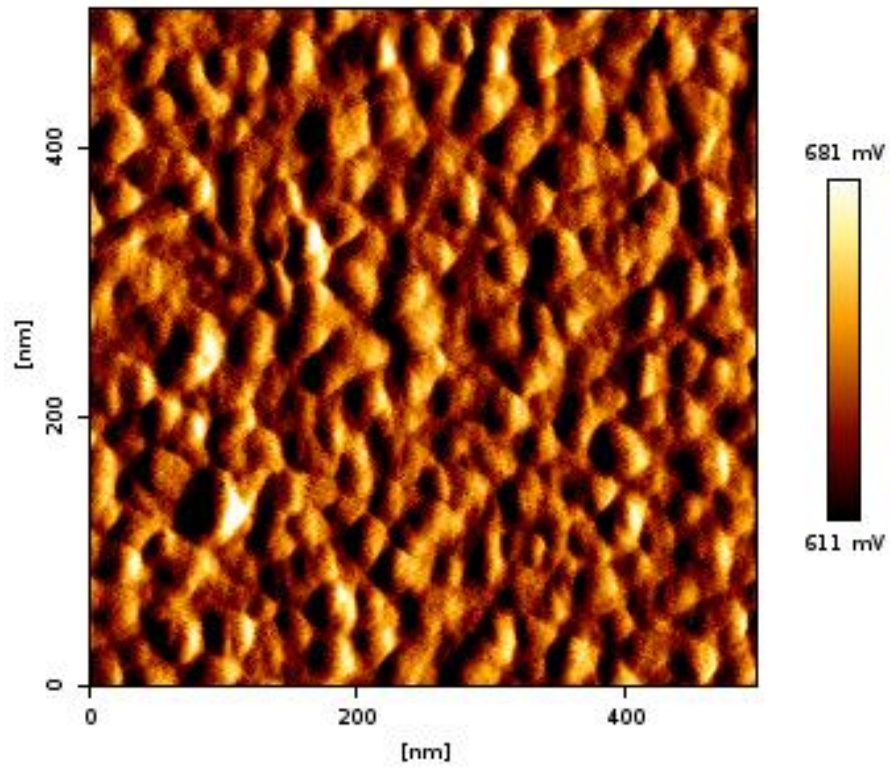


Fig.27a: AFM image of mTHPP-Chitosan HCl nanocomplex (0.5x0.5 μm)

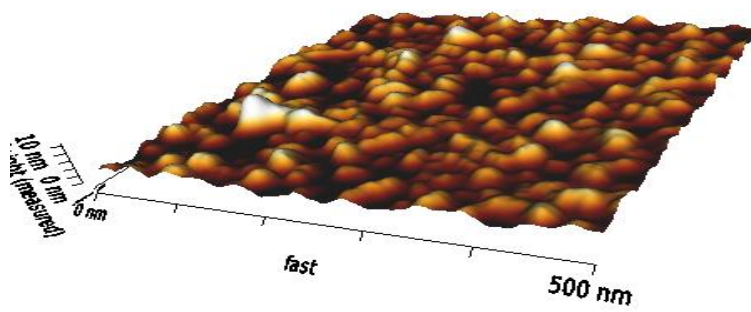


Fig.27b: AFM image of mTHPP-Chitosan HCl nanocomplex (0.5x0.5 μm)

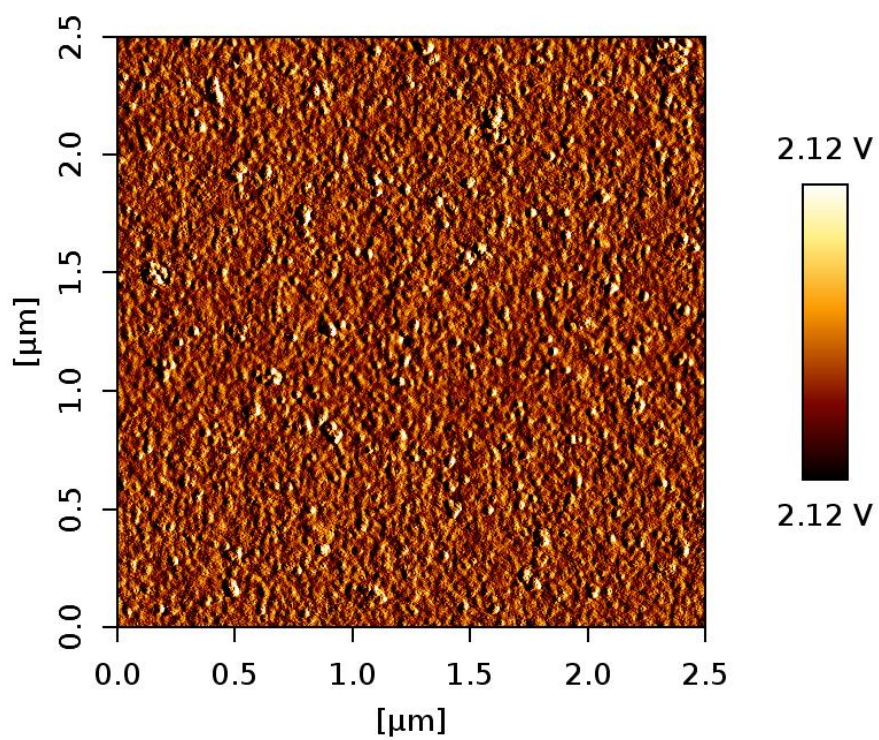


Fig.28a: AFM image of mTHPP-PVP nanocomplex (2.5 x 2.5 μm)

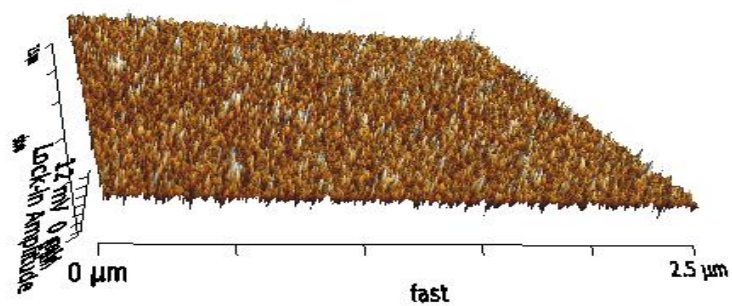
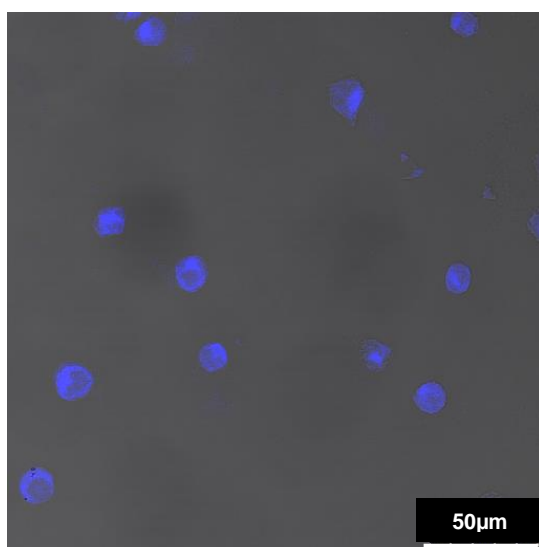


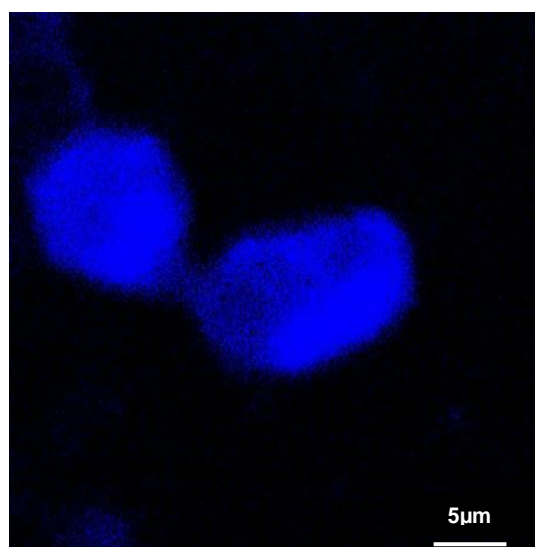
Fig.28b: AFM image of mTHPP-PVP nanocomplex (2.5 x 2.5 μm)

6. Confocal laser scanning microscopy

Confocal scanning microscopy is a tool to confirm intracellular delivery of fluorescent compounds. Electroporation internalizes NCs into JCs where they exhibit fluorescence upon excitation by laser. Looking at absorption spectrums (Fig.23, 24 & 25) of each NC, it is evident that all NCs have similar spectral properties due to presence of common photosensitizer (mTHPP) associated with different polymers which have merely changed the electron mobility of mTHPP to make different but yet similar NCs.

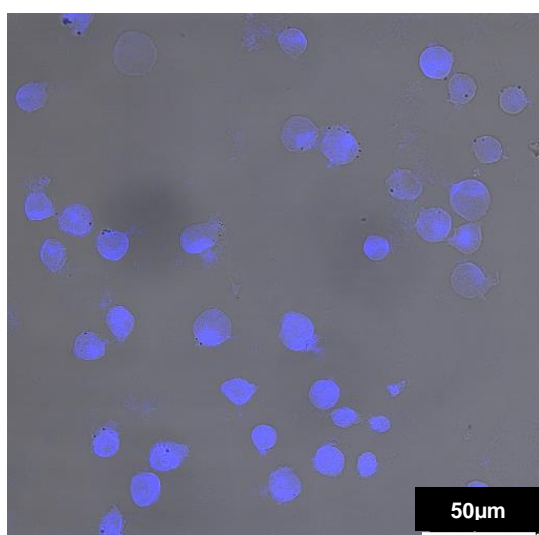


$\lambda_{exc} = 458\text{nm}$; $\lambda_{em} = 530\text{-}560\text{nm}$

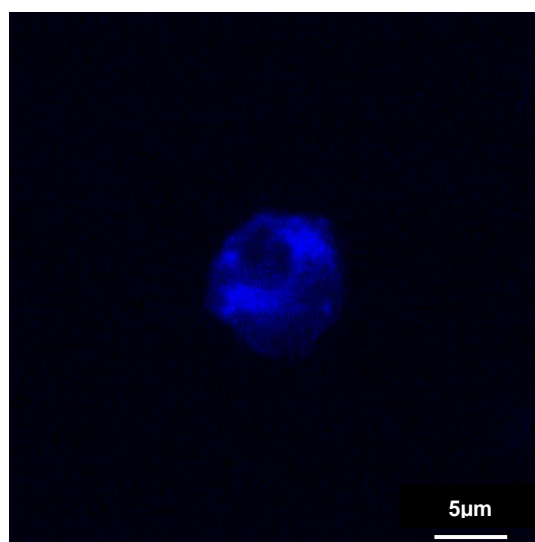


$\lambda_{exc} = 440\text{nm}$; $\lambda_{em} = 482\text{-}606\text{nm}$

Fig.29: Confocal image of mTHPP-PSS NC loaded JC ($\lambda_{exc} = 458\text{nm}$; $\lambda_{em} = 530\text{-}560\text{nm}$)



$\lambda_{exc} = 405\text{nm}$; $\lambda_{em} = 470\text{-}520\text{nm}$



$\lambda_{exc} = 440\text{nm}$; $\lambda_{em} = 455\text{-}580\text{nm}$

Fig.30: Confocal image of mTHPP-Protasan[®] NC loaded

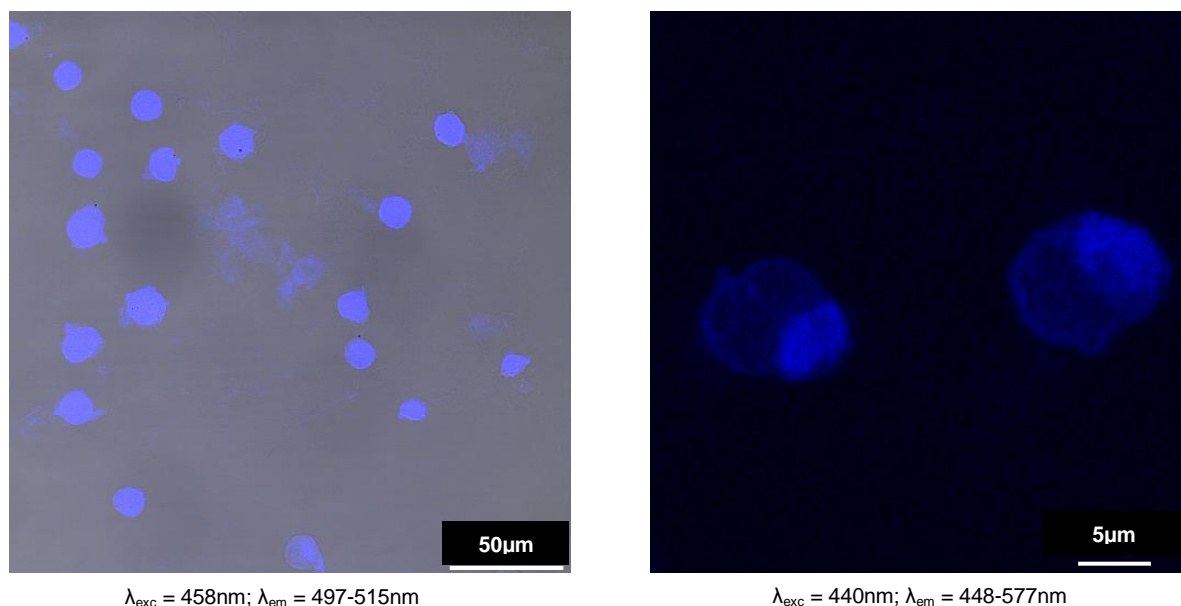


Fig.31: Confocal image of mTHPP-PVP NC loaded

7. Cell culture studies

7.1. Cellular toxicity studies

Cellular toxicity studies were performed on Polymer-mTHPP NC and electroporated blank JC. When the Polymer-mTHPP NCs have internalized into JC, their concentration must not affect viability of cells. Therefore, safe concentration of nanocomplex to JC for safe intracellular delivery was determined by dark toxicity study of Polymer-mTHPP NC with JC.

On other hand, while JC are subjected to electroporation, electric impulses are generated to form pores in the cell wall which can damage the cell resulting in cellular death. Therefore, optimization of electroporation parameters is equally important. Thus, overall objectives of cellular toxicity studies are optimization of sub-toxic concentration of Polymer-mTHPP NC and electroporation parameters for safe intracellular delivery of PNC into JC to develop an active, viable and efficient delivery system.

Comparison of dark toxicity profile of each NC by MTT assay of JCs showed toxicity in order of mTHPP-PSS > mTHPP-Chitosan > mTHPP-PVP (Fig. 32). The highest toxicity of mTHPP-PSS in comparison to its counterparts is attributed to its lower CE value in terms of monomers.

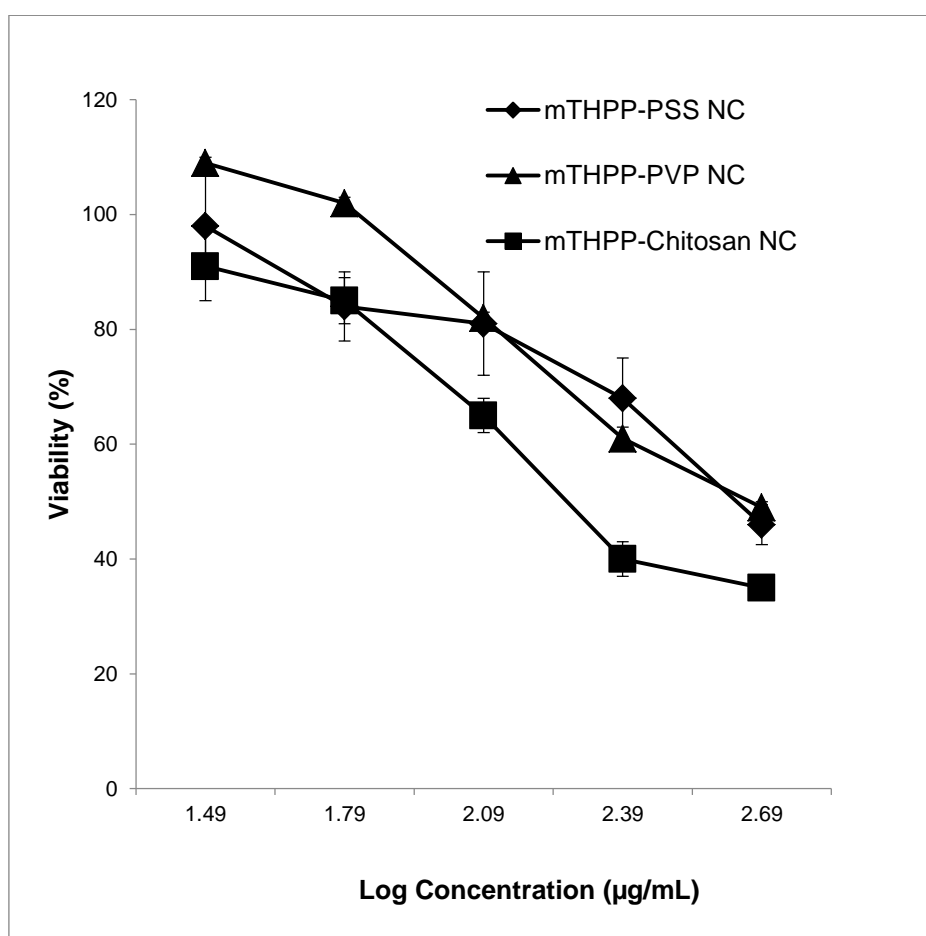
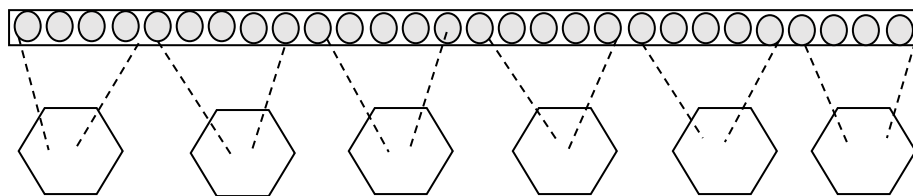


Fig. 32: In vitro dark toxicity of Jurkat cells (1×10^4) following incubation with serial dilutions of 1000 $\mu\text{g/mL}$ PSS NC, mTHPP-PVP NC and mTHPP-Chitosan NC
(Values are representative of 3 independent experiments and reported as mean \pm S.D.)

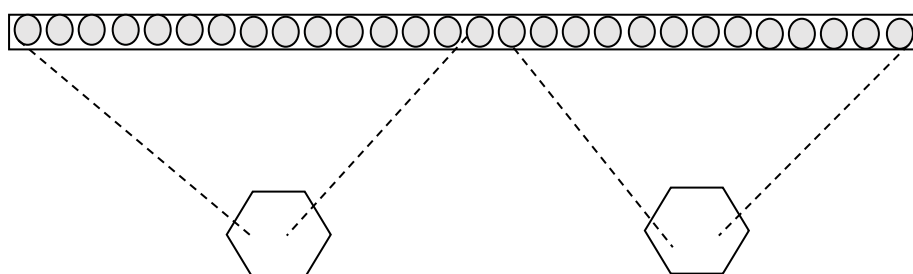
In order to form a NC with one mTHPP molecule, 6 PSS monomers are required while for mTHPP-PVP NC 27 monomers and for mTHPP-Chitosan 14 monomers are needed. Taking a chain of each polymer with equal number of monomers, PSS carries more numbers of mTHPP molecules than Chitosan and then PVP in their NC (Fig. 33). These monomers form physical bonding with mTHPP molecule and the mechanism of formation of intermolecular forces leading to nanocomplexation is described previously.

Interestingly, Chitosan is more toxic to cells due to amine cationic head than negatively charged PSS and neutral PVP polymers but after complexation with mTHPP the toxicity profile is altered. It can be attributed to mTHPP which plays key role in determining the toxicity to exposed cells. Chitosan having lower CE carries less

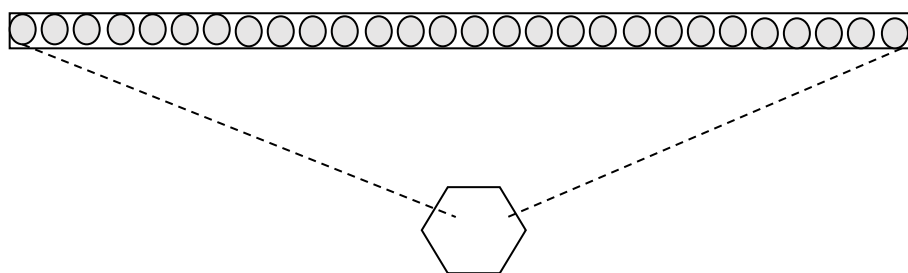
number of mTHPP in its NC than mTHPP-PSS, therefore later surpass the toxic potential over mTHPP-Chitosan due to its stronger CE.



(a) ~ 28 monomers of PSS bind with 6 mTHPP molecule



(b) ~ 28 monomers of Chitosan HCl bind with 2 mTHPP molecule



(c) ~ 28 monomers of PVP bind with 1 mTHPP molecule

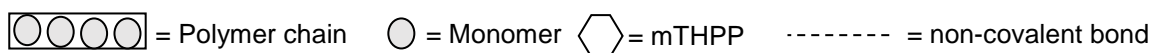


Fig. 33: Schematic representation of mTHPP-Polymer NCs showing molecular interaction between mTHPP and a polymer chain segment containing 28 monomers.

PVP is an inert and biocompatible polymer, and used as plasma volume expander (Motif, 1975). The CE of PVP is weakest among all PNCs, as evident from acquisition

of lowest amount of mTHPP for complexation out of the total mTHPP amount taken for experiment (Fig.22). Hence, mTHPP-PVP NC appears least toxic than its counterparts.

Despite a significant toxic potential in PDT associated with mTHPP-PVP and mTHPP-Chitosan NCs, a huge amount of polymer is required as an excipient which may in turn increases the cost of formulation. Thus PSS holds an ideal candidature for an excipient in polymeric NC based formulation of mTHPP among PVP and Chitosan, as previously explained. A schematic molecular model of PNC (Fig.33) vividly depicts the comparative mTHPP dependent toxic potential of all PNC. Taking ~28 monomers of each polymers complexing with mTHPP, PSS acquires 6 mTHPP molecule for complexation while chitosan forms complex with 2 mTHPP molecules and PVP with only 1 molecule. Thus the schematic molecular model and dark cytotoxicity results unravel the toxic potential of all 3 PNC following the order mTHPP-PSS > mTHPP-Chitosan > mTHPP-PVP.

Electroporation technique involves formation of nanosized pores in cell membrane using strong electrical fields, making cell membrane permeable with altered homeostasis (Rubinsky et al, 2007). Electroporation method was chosen for efficient delivery of Polymer-mTHPP NC into JCs because it is time saving, economic and involve only physical parameters in comparison to other biochemical methods in which use of chemicals can possibly alter physicochemical properties and influence intracellular delivery of Polymer-mTHPP NC. Upon comparing the viability of blank JC against electroporated JC (1×10^6 cells), later had shown 88% viability at 250V current, 250 μ F capacitance at 6.7ms time constant (Fig.34)

7.2. Intra-Jurkat-cellular quantification of mTHPP

Quantification of mTHPP delivered into JCs consists of two major steps; retrieval of mTHPP-Polymer NC from JC by cell lysis followed by extraction of mTHPP from polymer. Cell culture studies pertaining to investigation of xenobiotic metabolite cellular lysis and extraction are very important for investigations of cellular xenobiotic metabolite (Myers et al, 2011) and materials to be delivered into cell.

Triton X 100 is non-ionic surfactant and commonly used in cellular studies for cell lysis. The procedure makes use of 2% TritonX 100 (which breaks down cellular structure to isolate polymeric nanocomplexes and addition of ethanol (for mTHPP-PSS NC and mTHPP-PVP NC) and IPA (for mTHPP-Chitosan NC) resulted in further isolation of mTHPP from polymers. As the intracellular drug is often scanty therefore, fluorescence spectroscopy which is sensitive technique to quantify meagre amount of drug, was preferably used to estimate mTHPP.

Safe concentration of each NC; mTHPP-PSS NC (31µg/mL), mTHPP-Chitosan NC (47µg/mL) and mTHPP-PVP NC (94µg/mL) as determined by MTT assay were used for intra-Jurkat-cellular delivery. Electroporation causes accessibility of mTHPP to intracellular milieu in the form of complex with polymer. Breaking cells followed by isolating mTHPP from each polymer is challenging due to 2 steps extraction. However, the detergent TritonX 100 and ethanol/IPA served this purpose to estimate mTHPP as 0.39-0.53pg/cell upon taking 80×10^3 JC for electroporation with all mTHPP-Polymer nanocomplexes (Table 7). The mTHPP taken up by all Polymer-mTHPP nanocomplexes was between 4.7-5.6% and estimated dose of mTHPP to kill 75-80% A549 cells (1×10^4) by 80×10^3 JC ranges between 31-42 ng (Table.7).

Table 7: mTHPP uptake by JC by electroporation

mTHPP-Polymer NC	mTHPP uptake (%)	mTHPP/JC (pg)	mTHPP/80K JC (ng)
mTHPP-PSS NC	5.1 ± 1.6	0.4 ± 0.12	31 ± 9
mTHPP-Chitosan NC	5.6 ± 0.9	0.5 ± 0.08	42 ± 8
mTHPP-PVP NC	4.7 ± 0.9	0.5 ± 0.10	39 ± 8

Values are representative of 3 independent experiments reported as mean±S.D.

Upon escalating both, the concentration of nanocomplex as well as JC number taken for intracellular delivery, the cellular uptake of mTHPP must increase. If concentration of mTHPP-Polymer NC is increased beyond safe concentration then it can lead to cellular toxicity therefore amount of NC/mTHPP to be delivered is restricted only to safe concentration and techniques like electroporation can deliver up to 4.7-5.6%

mTHPP. In order to enhance the T lymphocyte-encapsulated amount of photosensitizer by increasing the number of JCs is feasible. Thus, in clinical practice the dose of photosensitizer can be optimised by varying the number of T lymphocytes for intracellular delivery depending upon cancer cells counting in blood or tumour volume.

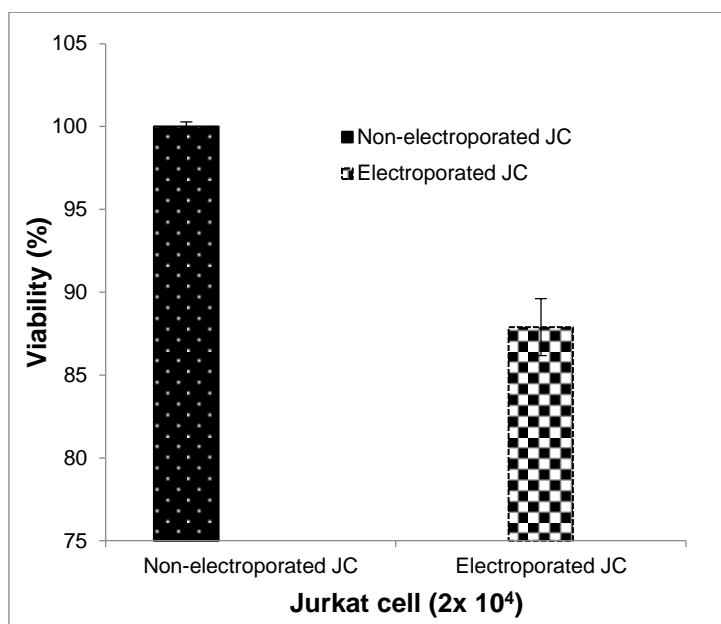


Fig. 34: Viability testing of electroporated 2×10^4 Jurkat cells reported as mean \pm S.D., n=4

7.3. Haemocompatibility studies

T cells express Fc receptors which mediate antibody-dependent cytotoxicity leading to destruction of target cells through interaction between target-specific antibodies and Fc receptors (Landazurimo-De et al, 1979). Erythrocytes are known to be victims of the immune system such as subsets of T cells bearing Fc receptors can break down erythrocytes (Katz et al, 1980). As T cell encapsulating Polymer-mTHPP NC is intended for direct administration into blood, encounter of T cells with RBC is evident. Therefore, the stability of the formulation in blood circulation and safeguard of blood cells from the T cell based delivery system are important.

Cellular wall acts as a barrier and allows intracellular and extracellular transport of drugs and other material by various mechanisms such as passive diffusion and carrier mediated transport (Sugano et al, 2010). Polymer-mTHPP NC may undergo passive diffusion to exit JCs because of the concentration gradient across the cellular membrane. The

size of Polymer-mTHPP NC is similar to other endogenous substances like DNA and viruses (Wang et al, 2008), therefore its active diffusion outside T lymphocytes in blood is inevitable. mTHPP and polymer are bound together with weak forces therefore NCs can dissociate into mTHPP and polymer. Chitosan has a cationic head and PSS possess negative charge. They may again form ion pair complex as well as free mTHPP may complex with substrates present in cell membrane, and undergo carrier mediated efflux from parent T cells (Ruifrok et al, 1981; Poirier et al, 2008).

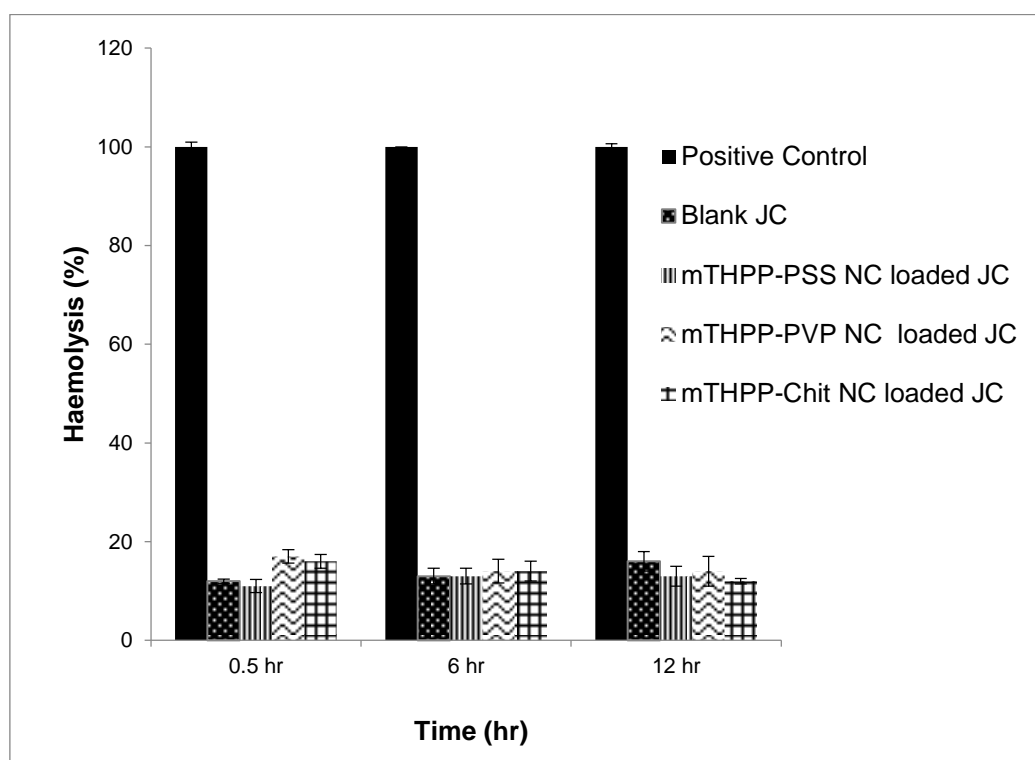


Fig. 35: In vitro hemolysis following incubation of human RBCs with 15×10^4 cells Blank JC, mTHPP-PSS NC, mTHPP-PVP NC and mTHPP-Chitosan HCl loaded JCs in normal saline. Positive Control shows 100% haemolysis (all values reported are mean \pm S.D., n=4).

All pathways leading to free mTHPP or NC escape from its T lymphocyte homing could be toxic to other blood cells. The extent of any adverse effect exerted through all diffusion pathways of NC, dissociated moieties and Jurkat cell itself while NC loaded Jurkat cell is present in blood was investigated by haemocompatibility studies viz, haemotoxicity studies and blood coagulation test (Fig.35 & Table 8).

The haemolysis study was designed by taking 150×10^3 each blank JCs and JCs (20×10^3) loaded with mTHPP-PSS NC, mTHPP-PVP NC and mTHPP-PSS NC in

normal saline (NS) against positive control (RBC with distilled water). Erythrocytes maintain its integrity in normal saline due to osmolality over incubation up to 12hr.

In case of positive control, addition of distilled water brings imbalance in fluid across erythrocyte cell membrane and transfer of extracellular fluid in RBC leads to cellular burst and death releasing Hb, is considered as 100% haemolysis used for estimation of haemotoxicity (Fig.35). Despite intact erythrocytes in NS, haemolysis only up to 14% after 12hr shown by blank and NC loaded JC is due to ATP release induced by experimental condition which involve varying level of oxygen, sheer stress while samples are under stirring (Sikora et al, 2014) at 40 rpm and haemotoxicity exhibited by JC (Arber et al, 1978). Overall haemolysis profiling indicates protective role of the T cell based delivery system in blood (Italia et al, 2009).

Table 8: Blood clotting studies with all Polymer-mTHPP NC

Samples	Time (Seconds)
Blood	130 \pm 5
Blood with mTHPP-PSS NC loaded JC	129 \pm 7
Blood with mTHPP-PVP NC loaded JC	130 \pm 4
Blood with mTHPP-Chitosan NC loaded JC	122 \pm 5

Values are representatives of 3 independent experiments and reported as mean \pm S.D.

Blood clotting is one of the host defence mechanism facilitating the repair of damaged vascular system. As leukocytes (e.g. T cells), erythrocytes and platelets are main player of blood clotting mechanism, therefore presence of T cell based delivery system may provoke the internal blood clotting. Blood clotting is assessed by the formation of fibrin fibres which arrest platelets and a platelet plug is formed appearing as clot. This platelet plug was checked every 30 seconds by needle for normal blood and those mixed with Polymer-mTHPP NCs loaded JC. Blood clotting studies showed the clotting time in presence of all three Polymer-mTHPP NCs loaded JC close to normal blood clotting time (Table 8). All mTHPP-Polymer NCs have shown no

deviation from the clotting time of normal blood i.e. 130 seconds which indicates protective role of cell based delivery system in systemic circulation.

7.4. In vitro anticancer activity

The phototoxic potential of all PNCs and intracellular released mTHPP from PNC, and ability of T lymphocytes to recognise and attack cancer cells were exploited together to kill A549 carcinoma cells. JC are transformed T lymphocytes (Schneider et al, 1977) acted as model cell for T lymphocytes and mTHPP as model drug for mTHPC.

Among all types of nanocarrier for delivery of mTHPP, nanocomplex is preferably chosen due to complex state of drug and polymer conjugate. As nanocomplex is merely association of mTHPP and polymer through physical bondings which may facilitates immediate release of mTHPP under certain condition. Other nanocarriers such as PEGylated moiety which helps accumulation of drug at tumor site, a steric hindrance between cancer cells and nanocarrier appears which reduces tumor cell uptake (Gabizon, 2001 & Hatakeyama et al, 2007). Polymeric nanoparticles of therapeutics with polymers such as PLGA or PLA forms polymer matrix in which drug is entrapped. Such nanoparticulate structure may not allow full exposure of drug to laser and even after exposure to light, fluorescence quenching is inevitable. It can increase the dose of drug to get desired anticancer photodynamic effect and thereby the cost of photodynamic treatment.

Moreover polymeric nanoparticles provoke sustained release of drug while in PIT, instant release of drug is desirable. On contrary, weak physical forces in nanocomplexes allows faster release of drug inside cell and interestingly the release is boosted under high intensity laser beam which can break down weak physical bonding to free mTHPP from polymer. Beside, any drug remaining bound with polymer itself is a fluorescent nanocomplex which is capable to exhibit photodynamic toxicity to destroy cancer cells.

The whole anticancer study comprises of two sets viz, dark toxicity study and laser induced toxicity study. In each set 20×10^3 , 40×10^3 and 80×10^3 JCs were used which include blank JC, electroporated blank JC and JC individually loaded with all three PNCs and only 10×10^3 A549 cells as negative control. In laser induced toxicity study,

cells were irradiated by 457nm wavelength at light dose 12J/mm^2 while dark toxicity samples were kept strictly away from any exposure to light (Fig.36).

The phototherapy with all three PNC loaded JCs at 457nm and light dose 12J/mm^2 shows different levels of toxicities. As the number of NC loaded JCs undergoing phototherapy exponentially increases from 20×10^3 JC to 80×10^4 JC, the anticancer activity also proportionally increases; together all 3 PNC loaded JCs (20×10^4) shows A549 toxicity between 49-53% and if all 3 PNC loaded JCs (40×10^3) are taken then exhibit 61-63% toxicity. Further upon taking all 3 PNC loaded JCs (80×10^3) a toxicity range between 75-80% is shown which is a significant toxic effect exerted on A549 cancer cells by immune cell based delivery system. Thus, the dose for a significant anticancer activity against 10×10^3 A549 cells was optimised as 31-42ng mTHPP encapsulated in 80K JC excited by 457nm light with 12J/mm^2 intensity. When PNC loaded JC number increases the dose of photosensitizer NC increases and under optimised LED (light emitting diode) parameters show an increased phototoxic effect. This indicates that the level of cancer cell toxicity is photosensitizer-dose dependent at optimized light dose (12J/mm^2) and the dose can be enhanced by increasing the number of JC encapsulating PNC.

The sub-toxic concentration of different PNCs against JC was first optimised in MTT assay (dark toxicity study). The toxicity exhibited by all PNCs is substantially due to mTHPP rather than polymer, therefore the subtoxic concentrations of all 3 PNCs contain almost same amount of mTHPP. Further, the mTHPP which is bound to respective polymers with weak physical bonds releases in JC homing alongwith nondissociated mTHPP which remains as PNC, both play active role to exert photodynamic activity.

Interestingly, mTHPP and PNC both are fluorescent and possess phototoxic effects, therefore upon excitation at 457nm, A549 cells are killed as a result of excitation of both released mTHPP and nondissociated mTHPP (nanocomplex). The A549 toxicity exerted by each PNC within same number of PNC loaded JC are almost comparable, however a relatively more anticancer effect associated with mTHPP-PSS NC is due to close matching of its $\lambda_{\text{max}}=446\text{ nm}$ with excitation wavelength $\lambda_{\text{exc}}=457\text{nm}$ of laser in comparison to mTHPP-Chitosan NC; $\lambda_{\text{max}}=412\text{nm}$ and mTHPP-PVP NC; $\lambda_{\text{max}}=426\text{nm}$.

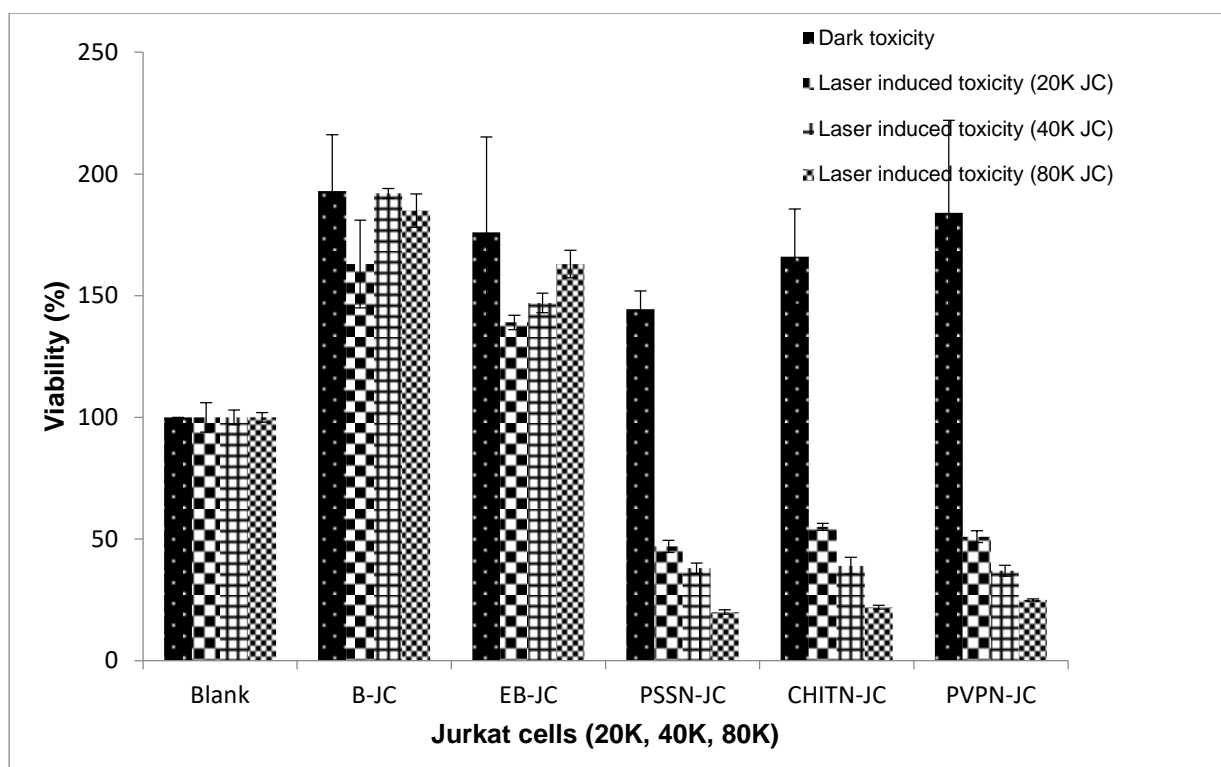


Fig.36: In vitro LED induced anticancer studies following, incubation of 20×10^3 – 80×10^3 JCs with 10×10^3 A549 cells over 4 hours, and irradiation at 457nm, light dose 12 J/mm^2 . Blank (control) =A549 cells, B-JC=Blank JC, EB-JC=Electroporated blank JC, PSSN-JC= mTHPP-PSS NC loaded JC, CHITN-JC= mTHPP-Chitosan loaded JC PVPN-JC=mTHPP-PVP loaded JC. Control shows 100% toxicity Values represent 3 independent experiments and reported as mean \pm S.D.

In vitro experimental condition provides an environment where JC remain in close proximity with A549 cells and JC binding with A549 cells through Tcell receptor is also possible. Thus, blank JC and electroporated blank JC show viability between 176-193% which is additive viabilities of A549 cell and JC.

Upon comparing light induced toxicity against dark toxicity, the phototoxic effect of PNC loaded JC on A549 cells during phototherapy is evident. In addition, together the electroporated blank JC and all 3 PNC loaded JC have shown a reduced viabilities in comparison to blank JC. As electroporated blank JC are killed during electroporation therefore they show 176% viability against 193% viability of blank JC which is due to the electroporation effect at optimised electroporation parameters on blank JC (Fig. 36).

Thus, the anticancer activity utilizing together the photosensitivity of PNC and, immunotoxic potential of JC is proven. Further this photo-immune cell based delivery system holds strong promise in an effective and safe photoimmunotherapy of cancer.

H. CONCLUSION

- Nanocomplexation of poorly soluble drug like mTHPP with water soluble polymer enhances aqueous solubility of the drug which not only overcomes the problem in formulation development but also suppress physiological limitations like accumulation and toxicity in tissues.
- As the ever expanding field of cancer therapy face several challenges, can be well confronted by exploiting the combined principles of PDT and adoptive cell based therapy for a safe, effective and economic management of cancer treatment.
- Loading of polymeric NCs of photosensitizer into T lymphocytes by electroporation is a shift in paradigm of designing a photo-immune cell based delivery system which combines the advantages of phototherapy and immunotherapy.

I. REFERENCES

- Abastado, J-P et al, World cancer report 2014. **2014**, *International Agency for Research on Cancer*. Lyon, France. 1-630
- Ackroyd R, Kelty C, Brown N, Reed M. The history of photodetection and photodynamic therapy. *Photochem. Photobiol.* **2001**, 74: 656–69
- Agostinis P, Berg K, Cengel KA, Foster TH, Girotti AW, Gollnick SO, Hahn SM, Hamblin MR, Juzeniene A, Kessel D, Korbelik M, Moan J, Mroz P, Nowis D, Piette J, Wilson BC, Golab J. Photodynamic therapy of cancer: an update. *CA Cancer J Clin.* **2011**, 61:250-81
- Ananya M. (<http://www.news-medical.net/health/What-are-Cytokines.aspx>)
- Anderson, B et al. Global cancer facts and figure, 3rd Edition. **2014**. *American Cancer Society*. 1-61
- Arber W, Henle W, Hofschneider PH, Humphrey JH, Klein J, Koldovský P, Koprowski H, Maaløe O, Melchers F, Rott R, Schweiger HG, Syruček L. In Vitro and in Vivo Investigations on Antibody-Dependent Cellular Cytotoxicity. *Current topics in microbiology and immunology.* **1978**, 80: 65-96
- Barrett DM, Liu X, Jiang S, June CH, Grupp SA, Zhao Y. Regimen-specific effects of RNA-modified chimeric antigen receptor T cells in mice with advanced leukemia. *Hum Gene Ther.* **2013**, 24: 717-27
- Bastien E, Schneider R, Hackbarth S, Dumas D, Jasniewski J, Röder B, Lina Bezdetnaya L, Lassalle H-P. PAMAM G4.5-chlorin e6 dendrimeric nanoparticles for enhanced photodynamic effects. *Photochem Photobiol Sci.* **2015**, 14: 2203-12
- Batist G, Gelmon KA, Chi KN, Miller WH Jr., Chia SK, et al. Safety, pharmacokinetics, and efficacy of CPX-1 liposome injection in patients with advanced solid tumors. *Clin Cancer Res.* **2009**, 15: 692-700
- Baxevanis CN, Perez SA, Papamichail M. Cancer immunotherapy. *Crit Rev Clin Lab Sci.* **2009**, 46: 167-89
- Bechet D, Couleaud P, Frochot C, Viriot ML, Guillemin F, Barberi-Heyob M. Nanoparticles as vehicles for delivery of photodynamic therapy agents. *Trends Biotechnol.* **2008**, 26: 612-21
- Berman B, Amini S, Valins W, Block S. Pharmacotherapy of actinic keratosis. *Expert Opin Pharmacother.* **2009**, 10: 3015-31
- Bharali D, Sahoo SK, Mozumdar A, Maitra A. Cross-linked polyvinylpyrrolidone nanoparticles: a potential carrier for hydrophilic drugs. *J Colloid Interface Sci.* **2003**, 15: 415-23.
- Blanco E, Kessinger CW, Sumer BD, Gao J. Multifunctional micellar nanomedicine for cancer therapy. *Exp Biol Med.* **2009**, 234: 123-31

Blaudszun AR, Moldenhauer G, Schneider M, Philippi A. A photosensitizer delivered by bispecific antibody redirected T lymphocytes enhances cytotoxicity against EpCAM-expressing carcinoma cells upon light irradiation. *J Control Release*. **2015**, 197: 58-68

Boyer JC, Vetrone F, Cuccia LA, Capobianco JA. Synthesis of colloidal upconverting NaYF₄ nanocrystals doped with Er³⁺, Yb³⁺ and Tm³⁺, Yb³⁺ via thermal decomposition of lanthanide trifluoroacetate precursors. *J Am Chem Soc*. **2006**, 126: 7444–45

Bonnett R, Photosensitizers of the porphyrin and phthalocyanine series for photodynamic therapy, *Chem Soc Rev*. **1995**, 24: 19–33.

Brown SB, Brown EZ, Walker I. The present and future role of photodynamic therapy in cancer treatment. *Lancet Oncol*. **2004**, 5: 497-08

Byrne KT, Côté AL, Zhang P, Steinberg SM, Guo Y, Allie R, Zhang W, Ernstoff MS, Usherwood EJ, Turk MJ. Autoimmune melanocyte destruction is required for robust CD8⁺ memory T cell responses to mouse melanoma. *J Clin Invest*. **2011**, 121: 1797-809

Castano AP, Demidova TN, Hamblin MR. Mechanism in photodynamic therapy: part three- photosensitizer pharmacokinetics, biodistribution, tumor localization and modes of tumor destruction. *Photodiagnosis Photodyn Ther*. **2005**, 2: 91-106

Chatterjee DK, Fong LS, Zhang Y. Nanoparticles in photodynamic therapy: an emerging paradigm. *Adv Drug Deliv Rev*. **2008**, 60:1627-37

Chen W, Zhang J. Using nanoparticles to enable simultaneous radiation and photodynamic therapies for cancer treatment. *J Nanosci Nanotechnology*. **2006**, 6: 1159–66

Chen Y, Zheng X-L, Fang D-L, Yang Y, Zhang J-K, Li H-L, Xu B , Lei Y, Ren K, Song X-R. Dual Agent Loaded PLGA Nanoparticles Enhanced Antitumor Activity in a Multidrug-Resistant Breast Tumoreenograft Model. *Int J Mol Sci*. **2014**, 15: 2761-72

Cho K, Wang Xu, Nie S, Chen Z, Shin DM. Therapeutic Nanoparticles for Drug Delivery in Cancer. *Clin Cancer Res*. **2008**, 14: 1310

Choudhary S, Nouri K, Elsaie ML. Photodynamic therapy in dermatology: A review. *Lasers Med Sci*. **2009**, 24: 971-80

Couzin-Frankel J. Breakthrough of the year 2013. Cancer immunotherapy. *Science*. **2013**, 342: 1432–1433

Chung JE, Tan S, Gao SJ, Yongvongsoontorn N, Kim SH, Lee JH, Choi HS. Yano H, Zhuo L, Kurisawa M, Ying JY. Self-assembled micellar nanocomplexes comprising green tea catechin derivatives and protein drug for cancer therapy. *Nat Nanotechnol*. **2014**, 11: 907-12

Daniell MD, Hill JS. A history of photodynamic therapy. *Aust NZJ Surg.* **1991**, 61: 340–48

Dardel F, Arden TV. Ion Exchangers. *Ullmann's Encyclopedia of Industrial Chemistry*, **2008**, Wiley-VCH, Weinheim.

Diamond I, McDonagh AF, Wilson CB, Granelli SI, Nielsen S, Jaenicke R. Photodynamic therapy of malignant tumours. *Lancet.* **1972**, ii: 1175-77

Di Corato R, Béalle G, Kolosnjaj-Tabi J, Espinosa A, Clément O, Silva AK, Ménager C, Wilhelm C. Combining magnetic hyperthermia and photodynamic therapy for tumor ablation with photoresponsive magnetic liposomes. *ACS Nano.* **2015**, 24: 2904-16

Dolmans DEJGJ, Fukumara D, Jain RK. Photodynamic therapy for cancer. *Nat Rev Cancer.* **2003**, 3: 380-87

Dougherty TJ. An update on photodynamic therapy applications. *J Clin Laser Med Surg.* **2002**, 20: 3-7

Dougherty TJ, Grindey GB, Fiel R, Weishaupt KR, Boyle DGJ. Photoradiation therapy II. Cure of animal tumors with hematoporphyrin and light. **1975**. *Natl. Cancer Inst.* 55: 115-21

Dougherty TJ, Kaufman JE, Goldfarb A, Weishaupt KR, Boyle D, Mittleman A. Photoradiation therapy for the treatment of malignant tumors. *Cancer Res.* **1978**, 38: 2628–35

Dranoff G. Cytokines in cancer pathogenesis and cancer therapy. *Nat Rev Cancer.* **2004**, 4: 11-22

Duncan R. The dawning era of polymer therapeutics. *Nat Rev Drug Discov.* **2003**, 5: 347-60

Ericson MB, Sandberg C, Stenquist B, et al. Photodynamic therapy of actinic keratosis at varying fluence rates: assessment of photobleaching, pain and primary clinical outcome. *Br J Dermatol.* **2004**, 151: 1204–12

Ferreira DM, Saga YY, Aluicio-Sarduy E, Tedesco AC. Chitosan nanoparticles for melanoma cancer treatment by Photodynamic Therapy and electrochemotherapy using aminolevulinic acid derivatives. *Curr Med Chem.* **2013**, 20:1904-11

Figge FHJ, Weiland GS, and Manganiello OJ. Cancer detection and therapy. Affinity of neoplastic, embryonic, and traumatized tissues for porphyrins and metalloporphyrins, *Proc Soc Exp Biol Med.* **1948**, 68: 640–41

Fisher, GH. *et al.* Induction and apoptotic regression of lung adenocarcinomas by regulation of a K-Ra transgene in the presence and absence of tumor suppressor genes. *Genes Dev.* **2001**, 15: 3249–62

Fröhlich E. The role of surface charge in cellular uptake and cytotoxicity of medical nanoparticles. *Int J Nanomedicine*. **2012**, 7: 5577–91

Fry TJ, Mackall CL. Interleukin 7: master regulator of peripheral T cell homeostasis? *Trends Immunol*. **2001**, 22:564-71

Gabizon AA. Stealth liposomes and tumor targeting: one step further in the quest for the magic bullet. *Clin Cancer Res*. **2001**, 7: 223-5

Hatakeyama H, Akita H, Kogure K, Oishi M, Nagasaki Y, et al. Development of a novel systemic gene delivery system for cancer therapy with a tumor-specific cleavable PEG-lipid. *Gene Ther*. **2007**, 14: 68-77

Heer S, Kompe K, Gudel HU, Haase M. Highly efficient multicolour upconversion emission in transparent colloids of lanthanide-doped NaYF₄ nanocrystals. *Adv Mater*. **2004**, 16: 2102–05

Hopper C, Niziol C, Sidhu M. The cost effectiveness of Foscan mediated photodynamic therapy (Foscan-PDT) compared with extensive palliative surgery and palliative chemotherapy for patients with advanced head and neck cancer in the UK. *Oral Oncol*. **2004**, 40: 372-82

Hur C, Nishioka NS, Gazelle GS. Cost effectiveness of photodynamic therapy for treatment of Barrett's esophagus with high grade dysplasia. *Dig Dis Sci*. **2003**, 48: 1273-83

Insinga A, Monestiroli S, Ronzoni S, Gelmetti V, Marchesi F, Viale A, Altucci L, Nervi C, Minucci S, Pelicci PG. Inhibitors of histone deacetylases induce tumor-selective apoptosis through activation of the death receptor pathway. *Nat Med*. **2005**, 11: 71–76

Italia JL, Bhatt DK, Bhardwaj V, Tikoo K, Kumar MN. PLGA nanoparticles for oral delivery of cyclosporine: nephrotoxicity and pharmacokinetic studies in comparison to Sandimmune Neoral. *J Control Release*. **2007**, 119:197-206

Italia JL, Yahya MM, Ravi Kumar MNV. Biodegradable Nanoparticles Improve Oral Bioavailability of Amphotericin B and Show Reduced Nephrotoxicity Compared to Intravenous Fungizone®. *Pharm Res*. **2009**, 6:1324-31

Jain M et al. Sustained loss of neoplastic phenotype by brief inactivation of MYC. *Science*. **2002**, 297:102-04

Johnson LA et al. Gene therapy with human and mouse T-cell receptors mediates cancer regression and targets normal tissues expressing cognate antigen. *Blood*. **2009**, 114:535-45

Josefsen LB, Boyle RW. Photodynamic therapy and the development of metal-based photosensitisers. *Met Based Drugs*. **2008**, 2008: 276109

Juzeniene A, Peng Q, Mohan J. Milestones in the development of photodynamic therapy and fluorescence diagnosis. *Photochem Photobiol Sci.* **2007**, 6:1234-45

Katz P, Fauci AS. Antibody dependent cellular toxicity mediated by subpopulation of human T lymphocytes; killing of human erythrocytes and autologous lymphoid cells. *Immunology.* **1980**, 39: 407-016

Khan DR. The Use of Nanocarriers for Drug Delivery in Cancer Therapy. *J Cancer Sci Ther.* **2010**, 2: 058-062

Kirkwood JM, Tarhini AA, Panelli MC, Moschos SJ, ZarourHM, Butterfield LH, Gogas HJ. Next generation of immunotherapyfor melanoma. *J ClinOncol.* **2008**, 26: 3445–55

Konan YN, Berton M, Gurny R, Allemann E. Enhanced photodynamic activity of meso-tetra(4-hydroxyphenyl)porphyrin by incorporation into sub-200 nm nanoparticles. *Eur J Pharm Sci.* **2003a**, 18: 241–49

Konan-Kouakou YN, Boch R, Gurny R, Allemann E. In vitro and in vivo activities of verteporfin-loaded nanoparticles. *J Control Release.* **2005**, 103: 83-91

Konan YN, Gurny R, Allemann E. State of the art in the delivery of photosensitizers for photodynamic therapy. *J Photochem Photobiol B.* **2002**, 66: 89-106

Konan YN, Gerny R, Favet J, Berton M, Gurny R, Allemann E. Preparation and characterization of sterile sub-200 nm meso-tetra(4-hydroxylphenyl)porphyrin-loaded nanoparticles for photodynamic therapy. *Eur J Pharm Biopharm.* **2003b**, 55: 115–24

Kourie JI. Interaction of reactive oxygen species with ion transport mechanisms. *Am J Physiol.* **1998**, 275: C1-24

Kraut EH, Fishman MN, Lorusso PM, Gordon MS, Rubin EH, et al. Final results of a phase I study of liposome encapsulated SN-38 (LESN38): Safety, pharmacogenomics, pharmacokinetics, and tumor response. *Journal of Clinical Oncology-ASCO Annual Meeting Proceedings* 23, **2005**

Kübler AC. Photodynamic therapy. *Med Laser Appl.* **2005**, 20: 37-45

Landazurimo-De MO, Silva A, Alvares J, Herberman RB. Evidence that natural cytotoxicity and antibody-dependent cellular cytotoxicity are mediated in humans by the same effector cell populations. *J Immunol.* **1979**, 123: 252-58

Lipson RL, Baldes EJ Olsen AM. The use of a derivative of hematoporphyrin in tumor detection, *J Natl Cancer Inst.* **1961**, 26: 1–11

Liu J, Blake SJ, Smyth MJ, Teng MW. Improved mouse models to assess tumor immunity and irAEs after combination cancer immunotherapies. *Clin Trans Immunology.* **2014**, 3: e22

Los M, Roodhart JM, Voest EE. Target practice: lessons from phase III trials with bevacizumab and vatalanib in the treatment of advanced colorectal cancer. *Oncologist*. **2007**, 12: 443-50

Lucky SS, Soo KC, Zhang Y. Nanoparticles in photodynamic therapy. *Chem Rev*. **2015**, 115: 1990-2042

Lukšienė Z. Photodynamic therapy: mechanism of action and ways to improve the efficiency of treatment. *Medicina*. **2003**, 39: 12

Maeda H, Wu J, Sawa T, Matsumura Y, Hori K. Tumor vascular permeability and the EPR effect in macromolecular therapeutics: a review. *J Control Release*. **2000**, 65: 271-84

Mahmoud G, Jedelská J, Strehlow B, Bakowsky U. Bipolar tetraether lipids derived from thermoacidophilic archaeon *Sulfolobus acidocaldarius* for membrane stabilization of chlorin e6 based liposomes for photodynamic therapy. *Eur J Pharm Biopharm*. **2015**, 95: 88-98

Mahnke K, Schonfeld K, Fondel S, Ring S, Karakhanova S, Wiedemeyer K, Bedke T, Johnson TS, Storn V, Schallenberg S, Enk AH. Depletion of CD4+CD25+ human regulatory T cells in vivo: kinetics of Treg depletion and alterations in immune functions in vivo and in vitro. *Int J Cancer*. **2007**, 120: 2723-33

Matsumura Y, Maeda HA. New concept for macromolecular therapeutics in cancer chemotherapy: mechanism of tumor tropic accumulation of proteins and the antitumor agent smancs. *Cancer Res*. **1986**, 46: 6387-92

McCarthy JR, Perez JM, Bruckner C, Weissleder R. Polymeric nanoparticle preparation that eradicates tumors. *Nano Lett*. **2005**, 5: 2552-56

McKeage K, Perry CM, Trastuzumab: a review of its use in the treatment of metastatic breast cancer overexpressing HER2. *Drugs*. **2002**, 62: 209-43

Melero I, Hervas-Stubbs S, Glennie M, Pardoll DM, Chen L. Immunostimulatory monoclonal antibodies for cancer therapy. *Nat Rev Cancer*. **2007**, 7: 95-106

Meyer-Betz F. Untersuchung über die biologische (photodynamische) Wirkung des Hamatoporphyrins und anderer Derivate des Blut- und Gallenfarbstoffs. *Dtsch Arch Klin Med*. **1913**, 112: 476-503

Milstein O, Hagin D, Lask A, Reich-Zeliger S, Shezen E, Ophir E, Eidelstein Y, Afik R, Antebi YE, Dustin ML, Reisner Y. CTLs respond with activation and granule secretion when serving as targets for T-cell recognition. *Blood*. **2011**, 117: 1042-52

Mitsunaga M, Nakajima T, Sano K, Choyke PL, Kobayashi H. Near-infrared Theranostic Photoimmunotherapy (PIT): Repeated Exposure of Light Enhances the Effect of Immunoconjugate. *Bioconjugate Chem*. **2012**, 23: 604-09

Mitsunaga M, Ogawa M, Kosaka N, Rosenblum LT, Choyke PL, Kobayashi H. Cancer cell-selective in vivo near infrared photoimmunotherapy targeting specific membrane molecules. *Nat Med.* **2011**, 17: 1685–91

Monfrecola G, Fabbrocini G, Pinton PC. Photodynamic therapy for non-melanoma skin cancers. *Curr Cancer Ther Rev.* **2009**, 5: 271-80

Morgana NY, Kramer-Marekb G, Smitha PD, Camphausenb K, Capalab J. Nanoscintillator Conjugates as Photodynamic Therapy-Based Radiosensitizers: Calculation of Required Physical Parameters. *Radiat Res.* **2009**, 17: 236–44

Motiff EA. Blood substitutes. *Can Anaesth Soc J.* **1975**, 22:12-9

Mroz P, Yaroslavsky A, Kharkwal GB, Hamblin MR. Cell Death Pathways in Photodynamic Therapy of Cancer. *Cancers.* **2011**, 3: 2516-39

Myers JN, Rekhadevi PV, Ramesh A. Comparative evaluation of different cell lysis and extraction methods for studying benzo(a)pyrene metabolism in HT-29 colon cancer cell cultures. *Cell Physiol Biochem.* **2011**, 28: 209-18

Nayak CS. Photodynamic therapy in dermatology. *Indian J Dermatol Venerol Leprol.* **2005**, 71: 155-60

Nazaran MH et al. BCc1, the novel antineoplastic nanocomplex, showed potent anticancer effects in vitro and in vivo. *Drug Des Devel Ther.* **2015**, 10: 59–70

Nazaran MH et al. The therapeutic effects of MSc1 nanocomplex, synthesized by nanochelating technology, on experimental autoimmune encephalomyelitic C57/BL6 mice. *Int J Nanomed.* **2014**, 9: 3841-53

Ochsner M. Photophysical and photobiological processes in the photodynamic therapy of tumours. *J Photochem Photobiol B.* **1997**, 39: 1-18

Okudaira K, Hokari R, Tsuzuki Y, Okada Y, Komoto S, Watanabe C, Kurihara C, Kawaguchi A, Nagao S, Azuma M, Yagita H, Miura. Blockade of B7-H1 or B7-DC induces an anti-tumor effect in a mouse pancreatic cancer model. *Int J Oncol.* **2009**, 35: 741-9

Oleinik NL, Evans HH. The photobiology of photodynamic therapy: Cellular targets and mechanisms. *Radiation Res.* **1998**, 150:146-56

Park S. Delivery of photosensitizers for photodynamic therapy. *Korean J Gastroenterol.* **2007**, 49: 300-13

Pass HI. Photodynamic therapy in oncology: Mechanisms and clinical use. *J Natl Cancer Inst.* **1993**, 85: 443-56

Persson J, Beyer I, Yumul R, Li Z, Kiem H-P, et al. Immuno-Therapy with Anti- TLA4 Antibodies in Tolerized and Non-Tolerized Mouse Tumor Models. *PLoS ONE*. **2011**, 6(7): e22303

Photos PJ, Bacakova L, Discher B, Bates FS, Discher DE. Polymer vesicles in vivo: correlations with PEG molecular weight. *J Control Release*. **2003**, 90: 323-34

Piacquadio DJ, Chen DM, Farber HF, et al. Photodynamic therapy with aminolevulinic acid topical solution and visible blue, light in the treatment of multiple actinic keratoses of the face and scalp – investigator-blinded, phase 3, multicenter trials. *Arch Dermatol*. **2004**, 140: 41–6

Pichierri, F. Dipole-dipole interactions in protein-protein complexes: a quantum mechanical study of the ubiquitin-Dsk2 complex. *QPI*. **2013**, 1:1-8

Pirollo KF, Nemunaitis, Leung PK, Nunan RJ, Adams J, Chang EH. Safety and Efficacy in Advanced Solid Tumors of a Targeted Nanocomplex Carrying the p53 Gene Used in Combination with Docetaxel: A Phase 1b Study *Mol Ther*. **2016**, Aug 2. doi: 10.1038/mt.2016.135. [Epub ahead of print]

Plaetzer K, Kiesslich T, Verwanger T, Krammer B. The modes of cell death induced by PDT: An overview. *Med Laser Appl*. **2003**, 18: 7-19

Poirier A, et al. Design, data analysis and simulation of in vitro drug transport kinetic experiments using a mechanistic in vitro model. *Drug Metab. Dispos*. **2008**, 36: 2434–44

Powell E, Lee Y-H, Partch R, Dennis D, Morey T, Varshney M, Pi-Pi complexation of bupivacaine and analogues with aromatic receptors: Implications for overdose remediation. *Int J Nanomedicine*. **2007**, 2: 449–59

Prime S, Littlewood T, Khan M, Elia G, Evan GI. Suppression of Myc-induced apoptosis in beta cellsexposes multiple oncogenic properties of Myc and triggers carcinogenic progression. *Mol Cell*. **1900**, 3: 565-77

Raab O. Über die Wirkung fluoreszierender Stoffe auf Infusorien. *Zeitung Biol*. **1900**, 39: 524–26

Reum N, Fink-Straube C, Klein T, hartmann RW, Lehr C-M, Schneider M. Multilayer Coating of Gold Nanoparticles with Drug-Polymer Coadsorbates. *Langmuir*. **2010**, 26: 16901–08

Reum N, Schneider M. Multilayer coating of gold nanoparticles (AuNP) with drug-polymer complex: Development and characterization. *Thesis*. **2011**, 1–129

Rothschild WG: Binding of hydrogen donors by peptide groups of lactams. Identity of the reaction sites. *J Am Chem Soc*. **1972**, 94: 8676–83

Roy I, Ohulchanskyy TY, Pudavar HE, Bergey EJ, Oseroff AR, Morgan J, Dougherty TJ, Prasad PN. Ceramic-based nanoparticles entrapping water-insoluble

photosensitizing anticancer drugs: a novel drug-carrier system for photodynamic therapy. *J Am Chem Soc.* **2003**, 125: 7860–65

Rubinsky B. Irreversible electroporation in medicine. *Technol. Cancer Res Treat.* **2007**, 6: 255-60

Ruifrok PG, Meijer DK. Transport of organic ions through lipid bilayers. *Naunyn Schmiedebergs Arch Pharmacol.* **1981**, 316: 266–72

Sandberg C, Stenquist B, Rosdahl I, et al. Important factors for pain during photodynamic therapy for actinic keratosis. *Acta DermatoVenereologica.* **2006**, 86: 404–8

Santos-Carballal B, Aldering LJ, Ritzefeld M, Pereira S, Sewald N, Moerschbacher BM, Götte M, Goycoolea FM. Physicochemical and biological characterization of chitosan-microRNA nanocomplexes for gene delivery to MCF-7 breast cancer cells. *Sci Rep.* **2015**, 5: 1-14

Saroj AL, Singh RK, Chandra S. Studies on polymer electrolyte poly(vinyl)pyrrolidone (PVP) complexed with ionic liquid: Effect of complexation on thermal stability, conductivity and relaxation behavior. *Material Science and Engineering B.* **2013**, 178: 231–38

Schneider U, Schwenk HU, Bornkamm G. Characterization of EBV-genome negative "null" and "T" cell lines derived from children with acute lymphoblastic leukemia and leukemic transformed non-Hodgkin lymphoma. *Int J Cancer.* **1977**, 19: 621-6

Schreck S, Pietzsch A, Kennedy B, Sâthe C, . Miedema PS, Techert A, Strocov VN, Schmitt T, Hennies F, Rubensson E, Föhlisch A. Ground state potential energy surfaces around selected atoms from resonant inelastic x-ray scattering. *Sci Rep.* **2016**, 20054: 1-7

Sharma D, Chelvi TP, Kaur J, Chakravorty K, De TK, Maitra A, Ralhan R. Novel Taxol formulation: polyvinylpyrrolidone nanoparticle-encapsulated Taxol for drug delivery in cancer therapy. *Oncol Res.* **1996**, 8: 281-06

Shi C, Khan SA, Wand K, Schneider M. Improved delivery of the natural anticancer drug tetrandrine. *Int J Pharm.* **2015**, 479: 41-51

Shih T, Lindley C. Bevacizumab: an angiogenesis inhibitor for the treatment of solid malignancies. *Clin Ther.* **2006**, 28:1779-802

Sikora, J.; Orlov, S. N.; Furuya, K.; Grygorczyk, R. Hemolysis is a primary ATP-release mechanism in human erythrocytes, *Blood.* **2014**, 124: 2150–57

Smits T, Moor ACE. New aspects in photodynamic therapy of actinic keratoses. *J Photochem Photobiol B: Biology.* **2009**, 96: 159-69

Songca SP, Oluwafemi OS. Photodynamic therapy: A new light for the developing world. *Afr J Biotechnol.* **2013**, 12: 3590-99

Sugano K, Kansu M, Artursson P, Avdeef A, Bendles S, Di L, Ecker GF, Faller B, Fischer H, Gerebtzoff G, Lennernaes S, Senner F. Coexistence of passive and carrier mediated processes in drug transport. *Nat Rev Drug Discov.* **2010**, 9: 597-614

Sutmuller RP, van Duivenvoorde LM, van Elsas A, Schumacher TN, Wildenberg ME, Allison JP, Toes RE, Offringa R, Melief CJ. Synergism of cytotoxic T lymphocyte associated antigen 4 blockade and depletion of CD25(+) regulatory T cells in antitumor therapy reveals alternative pathways for suppression of autoreactive cytotoxic T lymphocyte responses. *J Exp Med.* **2001**, 194: 823–32

Tersigni SH. Core-excited nanoparticles and methods of their use in the diagnosis and treatment of disease. *United State Patent.* **2012**, Patent no. US8,197,471,B1

Thakor A, Gambhir S. Nanooncology: The future of cancer diagnosis and therapy. *Ca Cancer J Clin.* **2013**, 63: 395-418

Torchilin VP. Targeted pharmaceutical nanocarriers for cancer therapy and imaging. *AAPS.* **2007**, J9: E128-47

Tschen EH, Wong DS, Pariser DM, et al: Photodynamic therapy using aminolaevulinic acid for patients with nonhyperkeratotic actinic keratoses of the face and scalp: Phase IV multicentre clinical trial with 12-month follow up. *Br J Dermatol.* **2006**, 155:1262-1269

Vivek R, Nipun Babu V, Thangam R, Subramanian KS, Kannan S. pH-responsive drug delivery of chitosan nanoparticles as Tamoxifen carriers for effective anti-tumor activity in breast cancer cells. *Colloids Surf B Biointerfaces.* **2013**, 111: 117-23

von Specht BU, Seinfeld H, Brendel W. Polyvinylpyrrolidone as a soluble carrier of proteins. *Hoppe Seylers Z Physiol Chem.* **1973**, 354: 1659-60

Wang X, Yang L, Chen ZG, and Shin DM. Application of nanotechnology in cancer therapy and imaging. *CA Cancer J Clin.* **2008**, 58: 97-110

Wang Y, Lin Y, Zhang H-g, Zhu J. A photodynamic therapy combined with topical 5-aminolevulinic acid and systemic hematoporphyrin derivative is more efficient but less phototoxic for cancer. *J Cancer Res Clin Oncol.* **2016**, 142: 813–821

Weissleder R, Ntziachristos V. Shedding light onto live molecular target. *Nat Med.* **2003**, 1: 123-8

Wieder ME, Hone DC, Cook MJ, Handsley MM, Gavrilovic J, Russell DA. Intracellular photodynamic therapy with photosensitizer-nanoparticle conjugates: cancer therapy using a 'Trojan horse'. *Photochem Photobiol Sci.* **2006**, 5: 727–34

Wijnja H, Pignatello JJ, Malekani K. Formation of pi-pi complexes between phenanthrene and model pi-acceptor humic subunits. *J Environ Qual.* **2004**, 33: 265-75

Wohrle D, Hirth A, Bogdahn-Rai T, Schnurpfeil G, Shopova M. Photodynamic therapy of cancer: second and third generations of photosensitizers. *Russ Chem Bull.* **1998**, 47: 807–16

Wu H, Zhu L, Torchilin VP. pH-sensitive-(histidine)-PEG/DSPE-PEG co-polymer micelles for cytosolic drug delivery. *Biomaterials.* **2013**, 34: 1213-22

Wu ZM, Ling L, Zhou LY, Guo XD, Jiang W, Qian Y, Luo KQ, Zhang LJ. Novel preparation of PLGA/HP55 nanoparticles for oral insulin delivery. *Nanoscale Res Lett.* **2012**, 7: 299

Yang T, Cui F-D, Choi M-K, Cho J-W, Chung S-J, Shim C-K, Kim D-D. Enhanced solubility and stability of PEGylated liposomal paclitaxel: *In vitro* and *in vivo* evaluation. *Int J Pharm.* **2007**, 338: 317-26

Zeisser-Labouebe M, Lange N, Gurny R, Delie F. Hypericin-loaded nanoparticles for the photodynamic treatment of ovarian cancer. *Int J Pharm.* **2006**, 326:174–81

Zhao N, Bagaria HG, Wong MS, Zu Y. A nanocomplex that is both tumor cell-selective and cancer gene-specific for anaplastic large cell lymphoma. *J Nanobiotechnology.* **2011**, 9: 1-12

Zijlmans HJ, Bonnet J, Burton J, Kardos K, Vail T, Niedbala RS, Tanke HJ. Detection of cell and tissue surface antigens using up-converting phosphors: a new reporter technology. *Anal Biochem.* **1999**, 267: 30–36

Website References

<http://goldbook.iupac.org/P04652.html>

<http://www.sciencemag.org/news/2013/12/sciences-top-10-breakthroughs-2013>

[Hum Gene Ther. 2013 Aug;24\(8\):717-27. doi: 10.1089/hum.2013.075.](http://hum.gene.com/2013/Aug;24(8):717-27)

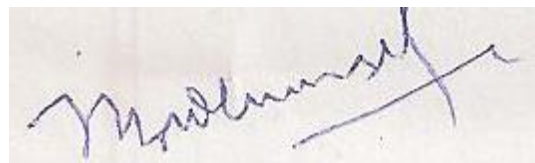
J. ERKLÄRUNG

Ich versichere, dass ich meine Dissertation

selbständig ohne unerlaubte Hilfe angefertigt und mich dabei keiner anderen als der von mir ausdrücklich bezeichneten Quellen bedient habe. Alle vollständig oder sinngemäß übernommenen sind Zitate als solche gekennzeichnet.

Die Dissertation wurde in der jetzigen oder einer ähnlichen Form noch bei keiner anderen Hochschule eingereicht und hat noch keinen sonstigen Prüfungszwecken gedient.

Marburg, den 03/11/2016



Mohammad Yahya Momin

.....

(Unterschrift mit Vor- und Zuname)

K. CURRICULUM VITAE

Name: Mohammad-Yahya Momin
Qualification: PhD (Pharmaceutics and Biopharmaceutics)
Pharmacist, M.S. (Pharmaceutics), B. Pharm.
Nationality: Indian
Gender: Male
Languages: English: Fluent; German: Middle level (B1)
Urdu and Hindi: Native speaker
E-mail id: mominzy@gmail.com

Academic and professional experience

PhD in Pharmaceutics and Biopharmaceutics (September 2014- December 2016)
Faculty of Pharmacy, Department of Pharmaceutics and Biopharmaceutics)
Philipps University of Marburg, Germany

Title of thesis: *“An injectable formulation of polymeric photosensitizer nanocomplex-encapsulated T lymphocytes in photodynamic therapy of cancer”*

- Synthesis and characterization of polymeric nanoparticles for drug delivery application (polymeric, solid lipid nanoparticle, polymeric nanocomplexes, liposomes)
- Internalization of polymeric nanoparticles into T cells (immune cell based delivery system)
- Electroporation
- Release studies with Franz diffusion cell
- Measurement of particles size, PDI and zeta potential by dynamic light scattering
- Analytical method development, validation, quantification by UV- and fluorescence spectroscopies
- Atomic force microscopy and Confocal laser scanning microscopy
- Cellular studies (cytotoxicity, anticancer, haemotoxicity studies)
- Photodynamic therapy
- Synthesis and characterization of solid lipid nanoparticles for drug delivery application
- Internalization of polymeric nanoparticles into T cells (immune cell based delivery system)

PhD Research Scholar (November 2011- April 2013)
Institute of Pharmacy, Department of Pharmacology and Toxicology, Free University of Berlin, Germany

Lecturer in Pharmaceutics (January 2009 – May 2011)
Dr. BN College of Pharmacy (Mumbai University, India)

- Lectures, conducting practical of Pharmaceutical Technology and supervision of undergraduates
- Mentorship

Research Associate Formulation R & D (3 months)

In 2008, **Ajanta Pharma Pvt. Ltd.**, Mumbai, India

- Optimization of pharmaceutical process for development of conventional dosage forms system

Master of Science

July 2005 – December 2007 in **Department of Pharmaceutics, National Institute of Pharmaceutical Education and Research (NIPER)-Mohali**, India

Title of thesis: *“Nanoparticulate Formulation of Amphotericin B for Oral Delivery”*

- Development and characterization of nanoparticles
- HPLC-*in vitro* and *in vivo* analytical method development and validation as per ICH guideline
- Enhancing poor bioavailability and aqueous solubility of challenging and difficult-to-deliver drug molecules
- Photon-imager for live tracking of fluorescent nanoparticles in animal (exposure)
- IPR (Intellectual Property Right)-searching patent data base and commercialization of patentable formulations

Bachelor in Pharmacy

August 2001 - May 2005 from **Bombay College of Pharmacy (Mumbai University)**, India

- All theories and practicals of pharmaceutical sciences
- Industrial training in manufacturing, research and development and quality control of solid and liquid oral delivery systems

GATE/Graduate Aptitude Test in Engineering (Pharmacy)

In March 2005 conducted by IIT (Indian Institute of Technology), Bombay, India
(GATE is a national level entrance exam for postgraduate studies)

NIPER national level entrance test (Pharmacy)

In May 2005 conducted by NIPER-Mohali
(GATE is a national level entrance exam for postgraduate studies)

Diploma in Pharmacy

August 1999 - May 2001, Mumbai University, India

Publications and presentations

Publications

- **Mohammad-Yahya Momin**, Shashank Reddy, Udo Bakowsky, Marc Schneider. Polymeric nanocomplex of porphyrine photosensitizer-loading into T lymphocyte for photo-immunotherapy of cancer. Manuscript under publication process

- **Mohammad-Yahya Momin**, Pramod Nair, Udo Bakowsky, Marc Schneider. Complexation potential of water soluble polymers with porphyrine for drug delivery: A comparative investigation based on UV spectroscopy and computational modelling. Manuscript under writing.
- K  chler S, Wolf NB, Heilmann S, Weindl G, Helfmann J, **Yahya MM**, Stein C, Sch  fer-Korting M. 3D-Wound healing model: Influence of morphine and solid lipid nanoparticles. *Journal of Biotechnology* 148(2010), 24–30 (Impact factor; 3.18)
- Italia JL, **Yahya MM**, Singh D, Ravi Kumar MN. Biodegradable Nanoparticles Improve Oral Bioavailability of amphotericin B and Show Reduced Nephrotoxicity Compared to Intravenous Fungizone[®]. *Pharmaceutical Research* 26(6):1324-31 (Impact factor; 3.42)

Presentations

- Poster- **MY Momin**, Shashank P. Reddy, U. Bakowsky, M. Schneider. Polymeric nanocomplexes of photosensitizers loaded T lymphocytes for photodynamic therapy of cancer. *NANO-SMAT 2016 May 18-20, 2016* in University of Texas, Arlington-USA
(Best scientific poster presentation award)
- Oral- **MY Momin**, Shashank P. Reddy, U. Bakowsky, M. Schneider. Polymeric nanocomplexes of photosensitizers loaded T lymphocytes for photodynamic therapy of cancer. *NANO-SMAT 2016 May 18-20, 2016* in University of Texas, Arlington-USA
- Poster- **MY Momin**, JL Italia, MNV Ravi Kumar. Development and *in vivo* evaluation of nanoparticulate formulation of Amphotericin B” at 35th Annual Meeting Exposition of Controlled Release, July 12-16, 2008 in New York-USA

Awards and Achievements

Scholarship

- Travel award by DAAD to attend NANOSMAT 2016 international conference, Texas, USA (2016)
- Philipps University of Marburg Scholarship for PhD
- Government of India national scholarship for M.S. (Pharmaceutics) (2005-2007)
- MESCO-Scholarship for Bachelor in Pharmacy und Diploma in Pharmacy(2001-2005)

Achievements

- **Best poster award** at University of Texas for PhD research work (2016)
- First prize as Human Relationship Award in UXL Training during M.S. in Pharmaceutics (2007)

- First prize for speech as “HIV AIDS Literate” in Diploma in Pharmacy (1999)
- First prize in essay writing competition in Urdu from Rotary Club Mumbai, India (1994)
- "Excellence in B. Pharmacy Award“ from MESCO (2005)

Computer proficiency

- End note
- MS Office
- In-design

Referees

- **Prof. Dr. M. Schneider**

Head of the Department
(Former Professor at Philipps Universität Marburg)
 Biopharmaceutics and Pharmaceutical Technology
 University of Saarland
 Campus A41 D-66123 Saarbruecken, Deutschland
 Tel: +49/68130-22438
 E-mail: marc.schneider@mx.uni-saarland.de

- **Prof. Dr. U. Bakowsky**

Head of the Department
 Pharmaceutics and Biopharmaceutics
 Philipps University of Marburg
 35039-Marburg, Deutschland
 Tel: +49/642128-25884 (Mo-Do)
 E-mail: ubakowsky@aol.com